Exhibit 6

IN RE JOHNSON & JOHNSON TALCUM POWDER PRODUCTS MARKETING, SALES PRACTICES, AND PRODUCTS LIABILITY LITIGATION
MDL NO. 16-2738 (FLW) (LHG)

Shu-Chun Su
2024-05-21

Credentials

My name is Shu-Chun Su. I have developed methods and published on issues related to the identification of asbestos by polarized light microscopy (PLM) throughout my more than forty-year career.

I was born in China. I majored in Geochemistry at the Department of Geology, Peking University, for my bachelor's, a six-year program mirroring science programs at Moscow University. My Optical Crystallography was a two-semester (40 weeks) course. So was Optical Mineralogy. These two courses are the foundations of identifying rock-forming minerals using PLM. American Geology departments teach these two subjects in several weeks, not as complete semester courses. I graduated from Peking University in 1964, and I worked as a geological engineer in the Geological Survey of Gansu Province of China for 14 years. My job was to identify rock and mineral samples collected by field geologists in the geological mapping of the Gansu Province using a Zeiss polarized light microscope. Serpentine asbestos (chrysotile) was a common mineral species among the field samples of ultramafic rocks in that area. I developed expertise in the identification of asbestos—and specifically chrysotile—during my work here.

In 1979, I attended the Institute of Geology, Chinese Academy of Science, for graduate studies and obtained my Master's Degree in Mineralogy in 1981. Then, I came to the United States to pursue my doctoral studies at Virginia Institute of Technology and State University under Professor Donald Bloss, the preeminent, world-renowned expert in optical crystallography. My doctoral thesis was the study of silicate minerals by light and electron microscopy and X-ray diffraction spectroscopy, which are the same techniques used to analyze asbestos. The identification of chrysotile and other asbestos minerals by light microscopy is something that I have been researching and publishing for more than forty years.

After obtaining my Ph.D. in geology in 1985, I did two years of postdoctoral research in the development of an automatic optical instrument for measuring minerals' refractive index invented by Professor Bloss. I went to work at the Research Center, Hercules Incorporated, a specialty chemical and aerospace company. I was the director of the Optical and Electron Microscopy Laboratory in Wilmington, Delaware. My job was to characterize materials produced and researched by the company using various optical and electron microscopy techniques. As part of this work, I characterized chrysotile and other types of asbestos by PLM.

In 1988, I was recruited to become a Technical Expert in the Bulk and Airborne Asbestos Programs by the National Voluntary Laboratory Accreditation Program (NVLAP) under the Department of Commerce, a government office regulating asbestos analysis laboratories. Since then, I've conducted approximately one thousand on-site audits of asbestos laboratories, mainly in the United States but also in Canada, Japan, and Korea. These audits assess the laboratories' managerial and

technical proficiency in conducting standardized PLM and TEM asbestos analyses. Every asbestos laboratory with (or seeking) NVLAP accreditation performs PLM asbestos analyses.

To date, I've authored 29 publications on asbestos analysis, which are identified in my biography, which is attached as **Exhibit A**.

In the area of airborne asbestos analysis, I have created 880 pages of comprehensive tables for the identification of amphibole asbestos, which has been widely used by airborne asbestos laboratories around the world.

My most well-known contribution to asbestos analysis is a standard operating procedure to quickly and accurately measure the refractive index (RI) of asbestos minerals (the primary diagnostic optical property of "fingerprinting" asbestos minerals) using the central stop dispersion staining technique by PLM. This procedure is accurate and highly efficient, reducing a lengthy ten-minute graphic solution of RI value into 10 seconds. This technique has been referred to as the "Su Method" by scientists practicing in this area and has been cited in textbooks addressing the identification of asbestos by PLM. The Su Method has been adopted by most analytical laboratories performing PLM analyses in the United States and overseas. In fact, Dr. William Longo's laboratory MAS reports that they themselves have been using my Su Method for Johnson's Baby Powder analyses.

In April 2024, at ASTM International's Michael Beard Conference on Asbestos Terminology, the organization presented me with an award recognizing my career-long contributions to asbestos analysis, including recognizing the "Su Method" as a significant achievement in PLM analytical procedures.

As noted above, I am an accomplished expert in the characterization of asbestos minerals by PLM. It has been a focus of my entire career. As such, I am uniquely qualified to assess whether or not a laboratory's PLM data identifying asbestos using my Su Method is reliable and accurate.

Scope of Analysis

I have been asked to review PLM data put forth by Dr. Longo's laboratory MAS in which he claims to identify "chrysotile" in Johnson's Baby Powder by PLM using central stop dispersion staining. I am being compensated at a rate of $800 per hour for my scientific analysis of this issue. I have not provided any deposition or trial testimony in the past four years.

A list of the MAS reports that I reviewed identifying "chrysotile" in Johnson's Baby Powder is identified in **Exhibit B**.

As I explain further below, I disagree with each and every single PLM identification of "chrysotile" in Johnson's Baby Powder made by Dr. Longo's laboratory in the reports that I have reviewed. The data presented by MAS demonstrate significant deficiencies in all areas, which leads me to conclude that the laboratory is incapable of performing the most fundamental aspects of PLM analysis or correctly identifying chrysotile by PLM. A summary of the analytical failings of MAS appears below and is expanded upon in the demonstrative materials that I have attached as **Exhibit C**. The bases for my opinions are my experience, education, training, my publications that are listed in **Exhibit A**, and the sources cited in this report and the attached **Exhibit C**.

Summary of Analysis

Dr. Longo's laboratory's identification of "chrysotile" in Johnson's Baby Powder by PLM is incorrect and unreliable for the following reasons:

1. **MAS's Procedure for Measuring Refractive Index Values is Inaccurate and Unreliable**

    a. **MAS Used Suppressed Light Intensity, Leading to Inaccurate and Unreliable Refractive Index Value Determination**

In order to accurately measure the RI value of a mineral by PLM, it is fundamental that the equipment used needs to be set appropriately. MAS routinely uses insufficient light intensity, as if the light intensity was suppressed, which in turn subdues the dispersion staining color, resulting in a subdued RI value and a subdued birefringence value. The result is that talc's high γ and the associated birefringence are suppressed, making the elongated talc particle look like chrysotile. If the light suppression is unintentional, then MAS has failed to conduct basic PLM procedures, such as adjusting the light intensity and aperture diaphragm to optimal condition to achieve a fully and adequately displayed dispersion staining color or accurately calibrating the objective lens so that it can measure particles size accurately (as I will discuss further below).

I describe examples of this problem on pages 2 through 5 of **Exhibit C**.

b. Inaccurate Refractive Index Measurement Procedure Leads to Unreliable Results

MAS routinely fails to accurately identify the RI value exhibited by particles in its PLM analyses. There are numerous instances of MAS assigning an RI value that is simply wrong (and incorrectly closer to values that may be associated with chrysotile rather than talc). Based on my review of the reports identified in **Exhibit B**, the data presented by MAS demonstrates a systematic failure to assign RI values correctly. I describe examples of this systematic problem on pages 6 through 11 of **Exhibit C**.

In addition, there are other instances in which a talc particle exhibits a distorted dispersion staining color due to the total reflection occurring at the liquid-solid interface that a proficient PLM analyst who understands the basic principles of the central stop dispersion staining technique would recognize as a common phenomenon. Instead, MAS used the distorted dispersion staining color for RI assignments, leading to incorrect RI value, which, in turn, led to the misidentification of talc particles as "chrysotile." I describe examples of this problem on pages 12 through 14 of **Exhibit C**.

c. Dr. Longo's Claim That Particle Sizes Change Refractive Index Values Is Wrong

A mineral's RI is a constant governed by their chemical composition and crystal structure. MAS's theory that chrysotile's RI increases as the particle size decreases is unfounded and defies basic principles of physics. In fact, if such a theory is proved, it would shake the very foundation of physics.

The National Institute of Standards and Technology (NIST) Standard Reference Material (SRM) 1866 chrysotile RI values, α 1.549 and γ 1.556, were measured by John Phelps, a scientist at NIST, on a single fiber using the spindle stage technique. I know these details because John Phelps was in communication with me during the measurements that became the published SRM reference values. The spindle stage technique was invented by Professor Donald Bloss, my Ph.D. supervisor. I am an expert in this technique and author of the computer program used in the spindle stage measurement procedure. The "chrysotile" fibers that MAS claims to identify in Johnson's Baby Powder by PLM cannot be any thinner than the NIST SRM 1866 single chrysotile fiber that serves as the data point for the certified RI values for this material. MAS's claim that the particle sizes of "chrysotile" it finds in PLM analyses of Johnson's Baby Powder are so unique is not only unfounded but also without the support of credible measurement data that directly refutes the claim. I describe this problem on pages 15 and 16 of **Exhibit C**.

Another critical fact is that certified NVLAP RI values of "Calidria" chrysotile—a unique form of chrysotile from California that MAS claims is similar to the "chrysotile" it finds by PLM in Johnson's Baby Powder—are α 1.555 and γ 1.560, which are only 0.004 - 0.006 higher than the SRM 1866 chrysotile, documented by NVLAP in "ANALYSIS SUMMARY FOR NIST BULK ASBESTOS PROFICIENCY TESTING February 2001, Test Round M12001." Again, MAS's claim that the particle sizes and RI values of the "chrysotile" it found in PLM analyses of Johnson's Baby Powder are a match for Calidria chrysotile are inaccurate and not supported by the data. I describe this problem on page 17 of **Exhibit C**.

d. MAS's Complete Misunderstanding of My Central Stop Dispersion Staining Color Conversion Tables Leads to Incorrect and Unreliable "Chrysotile" Identification

I have created and published procedures and reference tables that help analysts measure RI values of the six regulated asbestos minerals, including chrysotile. MAS relies upon my procedure and tables as part of its PLM analyses of Johnson's Baby Powder.

However, Dr. Longo completely misunderstood my reference table and claimed that the RI range of my chrysotile table represents the chrysotile's minimum and maximum RI values. This is not true.

To illustrate, in the International Organization for Standardization (ISO) chart included in the 22262-1 method, the possible α and γ RI ranges of chrysotile are only a small section (between the dotted lines in the following figure) of the dispersion staining color chart; the chart must cover the whole dispersion staining color spectrum, and the same is true of my conversion table. The ranges of the ISO chart and my table must be much wider than the RI range of chrysotile.

My table is the numerical version of the ISO graphic chart for people who understand the principle. For people who do not understand this basic principle of my procedure and tables, it is impossible to correctly perform the analytical procedure of RI measurement by dispersion staining technique.

Chrysotile

in Cargille 1.560 (E)

λ_m	α							γ						
(nm)	17°C	19°C	21°C	23°C	25°C	27°C	29°C	17°C	19°C	21°C	23°C	25°C	27°C	29°C
300	1.652	1.651	1.650	1.649	1.648	1.647	1.646	1.645	1.644	1.643	1.642	1.641	1.641	1.640
320	1.632	1.631	1.630	1.629	1.628	1.628	1.627	1.627	1.626	1.625	1.624	1.623	1.622	1.621
340	1.618	1.617	1.616	1.615	1.614	1.613	1.613	1.614	1.613	1.612	1.611	1.610	1.609	1.608
360	1.607	1.606	1.606	1.605	1.604	1.603	1.602	1.604	1.603	1.602	1.601	1.600	1.599	1.599
380	1.599	1.598	1.597	1.596	1.595	1.595	1.594	1.596	1.595	1.595	1.594	1.593	1.592	1.591
400	1.593	1.592	1.591	1.590	1.589	1.588	1.587	1.590	1.589	1.588	1.588	1.587	1.586	1.585
420	1.587	1.586	1.585	1.584	1.583	1.583	1.582	1.585	1.584	1.583	1.583	1.582	1.581	1.580
440	1.583	1.582	1.581	1.580	1.579	1.578	1.577	1.581	1.580	1.579	1.578	1.577	1.577	1.576
460	1.579	1.578	1.577	1.576	1.575	1.574	1.573	1.578	1.577	1.576	1.575	1.574	1.573	1.572
480	1.576	1.575	1.574	1.573	1.572	1.571	1.570	1.575	1.574	1.573	1.572	1.571	1.570	1.569
500	1.573	1.572	1.571	1.570	1.569	1.568	1.567	1.572	1.571	1.570	1.569	1.568	1.567	1.567
520	1.570	1.569	1.568	1.567	1.567	1.566	1.565	1.570	1.569	1.568	1.567	1.566	1.565	1.564
540	1.568	1.567	1.566	1.565	1.564	1.563	1.563	1.568	1.567	1.566	1.565	1.564	1.563	1.562
560	1.566	1.565	1.564	1.563	1.562	1.562	1.561	1.566	1.565	1.564	1.563	1.562	1.561	1.560
580	1.564	1.563	1.563	1.562	1.561	1.560	1.559	1.564	1.563	1.562	1.562	1.561	1.560	1.559
600	1.563	1.562	1.561	1.560	1.559	1.558	1.557	1.563	1.562	1.561	1.560	1.559	1.558	1.557
620	1.561	1.560	1.560	1.559	1.558	1.557	1.556	1.562	1.561	1.560	1.559	1.558	1.557	1.556
640	1.560	1.559	1.558	1.557	1.556	1.556	1.555	1.560	1.559	1.559	1.558	1.557	1.556	1.555
660	1.559	1.558	1.557	1.556	1.555	1.554	1.553	1.559	1.558	1.557	1.557	1.556	1.555	1.554
680	1.558	1.557	1.556	1.555	1.554	1.553	1.552	1.558	1.557	1.556	1.556	1.555	1.554	1.553
700	1.557	1.556	1.555	1.554	1.553	1.552	1.551	1.557	1.556	1.556	1.555	1.554	1.553	1.552
720	1.556	1.555	1.554	1.553	1.552	1.551	1.550	1.557	1.556	1.555	1.554	1.553	1.552	1.551
740	1.555	1.554	1.553	1.552	1.551	1.551	1.550	1.556	1.555	1.554	1.553	1.552	1.551	1.550
760	1.554	1.553	1.552	1.552	1.551	1.550	1.549	1.555	1.554	1.553	1.552	1.551	1.550	1.550
780	1.554	1.553	1.552	1.551	1.550	1.549	1.548	1.554	1.553	1.553	1.552	1.551	1.550	1.549
800	1.553	1.552	1.551	1.550	1.549	1.548	1.547	1.554	1.553	1.552	1.551	1.550	1.549	1.548
850	1.551	1.550	1.550	1.549	1.548	1.547	1.546	1.552	1.551	1.550	1.550	1.549	1.548	1.547
900	1.550	1.549	1.548	1.547	1.546	1.546	1.545	1.551	1.550	1.549	1.548	1.547	1.547	1.546
950	1.549	1.548	1.547	1.546	1.545	1.544	1.543	1.550	1.549	1.548	1.547	1.546	1.546	1.545
1000	1.548	1.547	1.546	1.545	1.544	1.543	1.542	1.549	1.548	1.547	1.546	1.546	1.545	1.544

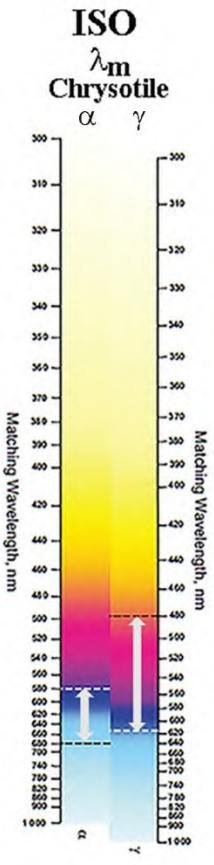

I describe this problem on pages 18 through 20 of **Exhibit C**.

e. Dr. Longo's Understanding of the Refractive Index Liquid's Effect on Mineral's Refractive Index Values Is Wrong

In 2022, I published a paper on the application of the dispersion staining technique to asbestos analysis. I recommended the use of 1.560 RI liquid for measuring the γ of Calidria chrysotile to improve the accuracy of measurement.

The only purpose of switching from 1.550 to 1.560 is to improve the accuracy of RI measurement because chrysotile's RI is a constant and does not change with the surrounding liquid medium.

When the same mineral is measured in two different RI liquids, its RI remains the same, but the matching wavelength λm changes accordingly: the lower liquid produces a shorter λm and the higher liquid produces a longer λm.

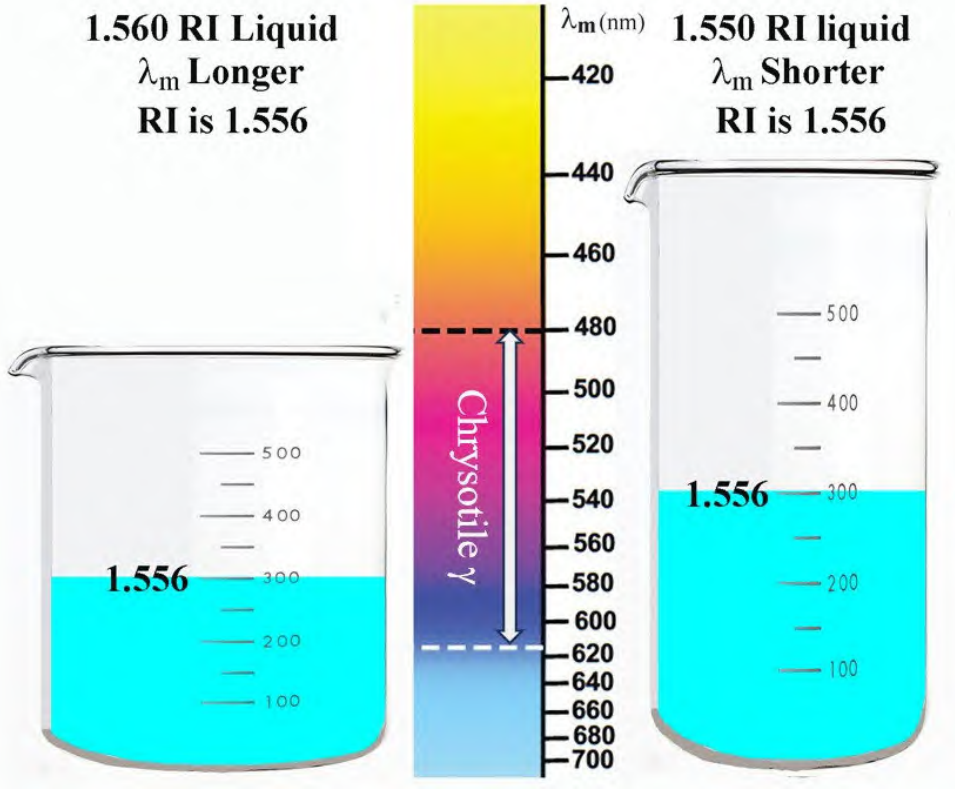

The above diagram shows two beakers; the left one is wider, representing 1.560 liquid, and the right one is thinner, representing 1.550 liquid. The volume of water represents the γ refractive index.

The 300 milliliters of water volume – γ value – does not change, but the water level – λ_m – changes from a shorter (upper) matching wavelength to a longer (lower) matching wavelength.

In 2022, Dr. Longo switched to 1.560 RI liquid. Without any background in optical crystallography, he mistakenly thought measuring in the 1.560 RI liquid would give his laboratory results different from those using 1.550 RI liquid. As noted below, MAS's use of the 1.560 RI liquid produced a suite of α and γ values similar to the 1.550 RI liquid values, none of which establish the

presence of chrysotile.

M71614-M71643-M71740 J&J Baby Powders

Date	MAS No.			γ		α	
				Low	High	Low	High
2023-02-28	M71614	001	1	1.564	1.564	1.561	1.561
			2	1.565	1.565	1.561	1.561
			3	1.568	1.568	1.557	1.560
			4	1.565	1.568	1.560	1.564
2023-10-19	M71643	001	1	1.566	1.566	1.561	1.561
			2	1.566	1.569	1.557	1.561
			3	1.561	1.561	1.552	1.552
			4	1.568	1.568	1.559	1.559
2024-02-15	M71740	001	1	1.564	1.564	1.560	1.560
			2	1.564	1.564	1.560	1.560
			3	1.565	1.565	1.562	1.562
			4	1.563	1.563	1.561	1.561
			Average	**1.565**	**1.565**	**1.559**	**1.560**
			Grand Average	**1.565**		**1.560**	

The above table summarizes 12 pairs of α and γ values from 2023 (M71614 and M71643) and 2024 (M71740) reports.

Three Types of Chrysotile

Type	α	γ	Birefringence	RI	Source
SRM 1866	1.549	1.556	0.007	Standard	NIST
Calidria	1.555	1.560	0.005	Significantly higher than 1866	NVLAP
New?	1.560*	1.565*	0.005	Significantly higher than Calidria	MAS

* Average of 12 samples in M71614, M71643, and M71740.

When I used the term "significantly higher" to describe Calidria chrysotile as compared to NIST SRM 1866 chrysotile, the RI values were in the area of .006 to .004 higher as described above. MAS's "chrysotile" is another "significantly higher" increase above Calidria chrysotile. Were those data credible (and they are not), MAS single-handedly discovered a new type of chrysotile, whose RI is significantly higher than the Calidria chrysotile as shown in the above table. Obviously, there has never been any report of the existence of such a unique type of chrysotile with such peculiar optical properties. MAS is simply wrong again.

I describe this problem on pages 21 and 22 of **Exhibit C**.

2. MAS's Procedure for Measuring Particle Sizes is Inaccurate and Unreliable

a. Scale Bars Are Completely Inaccurate

Mineral	Minimum (µm)	Average (µm)	Maximum (µm)	Reference
Talc	1.5	9.3	37.0	MAS (2017)
SG-210 Chrysotile	3.0	8.0	10.0	MAS (2023)

MAS reported the above talc particle size data from analyzing approximately 30 containers of Johnson & Johnson talcum powder products by SEM using image analysis software in 2017. The maximum particle size is 37 micrometers, which makes sense because the specification of Baby Powder is passing through a 325 mesh (44 micrometers) sieve.

Date	MAS No.	Chrysotile Length (µm)		
		Individual	Average	vs. Talc
2020-02-24 M70484	001-001	78.8	61.6	Same partcle size range as talc
	001-002	33.3		
	001-003	38.5		
	001-004	71.3		
	001-005	62.2		
	001-006	57.0		
	001-007	70.4		
	001-008	49.6		
	002-001	58.5		
	002-002	78.5		
	002-003	79.3		
2020-03-18 M71095	001-001	46.7	32.2	Same partcle size range as talc
	001-002	13.3		
	001-003	34.8		
	001-004	34.1		
2020-03-20 M70877	001-001	60.0	37.6	Same partcle size range as talc
	001-002	25.9		
	001-003	23.0		
	001-004	41.5		
2021-05-25 M71228	001-001	105.2	55.2	Same partcle size range as talc
	001-002	59.5		
	001-003	17.2		
	001-004	38.8		
2022-03-11 M71262	001-001	32.8	32.8	Same partcle size range as talc
	001-002	21.6		
	001-003	26.7		
	001-004	50.0		
2023-03-28 M71614	001-001	6.0	4.9	Same partcle size range as talc
	001-002	5.1		
	001-003	3.9		
	001-004	4.8		
2023-10-19 M71643	001-001	3.9	3.8	Same partcle size range as talc
	001-002	6.6		
	001-003	2.2		
	001-004	2.7		
2024-02-15 M71740	001-001	3.6	8.5	Same partcle size range as talc
	001-002	9.4		
	001-003	12.0		
	001-004	8.9		

The above table summarizes eight reports over the last five years. The dramatic variation of the "chrysotile" particle size, which is in the same size ranges as talc that can be seen in the PLM photomicrographs in each of the above reports, clearly indicates inaccurate scale bars, leading to inaccurate particle size measurements.

The creation of an accurate scale bar is a fundamental (and normally very easy) procedure of PLM. Over the years, MAS's systematic failure to create accurate scale bars for their analyses of Johnson's Baby Powder by PLM can only be attributed to the lack of basic expertise of MAS's analysts.

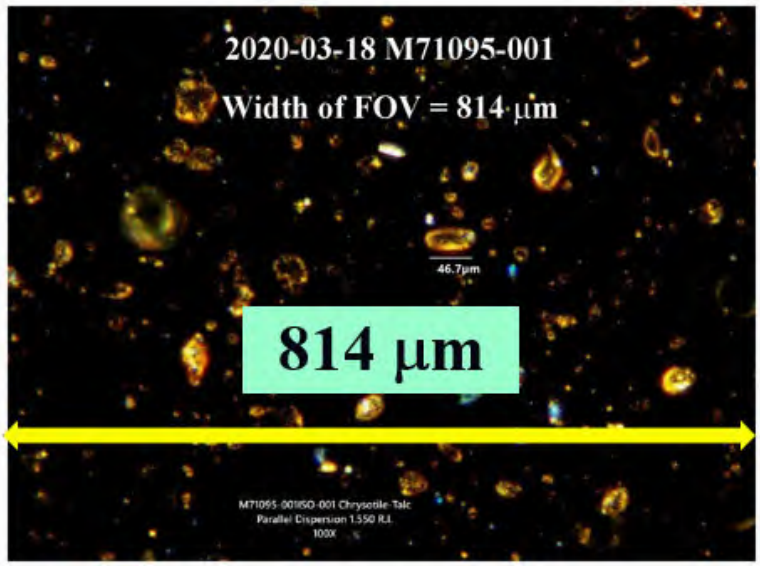

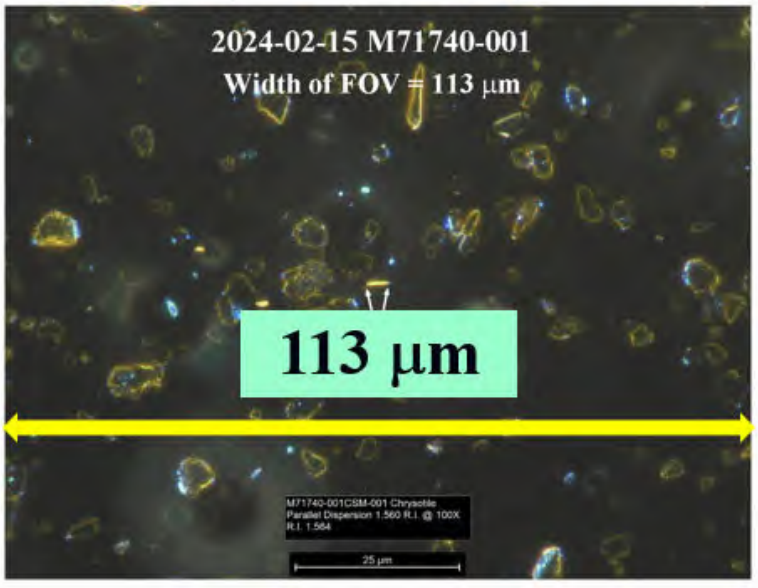

The width of the field of view (FOV) can be calculated from the scale bar length or the width of an object in the image. In the March 18, 2020 report M71095, the 814 µm field of view (FOV) width was wrong. Five years later, the mistake remained uncorrected. The February 15, 2024 report M71228 still reported a grossly wrong FOV width of 113 µm. Regardless of the microscope's make, Olympus

Nikon Leitz or Leica, the FOV width for a 10X objective lens is slightly over 1 mm or 1,000 µm.

What is important is that the particle sizes in these two micrographs with drastically different FOV widths are the same. That is because they are taken at the same magnification but the scales reported by MAS are wrong.

The only conclusion is that MAS is not capable of correctly performing PLM's most fundamental operation procedure: measuring the sizes of particles that it is analyzing. On occasion, the particle sizes are incorrect by ten times or more.

I describe this problem on pages 23 through 25 of **Exhibit C**.

b. If Chrysotile Was Truly Present In Johnson's Baby Powder, Its Particle Sizes Would Not Match Talc, as MAS Claims

Although MAS fails to correctly measure particle size by PLM, the micrographs in every Johnson's Baby Powder analytical report document the undeniable fact that the particle size of the claimed "chrysotile" matches the particle size of the surrounding talc. If that were true, it means the chrysotile's particle size was reduced to the particle size range of talc particles during the milling process of Johnson's Baby Powder production.

Chrysotile is a mineral with a very high tensile strength, around 100,000 pounds per square inch. It is so strong that it used to be woven into fabrics for making heat protection gears used in steel mills. It is also a super anti-abrasion additive used to make automobile braking shoes.

On the other hand, talc is the softest mineral on Earth. It is easily breakable.

The two minerals have drastically different grinding behaviors. When ground together, talc is easily and quickly ground into fine powders, whereas chrysotile is reduced to a particle size of hundreds of micrometers, significantly larger than talc. This differential grinding effect has been confirmed by US Pharmacopeia (2022) and Pier (2017).

Therefore, the "chrysotile" particles within the particle size range of talc powders cannot be chrysotile. They are talc.

I describe this problem on pages 26 through 52 of **Exhibit C**.

3. MAS's Procedure for Reporting Amounts of "Chrysotile" Identified in Johnson's Baby Powder is Inaccurate and Unreliable

a. Visually Estimated Percentages Are Inherently Unreliable

EPA bulk asbestos analysis procedure requires a point counting procedure for the asbestos quantification. The visual estimate procedure cannot quantify asbestos concentration at 0.00x% level, let alone 0.000x% level. NVLAP requires calibrated visual estimates (CVEs) for quantifying asbestos by PLM at the 1% level. Even at the 1% level, CVEs are difficult and require visual reference charts of the type that I have published. Yet MAS claims that it is capable of performing visual estimates of "chrysotile" concentrations beyond one ten thousandth of a percent without so much as a visual

reference chart against which to compare. There is no scientific justification for this claim and certainly no methodology or validation establishing the accuracy of these visual estimates by MAS.

I describe this problem on pages 53 through 64 of **Exhibit C**.

b. Fiber Per Gram Figures Based on Inappropriate Extrapolation from Unpublished Method with No Calculated Rate of Error

Dr. Longo's unpublished "concentration" preparation technique leads to highly variable and inappropriate extrapolated quantitative results. As an example, in the February 28, 2023 Valadez Report, a sample size of 0.000017 grams was used to extrapolate to 1 gram of Baby Powder—58,824 times extrapolation. Given the 0.0003 to 0.0006% chrysotile concentration claimed, a lenient 0.5% maximum allowed error, and a sample size of 0.000017 grams, the calculated Confidence Level is less than 50%, making the False Positive error rate greater than 50%. Such an irresponsible and unheard-of False Positive error rate is totally unacceptable as part of an analytical methodology. A responsible laboratory will never adopt such a sampling scheme to make the False Positive error rate greater than 50%. And such a methodology could never pass scrutiny to become an accepted method by any standards setting organization.

I describe this problem on pages 65 through 75 of **Exhibit C**.

4. MAS's Liquid Density Sample Preparation Procedures for "Chrysotile" are Inaccurate and Unreliable

2020 - 2024 HLS Resaults

Date	MAS No.			Light Fraction %
2020-09-17	M71666	001	1	17.0
			2	14.6
			3	13.4
2021-05-25	M71216	001	1	24.2
			2	21.4
			3	21.3
2023-02-28	M71614	001	1	15.9
2023-10-19	M71643	001	1	19.7
2024-02-15	M71740	001	1	25.7

While I have reviewed all of the reports included in **Exhibit B**, the above table includes the weight recovery fractions reported by MAS in a handful of Johnson's Baby Powder products over a five-year span. This small group of samples is illustrative of the high degree of variation in the sample preparation procedure as well as the inability of MAS's sample preparation procedure to effectively concentrate the "chrysotile" that it claims to find in Johnson's Baby Powder.

As shown in the table above, from 2020 to 2024 over a five year span using various different sample preparation techniques as described in MAS's reports, the heavy liquid separation sample preparation procedure produced a series of extremely inconsistent light fractions ranging from 13.4% to 24.2% in talcum powder products, which further produced "chrysotile" concentrations ranging from 0.003% to 0.01%. For Baby Powder samples consisting of 99.9% talcum powder, which should be in the heavy fraction, how possible is the light fraction more than 1%? It is beyond comprehension that

those ridiculous two-digit light fraction results did not make MAS realize something was grossly wrong with each and every sample preparation procedure that it tried over the course of five years.

The extremely high degree of volatility in weight recovery is not only a result of the deficiency in MAS's sample preparation procedure but also a clear indication of the non-existence of chrysotile. There is no chrysotile to concentrate regardless of the heavy liquid density separation process used.

I describe this problem on pages 76 and 77 of **Exhibit C.**

Conclusion

For the reasons stated above, I disagree with each and every single identification of "chrysotile" in Johnson's Baby Powder made by Dr. Longo's laboratory in the reports that I have reviewed. The data presented by MAS demonstrate systematic and chronic deficiencies in almost every aspect of operation, from the equipment setup and calibration to the sampling procedure, the sample preparation processes, the execution of the analytical procedure, and reporting quantification procedure, which leads me to conclude that the laboratory is incapable of performing the most basic aspects of PLM analytical procedure let alone correctly identifying chrysotile by PLM.

The following is a summary of MAS's systematic and chronic deficiencies:

- Inability to ensure a 95% Confidence Level of quantification.
- Inability to correctly interpret dispersion staining colors.
- Inability to calibrate dispersion staining colors.
- Inability to understand the relationship between the material's refractive index and the refractive index of liquids used for measurement.
- Inability to conduct calibrated visual estimate (CVE).
- Inability to check the internal consistency of analytical data.
- Inability to correctly measure particle size under a polarized light microscope.
- Inability to correctly create scale bars.
- Inability to understand the fundamental physics principles governing the relationship between a material's refractive index and physical dimension.
- Inability to understand the fundamental geological principles governing the formation of minerals and mineral ore deposits.

I hold all of the opinions that I expressed in this report and **Exhibit C** to a reasonable degree of scientific certainty.

By:_____
Dr. Shu-Chun Su

Date: May 21, 2024

Exhibit A – Biography

National Voluntary Laboratory Accreditation Program
National Institute of Standards and Technology
Department of Commerce
USA

Dr. Shu-Chun Su

Shu-Chun Su became an NVLAP Technical Expert for the Bulk and Airborne Asbestos Programs in 1988. Since then, he has conducted close to a thousand NVLAP on-site assessments of bulk and airborne asbestos laboratories in the USA, Canada, Japan, and Korea.

Skills and Expertise

Dr. Su is an accomplished expert in general and optical mineralogy, petrography, igneous and metamorphic petrology, geochemistry, crystal chemistry, powder and single crystal X-ray crystallography, digital image analysis, and various microscopy techniques, including polarized light microscopy, scanning electron microscopy, transmission electron microscopy, infra-red micro-spectroscopy, Raman micro-spectroscopy, confocal laser scanning microscopy, etc. Dr. Su's analytical approach to derive refractive indices at various wavelengths from dispersion staining data was recognized to be "Su's Method" by Professors R. E. Stoiber and S. A. Morse at Massachusetts University, Amherst, in "Crystal Identification with the Polarizing Microscope," Springer, 358pp, 1994. By applying this method to bulk asbestos analysis, he has developed a standardized procedure for rapidly and accurately determining refractive indices of asbestos fibers using the dispersion staining technique. The procedure has been used by more than 95% of asbestos laboratories in the USA, Canada, Japan, and Korea since 1994 and was formally published in 2003.

In the area of airborne asbestos analysis, Dr. Su has developed a computer program as well as detailed d-spacing and interfacial angle tables for the six regulated asbestos minerals plus winchite, richterite, and talc to assist the indexing and interpretation of zone-axis SAED (selected area electron diffraction) patterns. It's been widely used by airborne asbestos laboratories around the world.

Education, Work History, and Relevant Work Experience

Dr. Su obtained a B.S. in Geochemistry from Peking University, China, in 1964 and worked in the Central Laboratory, Geological Survey of Gansu Province for 17 years. After earning an M.S. in Mineralogy at the Institute of Geology and Geophysics, Chinese Academy of Sciences in 1981, Dr. Su came to the U.S. to pursue graduate study in crystal chemistry, optical crystallography, and silicate mineralogy with Professors F. Donald Bloss and Paul H. Ribbe at Virginia Polytechnic Institute and State University. After completing his Ph.D. in Geology/Mineralogy in 1985, he did post-doctoral research to develop an automated refractometer and joined Hercules Incorporated in 1987. Before his retirement in 2006, he was a Senior Research Scientist and Director of the Light and Electron Microscopy Laboratory at Hercules Research Center, Wilmington, Delaware. He is a Fellow of the Mineralogical Society of America.

Rev. 2024-02-22

29 Publications Relevant To Asbestos Analysis

2024 Su, S.C. The Unification of Becke Line and Dispersion Staining Techniques For the Determination of Refractive Index of Non-Opaque Materials. The Microscope. 70:3, 99–112. https://doi.org/10.59082/XCLR4173

2023 Su, S.C. The Calibration of Dispersion Staining Colors. The Microscope, 70:1, 3-21. https://doi.org/10.59082/HNQR9171

2022 Su, S.C. The Dispersion Staining Technique and Its Application to Measuring Refractive Indices of Non-opaque Materials, with Emphasis on Asbestos Analysis, The Microscope, 69:2, pp 51–69; https://doi.org/10.59082/ZGWM6676.

2022 Su, S.C. Area Percentage Charts to Aid Visual Estimation of Asbestos Concentration in Bulk Asbestos Samples. The Microscope, 69:4, 160-162. https://doi.org/10.59082/RPCG4507

2021 Su, S.C. Indexing and Interpretation of Zone-Axis SAED Patterns of Amphibole Asbestos Minerals in the Asbestos Analysis by Transmission Electron Microscopy. in Asbestos and Other Elongate Mineral Particles—New and Continuing Challenges in the 21st Century, ed. J. R. Millette and J. S. Webber (West Conshohocken, PA: ASTM International, 2021), 471–499. https://doi.org/10.1520/STP163220200071

2020 Su, S.C. A Comprehensive Suite of d-0 Look-Up Tables for Indexing Zone-Axis SAED Patterns of Amphibole Asbestos and Related Minerals. The Microscope, 68:3/4, 99-110, Appendix: Comprehensive Lattice Plane Spacing d and Interplanar Angle Tables of Asbestos and Talc Minerals. 888 pages

2014 Su, S.C. Can AHERA Bulk Asbestos Method Statistically Differentiate ACM from Non-ACM? Johnson Conference, July 21- 23, 2014. Burlington, Vermont.

2012 Su, S.C. Fundamental Flaws of AHERA Test Method for Determining Asbestos Concentration of Bulk Insulation Samples. Proceedings of Geological Society of America, Annual Meeting, November 4 - 7, 2012. Charlotte, North Carolina.

2005 Su, S.C. Analytical Sensitivity of Bulk Asbestos Analysis. Proceedings of 2005 ASTM Johnson Conference. July 18 - 22, 2005. Burlington, Vermont.

2005 Su, S.C. Dispersion Staining – A Versatile Complement to Becke Line Method for Refractive Index Determination. Special Supplement to Geochimica et Cosmochimica Acta, A727.

2004 Gunter, M.E., Weaver, R., Bandli, B.R., Bloss, F.D., Evans, S.H., and Su, S.C., Results from a McCrone spindle stage short course, a new version of EXCALIBR, and how to build a spindle stage. The Microscope, 52, 23-39.

2003 Su, S.C., A rapid and accurate procedure for the determination of refractive indices of asbestos minerals. American Mineralogist, 88, 1979-1982.

2001 Su, S.C., Applications of Dispersion Staining Technique in Image Analysis of Colorless Particles. Rieder, C. L., Ed., Proceedings of 59th Annual Meeting of the Microscopy Society of America, 817-818.

1993 Su, S.C., Determination of the refractive index of solids by dispersion staining method - An analytical approach. Rieder, C. L., Ed., Proceedings of 51st Annual Meeting of the Microscopy Society of America, 456-457.

1992 Su, S.C., Calibration of refractive index liquids using optical glass standards with dispersion staining technique. The Microscope, 40, 95-108.

1989 Gunter, M.E., Bloss, F.D., and Su, S.C., Computer programs for the spindle stage and double-variation method. The Microscope, 37, 167-171.

1988 Gunter, M.E., Bloss, F.D., and Su, S.C., EXCALIBR revisited. American Mineralogist, 73, 1481-1482.

1987 Peacor, D.R., Dunn, P.J., Su, S.C., and Innes, J., Ribbeite, a unit-cell twinned polymorph of alleghanyite and member of the leucophoenicite group from Kombat Mine, Namibia. American Mineralogist, 72, 213-216.

1987 Solie, D.N. and Su, S.C., An occurrence of barium-rich mica from Alaska Range. American Mineralogist, 72, 995-999.

1987 Dunn, P.J., Peacor, D.R., Ramik, R.A., Su, S.C., and Rouse, R.C., Franklinfurnaceite, a Ca-Mn-Fe3+-Zn layer silicate related to chlorite, from Franklin, New Jersey. American Mineralogist, 72, 812-815.

1987 Su, S.C., Bloss, F.D. and Gunter, M.E., Procedures and computer programs to refine the double variation method. American Mineralogist, 72, 1011-1013.

1987 Dunn, P.J., Peacor, D.R., Su, S.C., Wicks, F.J. and Parker, F.J., Parabrandite, the manganese analogue of talmessite, from Sterling Hill, Ogdensburg, New Jersey. Neues Jahrbuch fur Mineralogie, Abhandlungen, 157, 113-119.

1986 Su, S.C., Ribbe, P.H., and Bloss, F.D., and Warner, J.K., Optical properties of the high albite (analbite)-high sanidine solid solution series. American Mineralogist, 71, 1393-1398.

1986 Su, S.C., Ribbe, P.H., Bloss, F.D., and Goldsmith, J.R., Optical properties of single crystals in the order-disorder series low-high albite. American Mineralogist, 71, 1393-1398.

1986 Su, S.C., Ribbe, P.H., and Bloss, F.D., Alkali feldspars: Structural states determined from composition and optic axial angle 2V. American Mineralogist, 71, 1285-1296.

1986 Dunn, P.J., Peacor, D.R., Su, S.C., Nelen, J.A., and Knorring, O. von, Johninnesite, a new sodium manganese arsenosilicate from the Kombat Mine, Namibia. Mineralogical Magazine, 50, 667-670.

1984 Su, S.C., Bloss, F.D., Extinction angles for amphiboles or pyroxenes: A cautionary note. American Mineralogist, 69, 399-403.

1984 Su, S.C., Bloss, F.D., Ribbe, P.H., and Stewart, D.B., Optic axial angle, a precise measure of Al,Si ordering in T1 tetrahedral sites of K-rich feldspars. American Mineralogist, 71, 1384-1392.

1983 Bloss, F.D., Gunter, M., Su, S.C., and Wolfe, E.H., Gladstone-Dale constant: A new approach. Canadian Mineralogist, 21, 93-99.

2 Book Reviews Relevant to Asbestos Analysis

1989 Su, S.C., Introduction to Optical Mineralogy, by William D. Nesse, Oxford University Press, New York, 1986, 325p. American Mineralogist, 74, 506.

1986 Su, S.C., Optical Mineralogy, Second Edition, by David Shelley, Elsevier Science Publishing Co., Inc., New York, 1985, 321 p. American Mineralogist, 71, 1060.

28 Presentations Relevant to Asbestos Analysis

2017 Su, S.C., Instructor, Short Course on Optical Crystallography and The Spindle Stage. University of Idaho (January 30 – February 3, Moscow, Idaho)

2003 Su, S.C., Instructor, Short Course on Optical Crystallography and The Spindle Stage. INTER/MICRO-03 (July 11-13, Chicago, Illinois)

1999 Su, S.C., Instructor, Short Course on The Spindle Stage. INTER/MICRO-99 (July 2-3, Chicago, Illinois)

1998 Su, S.C., Estimating the Refractive Index Difference between a Solid Particle and an Immersion Liquid. INTER/MICRO-98 (August 10-14, Chicago, Illinois)

1997 Su, S.C., Improve the Proficiency in Asbestos Identification by Polarized Light Microscopy. The 15th Annual Conference of the Environmental Information Association (former National Asbestos Council), March 22 - 25, Las Vegas, Nevada.

1996 Su, S.C., Understanding Detection Limit and Analytical Sensitivity in TEM Airborne Asbestos Analysis. NVLAP Annual Regional Meetings (East Region: October 4, Philadelphia, PA; Central Region: October 25, Minneapolis, MN; West Region: November 1, San Francisco, CA)

1996 Su, S.C., Back to Basics for Bulk Asbestos Analysis. NVLAP Annual Regional Meetings (East Region: October 4, Philadelphia, PA; Central Region: October 25, Minneapolis, MN; West Region: November 1, San Francisco, CA)

1995 Su, S.C., Improving Accuracy in Refractive Index Measurement in Bulk Asbestos Analysis. NVLAP Annual Regional Meetings (East Region: September 15, Cincinnati, OH; Central Region: October 6, Houston, TX; West Region: October 27, Los Angeles, CA).

1995 Su, S.C., Identifying Tremolite, Actinolite, and Anthophyllite in Bulk Asbestos Samples. NVLAP Annual Regional Meetings (East Region: September 15, Cincinnati, OH; Central Region: October 6, Houston, TX; West Region: October 27, Los Angeles, CA).

1995 Su, S.C., Cooke, P.M., Perkins, R.L., and Harvey, B., Analysis of Bulk Materials for Asbestos: The Problems and Solutions. Professional Development Seminars, Environmental Management '95, the 12th Annual Conference of the Environmental Information Association (former National Asbestos Council), April 22-26, Tempa, Florida.

1994 Su, S.C., Measuring/recording refractive indices of asbestos fibers in NVLAP accredited environmental laboratories. NVLAP Annual Regional Meetings (West Region: June 29, Seattle, WA; Central Region: July 22, Chicago, IL; East Region: August 24, Gaithersburg, MD).

1994 Su, S.C., Determination of refractive indices of Asbestos Minerals. INTER/MICRO-94 (July 18-21, Chicago, Illinois).

1993 Su, S.C., Determination of the refractive index of solids by dispersion staining method - An analytical approach. 51st Annual Meeting of the Microscopy Society of America (July 31 - August 4, Cincinnati, Ohio).

1990 Su, S.C., A computer program for rapidly and accurately orienting single crystals by X-ray precession method. Symposium in Honor of Professor F. Donald Bloss (July 22-25, Blacksburg, Virginia).

1989 Su, S.C., Application of Spindle Stage to determining the birefringence of Synthetic fibers. The 28th Annual Meeting of Eastern Analytical Symposium (September 24-29, New York City, New York).

1989 Instructor, Short Course on Spindle Stage and Computer Methods. August 14-18. Offered jointly by McCone Research Institute and Virginia Polytechnic Institute and State University, Blacksburg, Virginia.

1989 Instructor, Short Course on Immersion Methods and Crystal Optics. August 7 - 11. Offered jointly by McCrone Research Institute and Virginia Polytechnic Institute and State University, Blacksburg, Virginia.

1986 Instructor, Short Course on Optical Identification of Crystals and Minerals. Virginia Polytechnic Institute and State University, Blacksburg, Virginia.

1986 Instructor, Short Course on Spindle Stage and Computer Methods. Virginia Polytechnic Institute and State University, Blacksburg, Virginia.

1986 Su, S.C., Ribbe, P.H., and Bloss, F.D., Optical, X-ray and microprobe study of low plagioclase single crystals: Discriminant analysis of discontinuities. The 14th General Meeting, the International Mineralogical Association (July 13-18, Stanford, California), Abstract with Programs, p.267.

1986 Su, S.C., Ribbe, P.H., and Bloss, F.D., Optical properties of alkali feldspars. Invited paper for the Symposium on Optical Properties of Minerals. The 14th General Meeting, the International Mineralogical Association (July 13-18, Stanford, California), Abstract with Programs, p.240.

1986 Su, S.C., Ribbe, P.H. and Bloss, F.D., Alkali feldspars: structural state determined from composition and optical angle 2V. The 99th Annual Meeting of Geological Society of America, Abstracts with Programs, 18, 766.

1985 Instructor, Short Course on Optical Identification of Crystals and Minerals. Virginia

Polytechnic Institute and State University, Blacksburg, Virginia.

1985 Instructor, Short Course on Spindle Stage and Computer Methods. Virginia Polytechnic Institute and State University, Blacksburg, Virginia.

1985 Su, S.C., Ribbe, P.H., and Bloss, F.D., Structural states and properties of a low-high albite series of single crystal. The 98th Annual Meeting of the Geological Society of America, Abstract with Programs, 17, 729.

1984 Warner, J.K., Su, S.C., Ribbe, P.H., and Bloss, F.D., Optical properties of the analbite-high sanidine solid solution series. The 97th Annual Meeting of Geological Society of America, Abstract with Programs, 16, 687.

1983 Su, S.C., Bloss, F.D., Ribbe, P.H., and Stewart, D.B., Optical axial angle, a precise measure of Al, Si content of the T1 tetrahedral sites in K-rich alkali feldspars. The 96th Annual Meeting of Geological Society of America Abstracts with Programs, 15, 701.

1983 Su, S.C., Bloss, F.D., Ribbe, P.H., and Stewart, D.B., Rapid and precise optical determination of Al, Si ordering in potassic feldspars. The 3rd NATO Advanced Study Institute on Feldspars, Feldspathoids and Their Paragenesis, June 26-July 6, Rennes, France.

Exhibit B – List of MAS Reports Reviewed in Which MAS Identifies "Chrysotile" by PLM in Johnson's Baby Powder Products

Date	MAS Project Number(s)
2/24/2020	M70484
3/6/2020	M66515 & M66516
3/18/2020	M71095
3/20/2020	M70877
4/6/2020	M71046
5/14/2020	M71095 Rev 1
9/16/2020	M71109-M71111
9/17/2020	M71166
9/23/2020	M71095 Rev 2
9/29/2020	M71166 Sup 1
12/8/2020	M71166 Sup 2
1/25/2021	M71211
2/9/2021	M71241
3/23/2021	M65329-013; M66507-001; M66508-001; M66509-001; M66513-001; M67420-001; M67420-002; M67420-004; M67420-005
4/13/2021	M71216
5/25/2021	M71228
6/4/2021	M70859
8/20/2021	M70877
3/11/2022	M71262
2/28/2023	M71614
10/19/2023	M71643
11/28/2023	M71730
2/15/2024	M71740

Exhibit C – Demonstrative Materials

IN RE JOHNSON & JOHNSON TALCUM POWDER PRODUCTS MARKETING, SALES PRACTICES, AND PRODUCTS LIABILITY LITIGATION

MDL NO. 16-2738 (FLW) (LHG)

MDL Report

Shu-Chun Su, Ph.D.

May 21, 2024

Dr. Shu-Chun Su's Analysis of MAS's Analytical Results

Incorrect RI Measurement Procedure: Suppressed Light Intensity

Incorrect RI Measurement Procedure

MAS Misidentified Talc as Chrysotile

2023-02-28 - Valadez Bottle Report

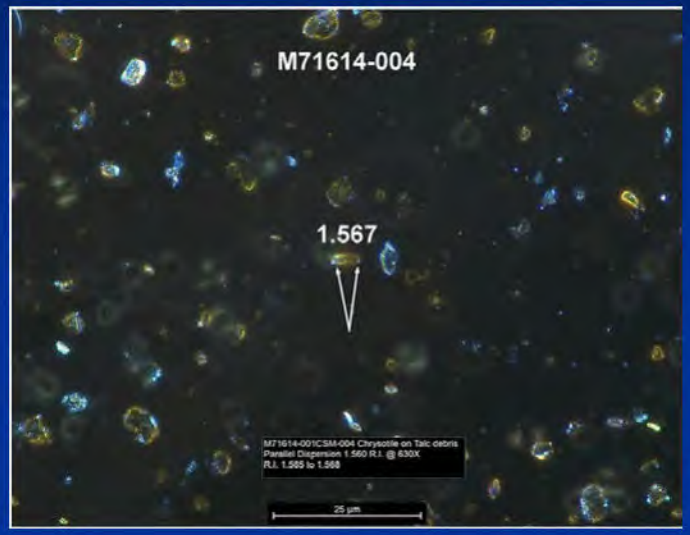

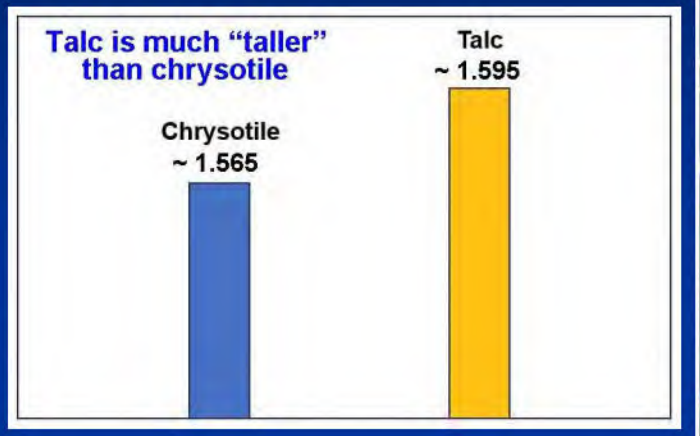

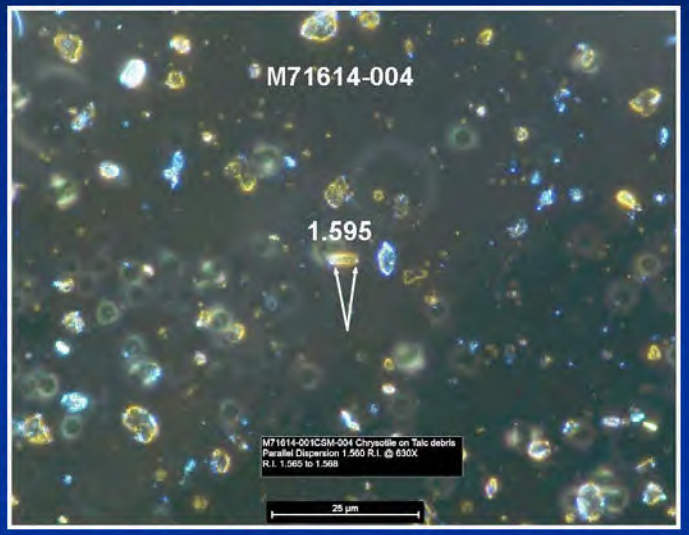

Suppressed

Unsuppressed

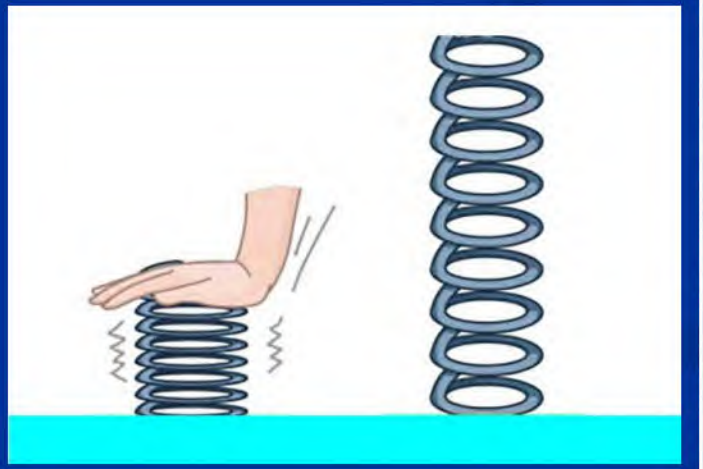

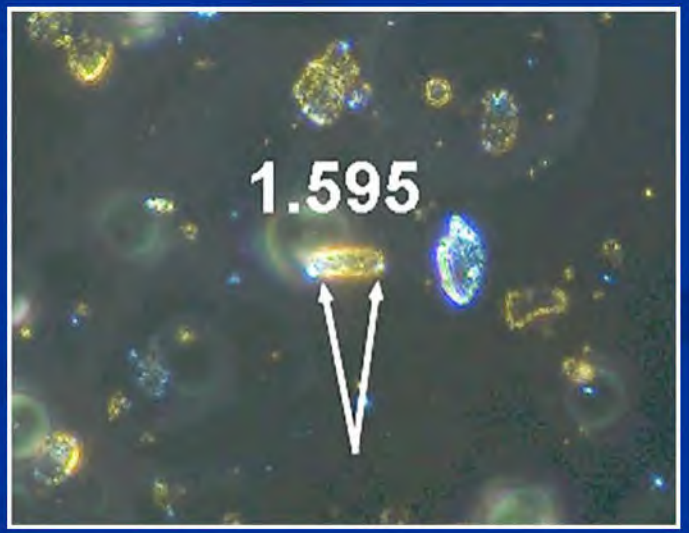

Another Example of MAS's Suppressed Illumination

2021-06-04 M70859 JPB-UK

Original illumination was suppressed

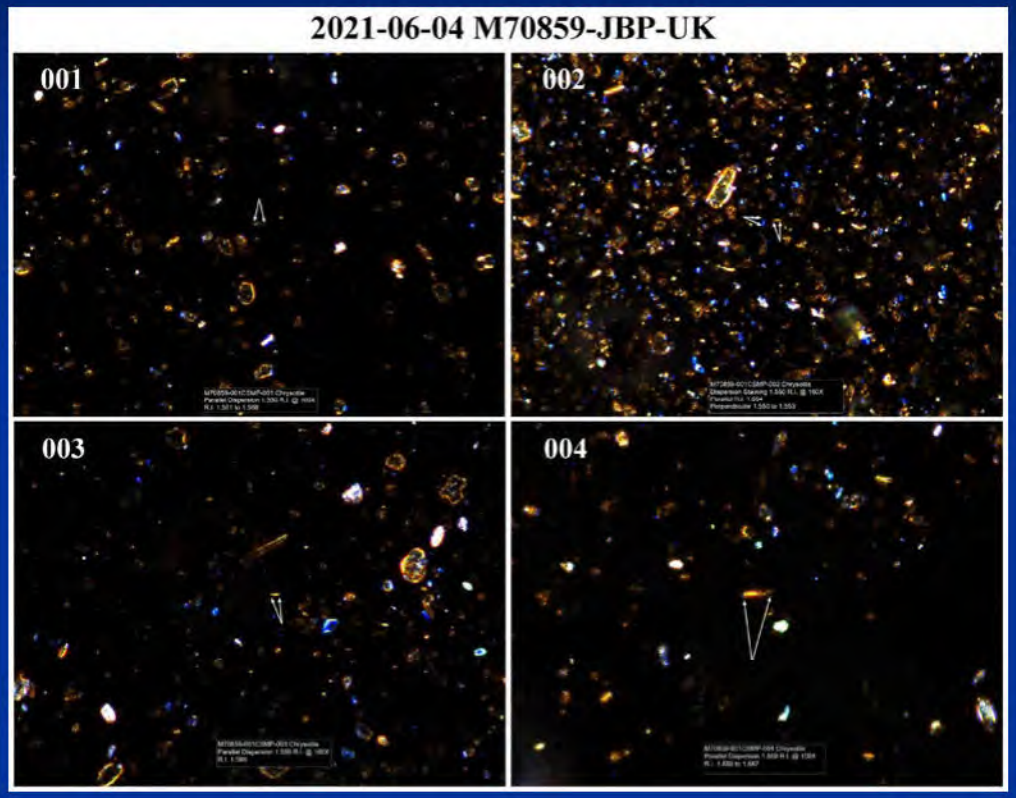

Illumination unsuppressed

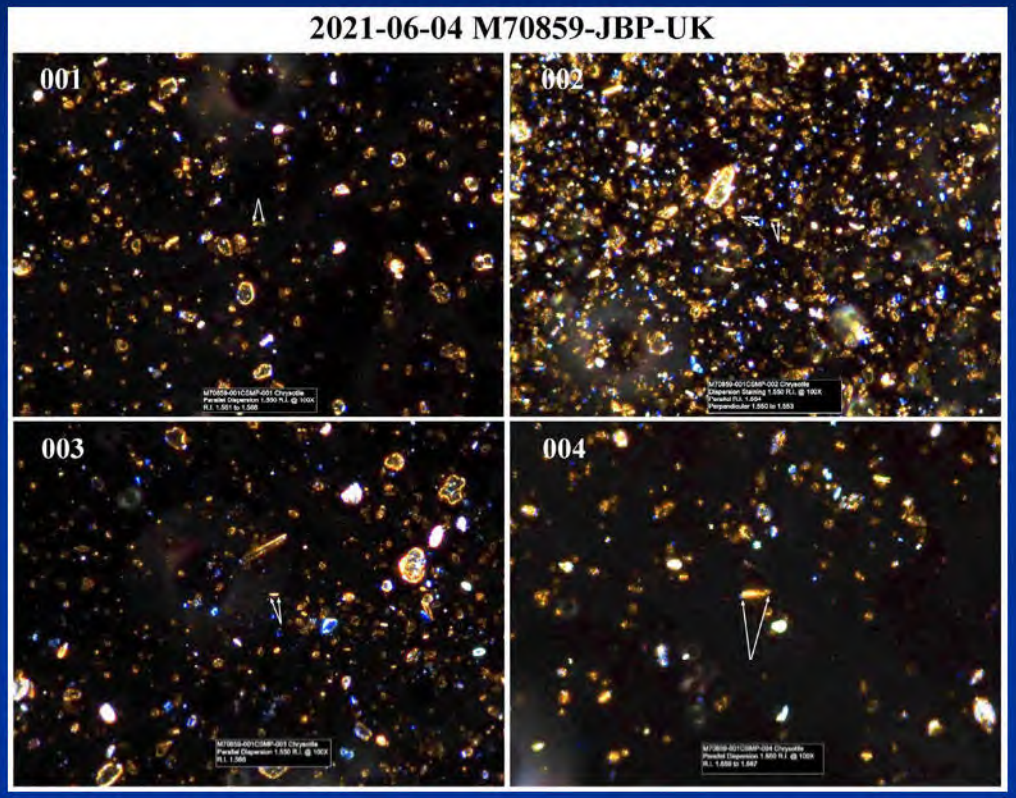

Correct analysis can only be conducted when the illumination is unsuppressed.

One More Example of MAS's Suppressed Illumination

2022-03-11 M71612 Klayman JPB & STS

Original illumination was suppressed

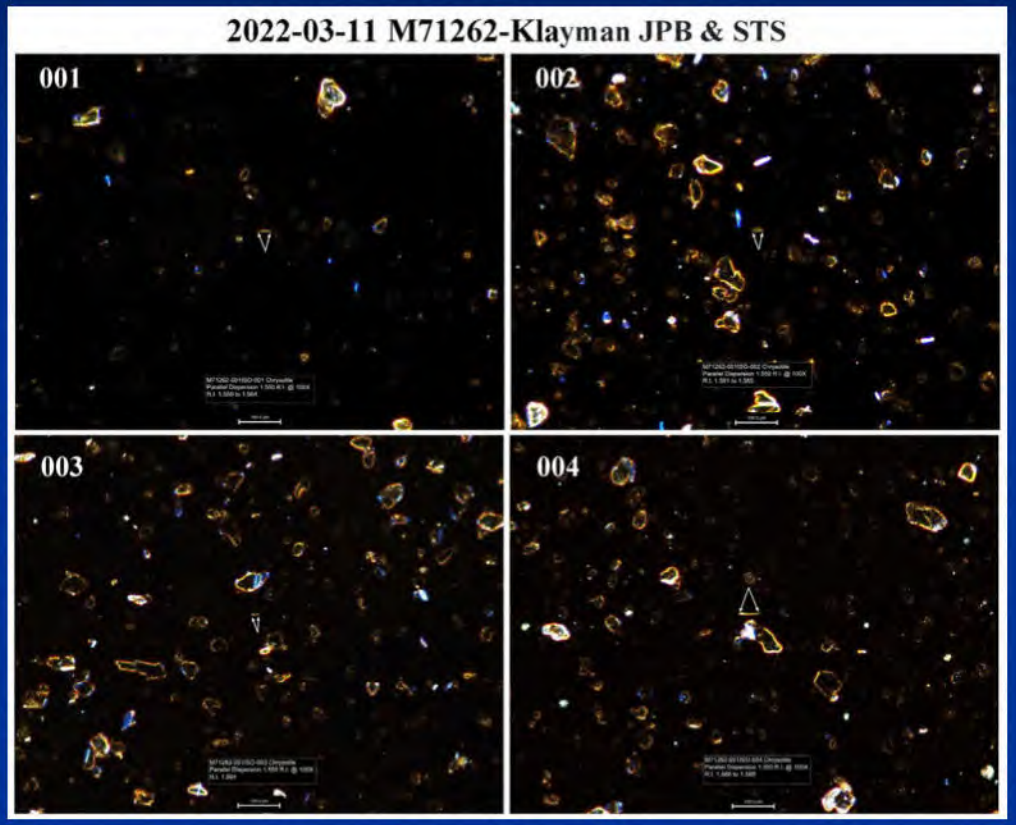

Illumination unsuppressed

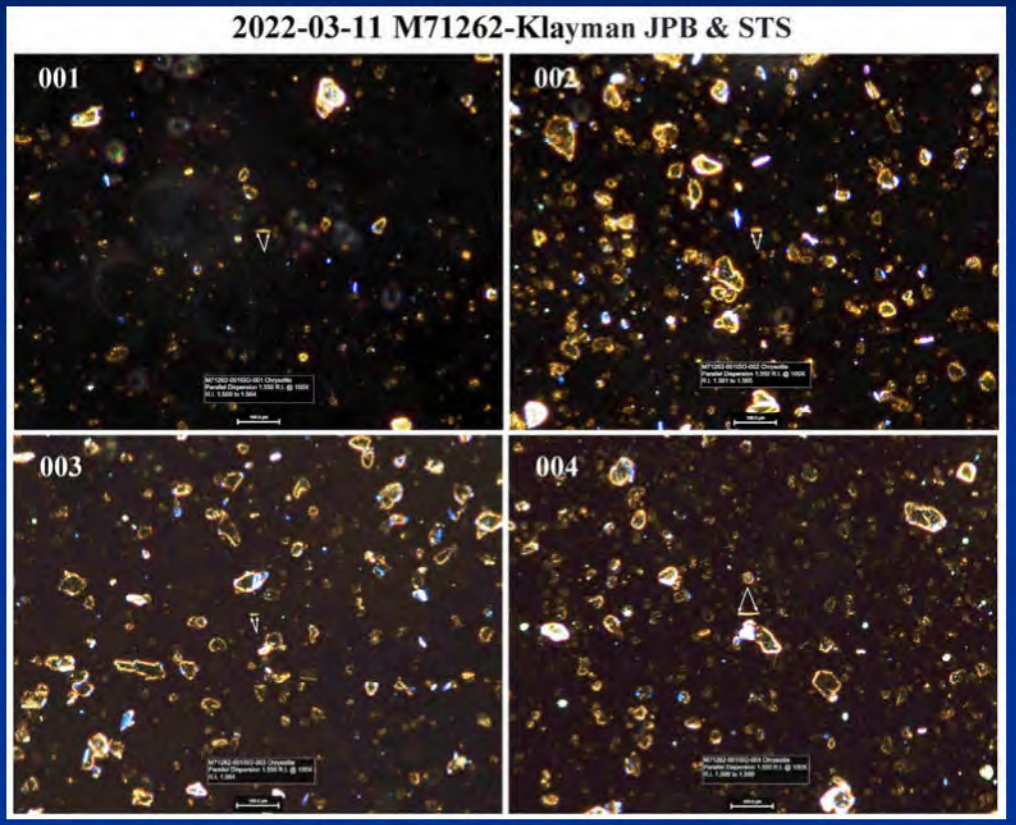

Correct analysis can only be conducted when the illumination is unsuppressed.

Dr. Shu-Chun Su's Analysis of MAS's Analytical Results

Incorrect RI Measurement Procedure:
Inaccurate RI Values

Incorrect RI Measurement Procedure

2023-02-28 - Valadez Bottle Report

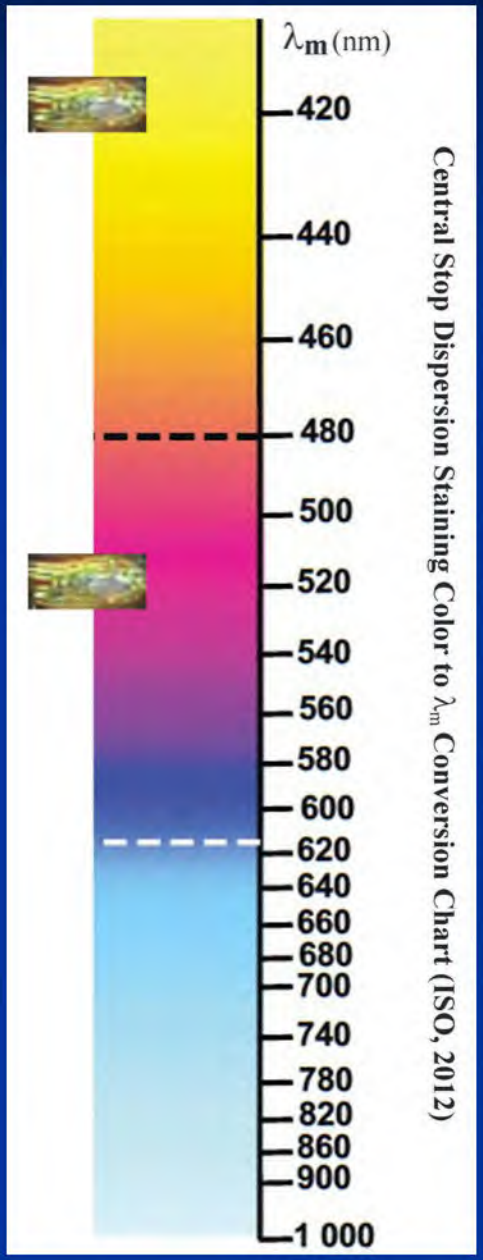

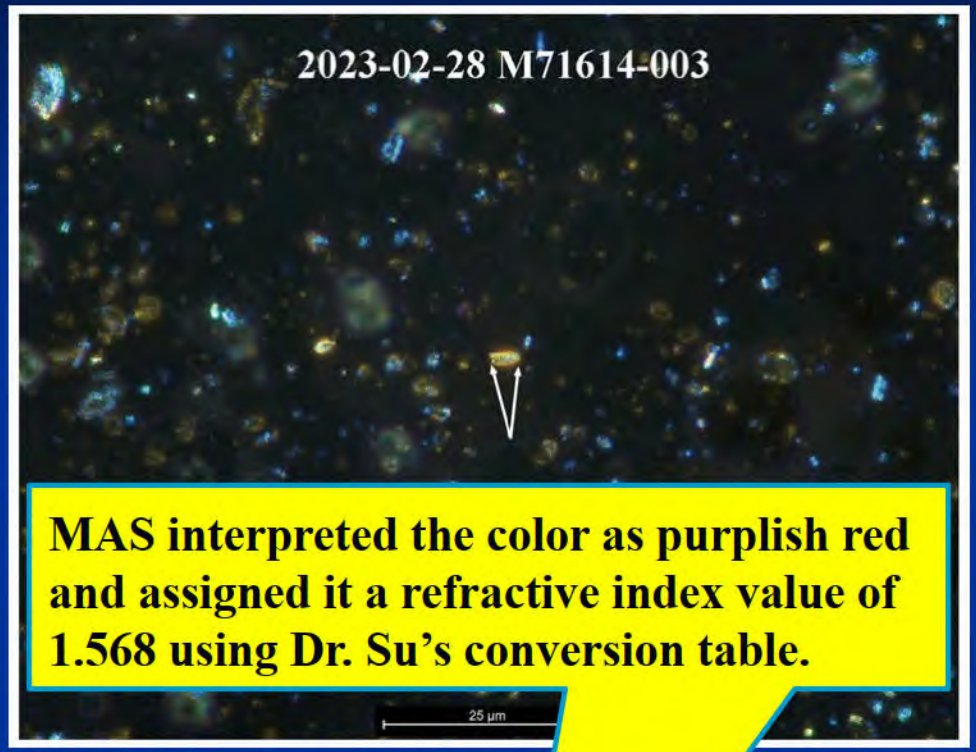

MAS interpreted the color as purplish red and assigned it a refractive index value of 1.568 using Dr. Su's conversion table.

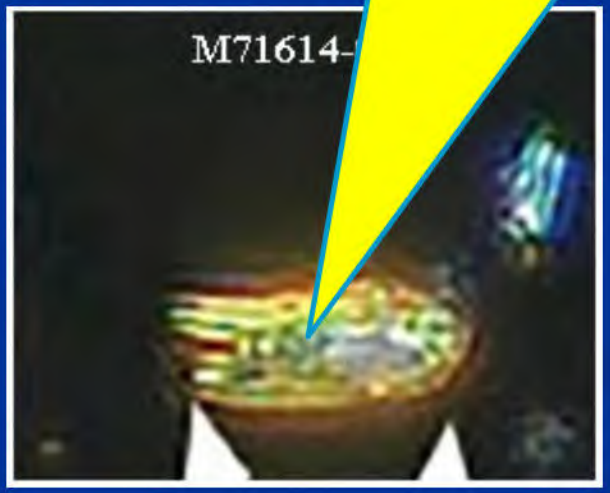

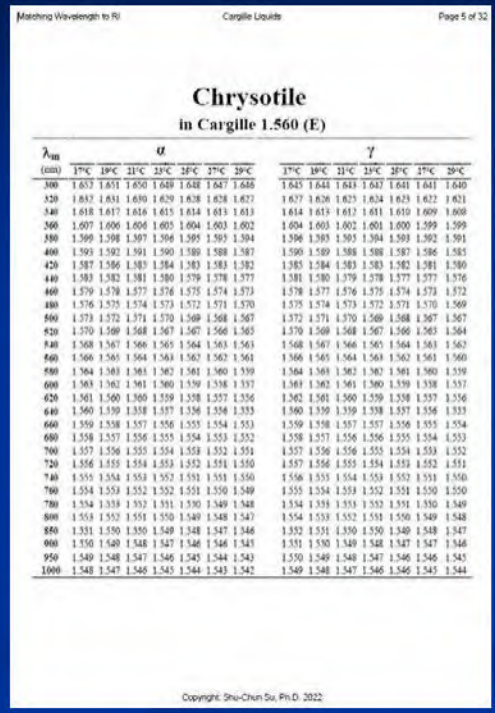
Matching Wavelength to RI — Cargille Liquids — Page 5 of 32

Chrysotile
in Cargille 1.560 (E)

λ_m (nm)	α 17°C	α 19°C	α 21°C	α 23°C	α 25°C	α 27°C	α 29°C	γ 17°C	γ 19°C	γ 21°C	γ 23°C	γ 25°C	γ 27°C	γ 29°C
500	1.653	1.651	1.650	1.649	1.648	1.647	1.646	1.645	1.644	1.643	1.642	1.641	1.641	1.640
520	1.633	1.631	1.630	1.629	1.628	1.628	1.627	1.627	1.626	1.625	1.624	1.623	1.622	1.621
540	1.618	1.617	1.616	1.615	1.614	1.613	1.613	1.614	1.613	1.612	1.611	1.610	1.609	1.608
560	1.607	1.606	1.606	1.605	1.604	1.603	1.602	1.604	1.603	1.602	1.601	1.600	1.599	1.599
580	1.599	1.598	1.597	1.596	1.595	1.595	1.594	1.596	1.595	1.595	1.594	1.593	1.592	1.591
600	1.593	1.592	1.591	1.590	1.589	1.588	1.587	1.590	1.589	1.588	1.588	1.587	1.586	1.585
620	1.587	1.586	1.585	1.584	1.583	1.583	1.582	1.585	1.584	1.583	1.583	1.582	1.581	1.580
640	1.583	1.582	1.581	1.580	1.579	1.578	1.577	1.581	1.580	1.579	1.578	1.577	1.577	1.576
660	1.579	1.578	1.577	1.576	1.575	1.574	1.573	1.578	1.577	1.576	1.575	1.574	1.573	1.572
680	1.576	1.575	1.574	1.573	1.572	1.571	1.570	1.575	1.574	1.573	1.572	1.571	1.570	1.569
700	1.573	1.572	1.571	1.570	1.569	1.568	1.567	1.572	1.571	1.570	1.569	1.568	1.567	1.567
720	1.570	1.569	1.568	1.567	1.567	1.566	1.565	1.570	1.569	1.568	1.567	1.566	1.565	1.564
740	1.568	1.567	1.566	1.565	1.564	1.563	1.563	1.568	1.567	1.566	1.565	1.564	1.563	1.562
760	1.566	1.565	1.564	1.563	1.562	1.562	1.561	1.566	1.565	1.564	1.563	1.562	1.561	1.560
780	1.564	1.563	1.563	1.562	1.561	1.560	1.559	1.564	1.563	1.562	1.562	1.561	1.560	1.559
800	1.563	1.562	1.561	1.560	1.559	1.558	1.557	1.563	1.562	1.561	1.560	1.559	1.558	1.557
820	1.561	1.560	1.560	1.559	1.558	1.557	1.556	1.562	1.561	1.560	1.559	1.558	1.557	1.556
840	1.560	1.559	1.558	1.557	1.556	1.556	1.555	1.560	1.559	1.559	1.558	1.557	1.556	1.555
860	1.559	1.558	1.557	1.556	1.555	1.554	1.553	1.559	1.558	1.557	1.557	1.556	1.555	1.554
880	1.558	1.557	1.556	1.555	1.554	1.553	1.552	1.558	1.557	1.556	1.556	1.555	1.554	1.553
900	1.557	1.556	1.555	1.554	1.553	1.552	1.551	1.557	1.556	1.556	1.555	1.554	1.553	1.552
920	1.556	1.555	1.554	1.553	1.552	1.551	1.550	1.557	1.556	1.555	1.554	1.553	1.552	1.551
940	1.555	1.554	1.553	1.552	1.551	1.551	1.550	1.556	1.555	1.554	1.553	1.552	1.551	1.550
960	1.554	1.553	1.552	1.552	1.551	1.550	1.549	1.555	1.554	1.553	1.552	1.551	1.550	1.550
980	1.554	1.553	1.552	1.551	1.550	1.549	1.548	1.554	1.553	1.553	1.552	1.551	1.550	1.549
1000	1.553	1.552	1.551	1.550	1.549	1.548	1.547	1.554	1.553	1.552	1.551	1.550	1.549	1.548
850	1.551	1.550	1.550	1.549	1.548	1.547	1.546	1.552	1.551	1.550	1.550	1.549	1.548	1.547
900	1.550	1.549	1.548	1.547	1.546	1.546	1.545	1.551	1.550	1.549	1.548	1.547	1.547	1.546
950	1.549	1.548	1.547	1.546	1.545	1.544	1.543	1.550	1.549	1.548	1.547	1.546	1.546	1.545
1000	1.548	1.547	1.546	1.545	1.544	1.543	1.542	1.549	1.548	1.547	1.546	1.546	1.545	1.544

Copyright Shu-Chun Su, Ph.D. 2022

M71614-003's pale yellow dispersion staining color corresponds to a matching wavelength of 410 nm, which is conversed to an RI of 1.593, indicating it is the γ' of talc.

Incorrect RI Measurement Procedure

2023-11-28 - Henderson-Longo Supp. J&J Report

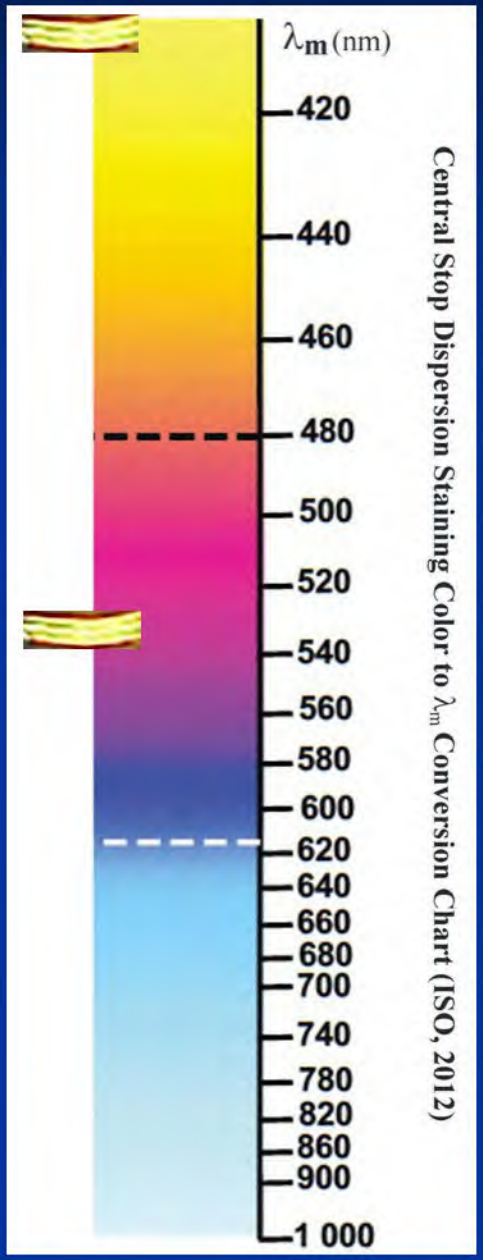

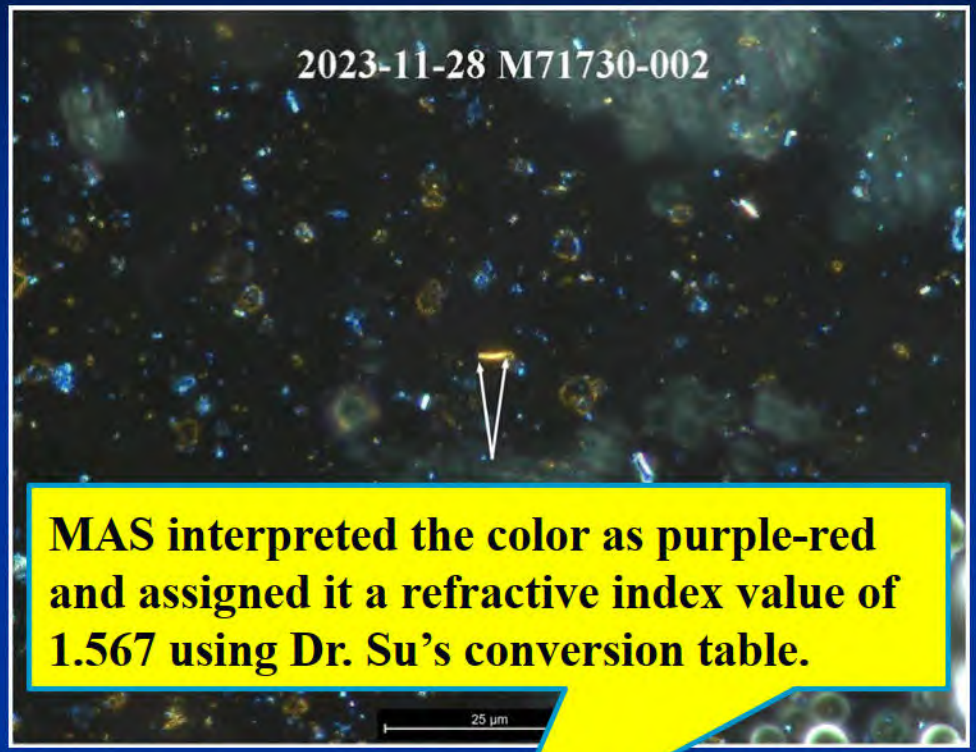

MAS interpreted the color as purple-red and assigned it a refractive index value of 1.567 using Dr. Su's conversion table.

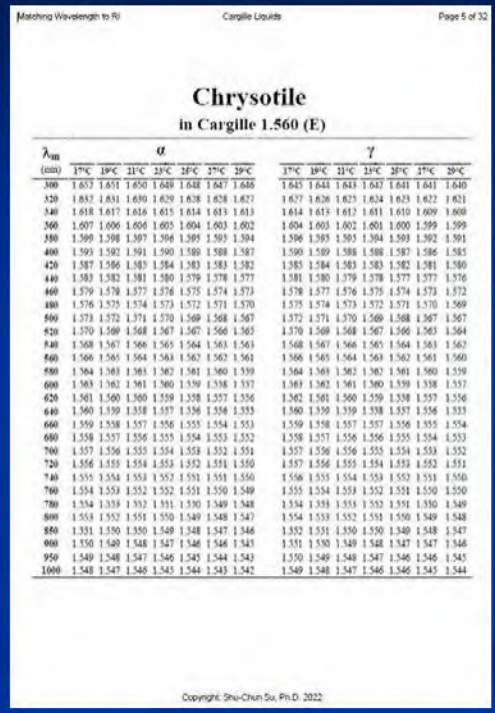
Matching Wavelength to RI — Cargille Liquids — Page 5 of 32

Chrysotile
in Cargille 1.560 (E)

λ_m (nm)	α 17°C	α 19°C	α 21°C	α 23°C	α 25°C	α 27°C	α 29°C	γ 17°C	γ 19°C	γ 21°C	γ 23°C	γ 25°C	γ 27°C	γ 29°C
500	1.653	1.651	1.650	1.649	1.648	1.647	1.646	1.645	1.644	1.643	1.642	1.641	1.641	1.640
520	1.643	1.641	1.639	1.639	1.638	1.638	1.637	1.637	1.636	1.635	1.634	1.633	1.632	1.631
540	1.618	1.617	1.616	1.615	1.614	1.613	1.613	1.614	1.613	1.612	1.611	1.610	1.609	1.608
560	1.607	1.606	1.606	1.605	1.604	1.603	1.602	1.604	1.603	1.602	1.601	1.600	1.599	1.599
580	1.599	1.598	1.597	1.596	1.595	1.595	1.594	1.596	1.595	1.595	1.594	1.593	1.592	1.591
600	1.593	1.592	1.591	1.590	1.589	1.588	1.587	1.590	1.589	1.588	1.588	1.587	1.586	1.585
620	1.587	1.586	1.585	1.584	1.583	1.583	1.582	1.585	1.584	1.583	1.583	1.582	1.581	1.580
640	1.583	1.582	1.581	1.580	1.579	1.578	1.577	1.581	1.580	1.579	1.578	1.577	1.577	1.576
660	1.579	1.578	1.577	1.576	1.575	1.574	1.573	1.578	1.577	1.576	1.575	1.574	1.573	1.572
680	1.576	1.575	1.574	1.573	1.572	1.571	1.570	1.575	1.574	1.573	1.572	1.571	1.570	1.569
700	1.573	1.572	1.571	1.570	1.569	1.568	1.567	1.572	1.571	1.570	1.569	1.568	1.567	1.567
720	1.570	1.569	1.568	1.567	1.567	1.566	1.565	1.570	1.569	1.568	1.567	1.566	1.565	1.564
740	1.568	1.567	1.566	1.565	1.564	1.563	1.563	1.568	1.567	1.566	1.565	1.564	1.563	1.563
760	1.566	1.565	1.564	1.563	1.562	1.562	1.561	1.566	1.565	1.564	1.563	1.562	1.561	1.560
780	1.564	1.563	1.563	1.562	1.561	1.560	1.559	1.564	1.563	1.562	1.562	1.561	1.560	1.559
800	1.563	1.562	1.561	1.560	1.559	1.558	1.557	1.563	1.562	1.561	1.560	1.559	1.558	1.557
820	1.561	1.560	1.560	1.559	1.558	1.557	1.556	1.562	1.561	1.560	1.559	1.558	1.557	1.556
840	1.560	1.559	1.558	1.557	1.556	1.556	1.555	1.560	1.559	1.559	1.558	1.557	1.556	1.555
860	1.559	1.558	1.557	1.556	1.555	1.554	1.553	1.559	1.558	1.557	1.557	1.556	1.555	1.554
880	1.558	1.557	1.556	1.555	1.554	1.553	1.552	1.558	1.557	1.556	1.556	1.555	1.554	1.553
900	1.557	1.556	1.555	1.554	1.553	1.552	1.551	1.557	1.556	1.556	1.555	1.554	1.553	1.552
920	1.556	1.555	1.554	1.553	1.552	1.551	1.550	1.557	1.556	1.555	1.554	1.553	1.552	1.551
940	1.555	1.554	1.553	1.552	1.551	1.551	1.550	1.556	1.555	1.554	1.553	1.552	1.551	1.550
960	1.554	1.553	1.552	1.552	1.551	1.550	1.549	1.555	1.554	1.553	1.552	1.551	1.550	1.550
980	1.554	1.553	1.552	1.551	1.550	1.549	1.548	1.554	1.553	1.552	1.551	1.550	1.549	1.549
1000	1.553	1.552	1.551	1.550	1.549	1.548	1.547	1.554	1.553	1.552	1.551	1.550	1.549	1.548
850	1.551	1.550	1.550	1.549	1.548	1.547	1.546	1.552	1.551	1.550	1.550	1.549	1.548	1.547
900	1.550	1.549	1.548	1.547	1.547	1.546	1.545	1.551	1.550	1.549	1.548	1.547	1.547	1.546
950	1.549	1.548	1.547	1.546	1.545	1.544	1.543	1.550	1.549	1.548	1.547	1.546	1.546	1.545
1000	1.548	1.547	1.546	1.545	1.544	1.543	1.542	1.549	1.548	1.547	1.546	1.546	1.545	1.544

Copyright Shiu-Chun Su, Ph.D. 2022

M71730-002's pale yellow dispersion staining color corresponds to a matching wavelength of 400 nm, which is conversed to an RI of 1.597, indicating it is the γ' of talc.

Incorrect RI Measurement Procedure

2024-02-15 M71740 Analysis of JBP (Rochelle Kirch) Compiled Notebook

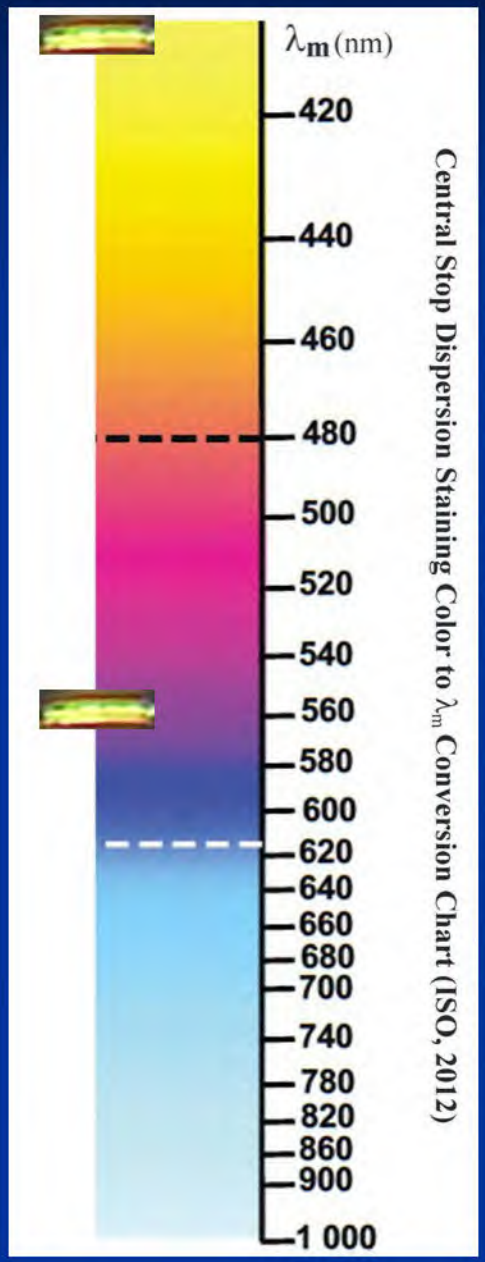

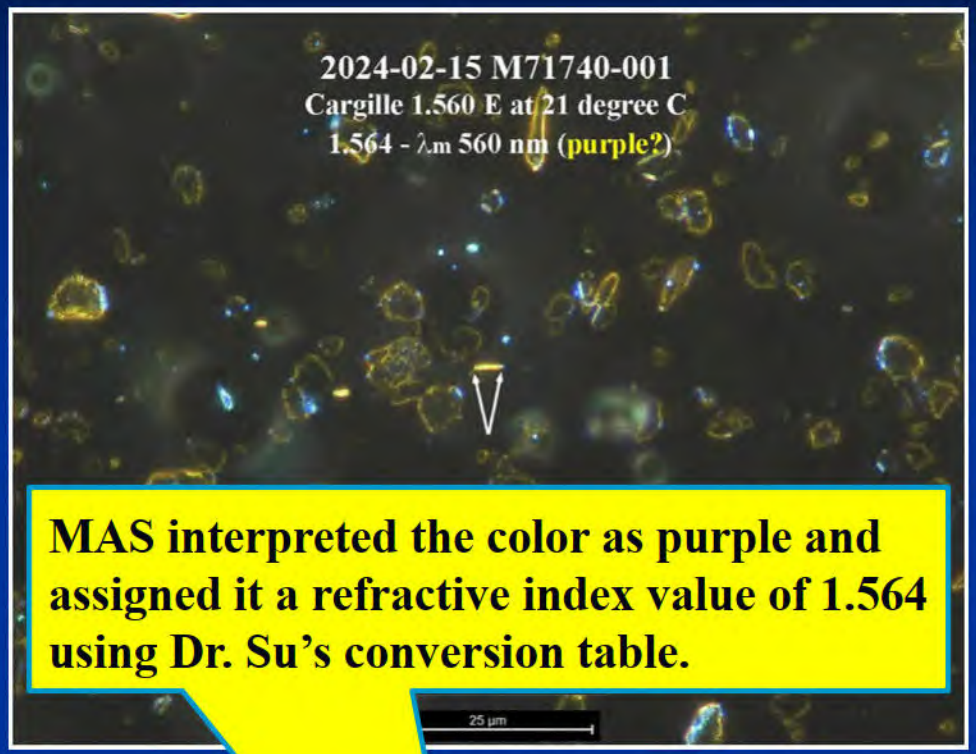

MAS interpreted the color as purple and assigned it a refractive index value of 1.564 using Dr. Su's conversion table.

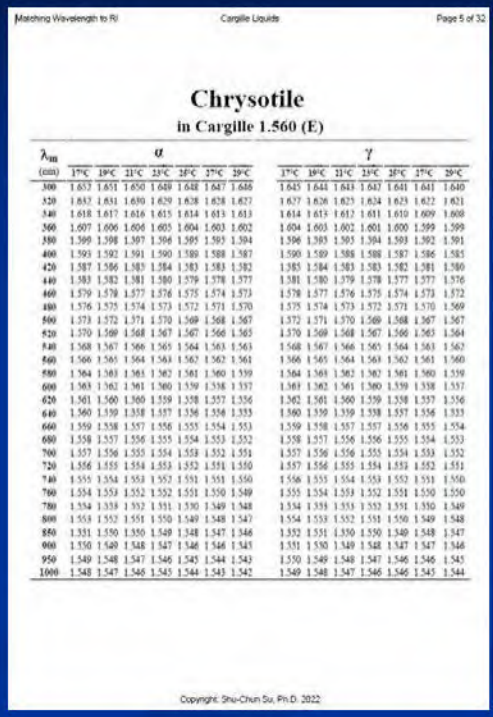
Matching Wavelength to RI — Cargille Liquids — Page 5 of 32

Chrysotile
in Cargille 1.560 (E)

λ_m	α							γ						
(nm)	17°C	19°C	21°C	23°C	25°C	27°C	29°C	17°C	19°C	21°C	23°C	25°C	27°C	29°C
500	1.573	1.572	1.571	1.570	1.569	1.568	1.567	1.572	1.571	1.570	1.569	1.568	1.567	1.567
520	1.570	1.569	1.568	1.567	1.567	1.566	1.565	1.570	1.569	1.568	1.567	1.566	1.565	1.564
540	1.568	1.567	1.566	1.565	1.564	1.563	1.563	1.568	1.567	1.566	1.565	1.564	1.563	1.563
560	1.566	1.565	1.564	1.563	1.562	1.562	1.561	1.566	1.565	1.564	1.563	1.562	1.561	1.560
580	1.564	1.563	1.563	1.562	1.561	1.560	1.559	1.564	1.563	1.562	1.562	1.561	1.560	1.559
600	1.563	1.562	1.561	1.560	1.559	1.558	1.557	1.563	1.562	1.561	1.560	1.559	1.558	1.557
620	1.561	1.560	1.560	1.559	1.558	1.557	1.556	1.562	1.561	1.560	1.559	1.558	1.557	1.556
640	1.560	1.559	1.558	1.557	1.556	1.556	1.555	1.560	1.559	1.559	1.558	1.557	1.556	1.555
660	1.559	1.558	1.557	1.556	1.555	1.554	1.553	1.559	1.558	1.557	1.557	1.556	1.555	1.554
680	1.558	1.557	1.556	1.555	1.554	1.553	1.552	1.558	1.557	1.556	1.556	1.555	1.554	1.553
700	1.557	1.556	1.555	1.554	1.553	1.552	1.551	1.557	1.556	1.556	1.555	1.554	1.553	1.552
720	1.556	1.555	1.554	1.553	1.552	1.551	1.550	1.557	1.556	1.555	1.554	1.553	1.552	1.551
740	1.555	1.554	1.553	1.552	1.551	1.551	1.550	1.556	1.555	1.554	1.553	1.552	1.551	1.550
760	1.554	1.553	1.552	1.552	1.551	1.550	1.549	1.555	1.554	1.553	1.552	1.551	1.550	1.550
780	1.554	1.553	1.552	1.551	1.550	1.549	1.548	1.554	1.553	1.553	1.552	1.551	1.550	1.549
800	1.553	1.552	1.551	1.550	1.549	1.548	1.547	1.554	1.553	1.552	1.551	1.550	1.549	1.548
850	1.551	1.550	1.550	1.549	1.548	1.547	1.546	1.552	1.551	1.550	1.550	1.549	1.548	1.547
900	1.550	1.549	1.548	1.547	1.546	1.546	1.545	1.551	1.550	1.549	1.548	1.547	1.547	1.546
950	1.549	1.548	1.547	1.546	1.545	1.544	1.543	1.550	1.549	1.548	1.547	1.546	1.546	1.545
1000	1.548	1.547	1.546	1.545	1.544	1.543	1.542	1.549	1.548	1.547	1.546	1.546	1.545	1.544

Copyright Shiu-Chun Su, Ph.D. 2022

M71740-001's pale yellow dispersion staining color corresponds to a matching wavelength of 400 nm, which is conversed to an RI of 1.597, indicating it is the γ' of talc.

Dr. Shu-Chun Su's Analysis of MAS's Analytical Results

Incorrect RI Measurement Procedure:
Problem Persists for Years

Incorrect RI Measurement Procedure

2021-05-25 M71228 OTShelf JBP Purchased Argentina

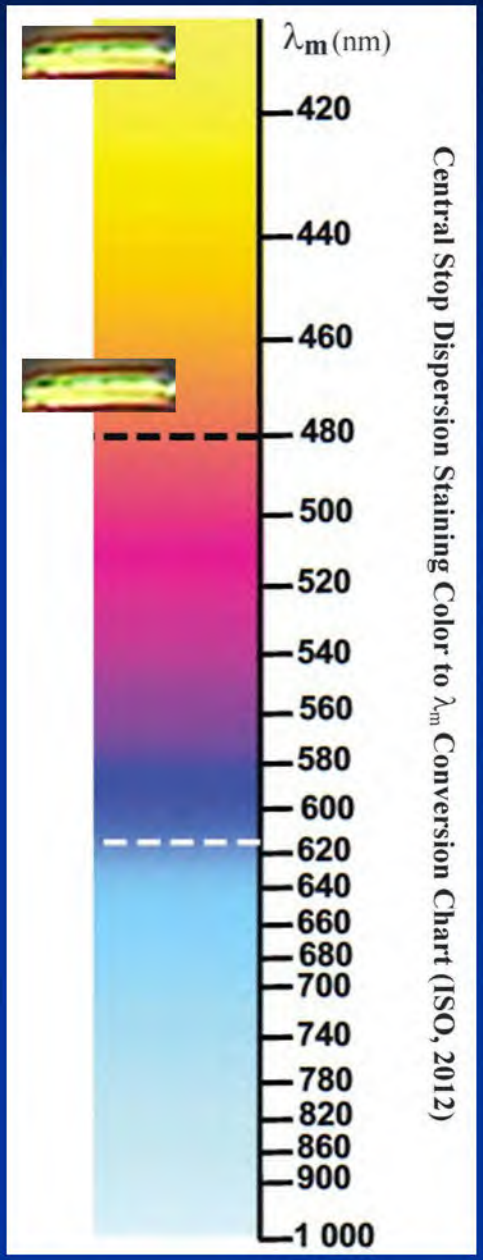

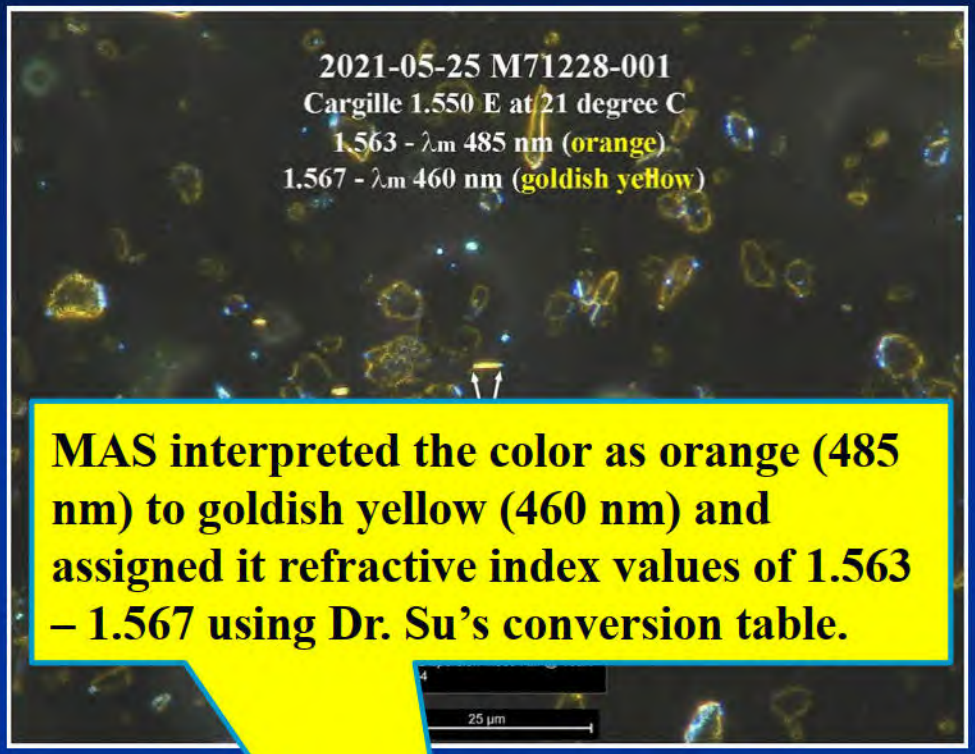

MAS interpreted the color as orange (485 nm) to goldish yellow (460 nm) and assigned it refractive index values of 1.563 – 1.567 using Dr. Su's conversion table.

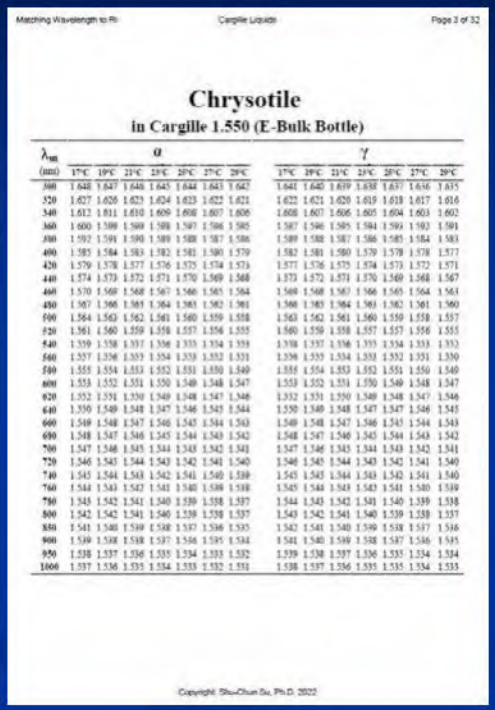

Chrysotile
in Cargille 1.550 (E-Bulk Bottle)

λ_m (nm)	α 17°C	α 19°C	α 21°C	α 23°C	α 25°C	α 27°C	α 29°C	γ 17°C	γ 19°C	γ 21°C	γ 23°C	γ 25°C	γ 27°C	γ 29°C
500	1.648	1.647	1.646	1.645	1.644	1.643	1.642	1.641	1.640	1.639	1.638	1.637	1.636	1.635
520	1.627	1.626	1.625	1.624	1.623	1.622	1.621	1.622	1.621	1.620	1.619	1.618	1.617	1.616
540	1.612	1.611	1.610	1.609	1.608	1.607	1.606	1.608	1.607	1.606	1.605	1.604	1.603	1.602
560	1.600	1.599	1.598	1.598	1.597	1.596	1.595	1.597	1.596	1.595	1.594	1.593	1.592	1.591
580	1.592	1.591	1.590	1.589	1.588	1.587	1.586	1.589	1.588	1.587	1.586	1.585	1.584	1.583
600	1.585	1.584	1.583	1.582	1.581	1.580	1.579	1.582	1.581	1.580	1.579	1.578	1.578	1.577
620	1.579	1.578	1.577	1.576	1.575	1.574	1.573	1.577	1.576	1.575	1.574	1.573	1.572	1.571
640	1.574	1.573	1.572	1.571	1.570	1.569	1.568	1.573	1.572	1.571	1.570	1.569	1.568	1.567
660	1.570	1.569	1.568	1.567	1.566	1.565	1.564	1.569	1.568	1.567	1.566	1.565	1.564	1.563
680	1.567	1.566	1.565	1.564	1.563	1.562	1.561	1.566	1.565	1.564	1.563	1.562	1.561	1.560
700	1.564	1.563	1.562	1.561	1.560	1.559	1.558	1.563	1.562	1.561	1.560	1.559	1.558	1.557
720	1.561	1.560	1.559	1.558	1.557	1.556	1.555	1.560	1.559	1.558	1.557	1.557	1.556	1.555
740	1.559	1.558	1.557	1.556	1.555	1.554	1.553	1.558	1.557	1.556	1.555	1.554	1.553	1.552
760	1.557	1.556	1.555	1.554	1.553	1.552	1.551	1.556	1.555	1.554	1.553	1.552	1.551	1.550
780	1.555	1.554	1.553	1.552	1.551	1.550	1.549	1.555	1.554	1.553	1.552	1.551	1.550	1.549
800	1.553	1.552	1.551	1.550	1.549	1.548	1.547	1.553	1.552	1.551	1.550	1.549	1.548	1.547
820	1.552	1.551	1.550	1.549	1.548	1.547	1.546	1.552	1.551	1.550	1.549	1.548	1.547	1.546
840	1.550	1.549	1.548	1.547	1.546	1.545	1.544	1.550	1.549	1.548	1.547	1.547	1.546	1.545
860	1.549	1.548	1.547	1.546	1.545	1.544	1.543	1.549	1.548	1.547	1.546	1.545	1.544	1.543
880	1.548	1.547	1.546	1.545	1.544	1.543	1.542	1.548	1.547	1.546	1.545	1.544	1.543	1.542
900	1.547	1.546	1.545	1.544	1.543	1.542	1.541	1.547	1.546	1.545	1.544	1.543	1.542	1.541
920	1.546	1.545	1.544	1.543	1.542	1.541	1.540	1.546	1.545	1.544	1.543	1.542	1.541	1.540
940	1.545	1.544	1.543	1.542	1.541	1.540	1.539	1.545	1.545	1.544	1.543	1.542	1.541	1.540
960	1.544	1.543	1.542	1.541	1.540	1.539	1.538	1.545	1.544	1.543	1.543	1.541	1.540	1.539
980	1.543	1.542	1.541	1.540	1.539	1.538	1.537	1.544	1.543	1.542	1.541	1.540	1.539	1.538
1000	1.542	1.542	1.541	1.540	1.539	1.538	1.537	1.543	1.542	1.541	1.540	1.539	1.538	1.537
1050	1.541	1.540	1.539	1.538	1.537	1.536	1.535	1.542	1.541	1.540	1.539	1.538	1.537	1.536
1100	1.539	1.538	1.538	1.537	1.536	1.535	1.534	1.541	1.540	1.539	1.538	1.537	1.536	1.535
1150	1.538	1.537	1.536	1.535	1.534	1.533	1.532	1.539	1.538	1.537	1.536	1.535	1.534	1.534
1200	1.537	1.536	1.535	1.534	1.533	1.532	1.531	1.538	1.537	1.536	1.535	1.535	1.534	1.533

M71228-001's pale yellow dispersion staining color corresponds to a matching wavelength of 400 nm, which is conversed to an RI of 1.597, indicating it is the γ' of talc.

Incorrect RI Measurement Procedure

The variation of dispersion staining color is due to the total reflection

It is wrong for MAS to interpret the purple-red CSDS color at the edge as the representative color for the RI assignment because it fits the inaccurate chrysotile theory. It is a distorted CS color due to total reflection at the liquid-solid interface. The pale yellow is the right color to choose.

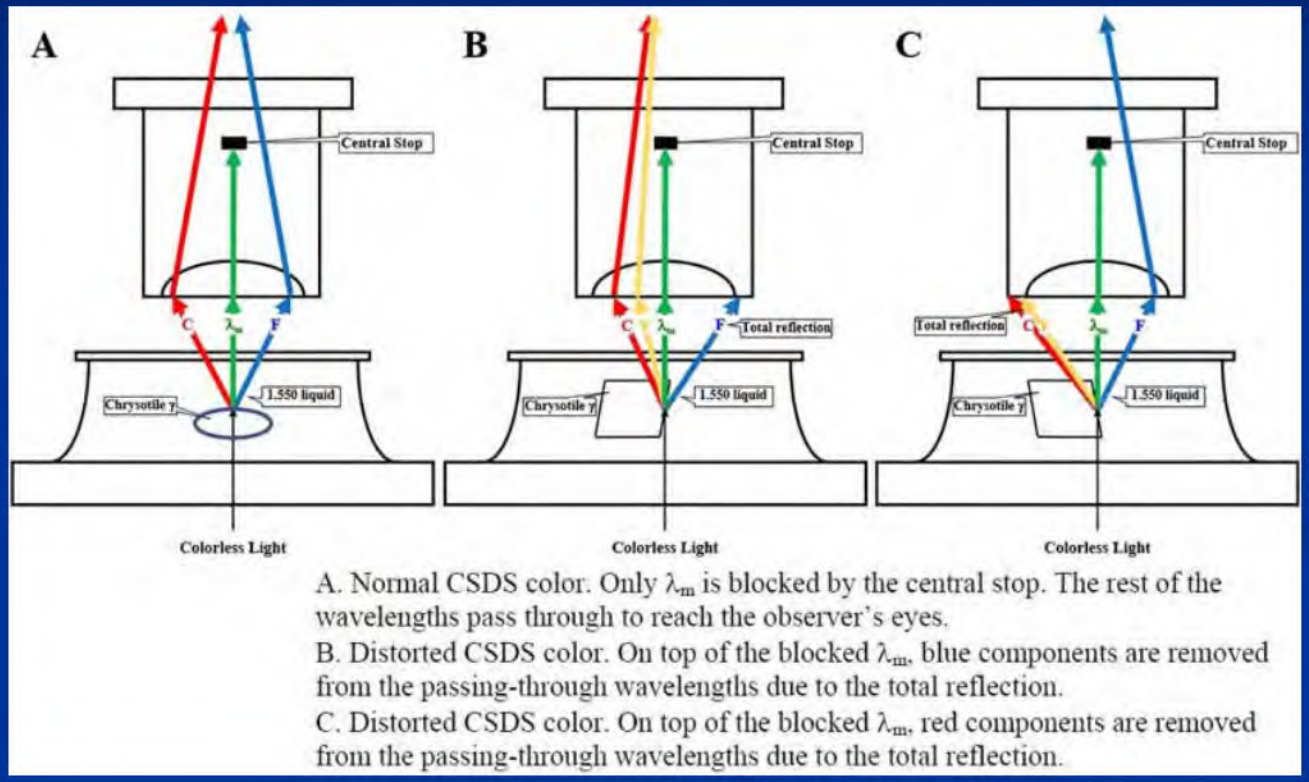

A. Normal CSDS color. Only λ_m is blocked by the central stop. The rest of the wavelengths pass through to reach the observer's eyes.
B. Distorted CSDS color. On top of the blocked λ_m, blue components are removed from the passing-through wavelengths due to the total reflection.
C. Distorted CSDS color. On top of the blocked λ_m, red components are removed from the passing-through wavelengths due to the total reflection.

This image explains the physics of how total reflection occurs.
By failing to consider the distortion of dispersion staining colors caused by total reflection, MAS used the wrong dispersion staining color and assigned incorrect RI values.

There is No Variability of Refractive Index within a Bundle

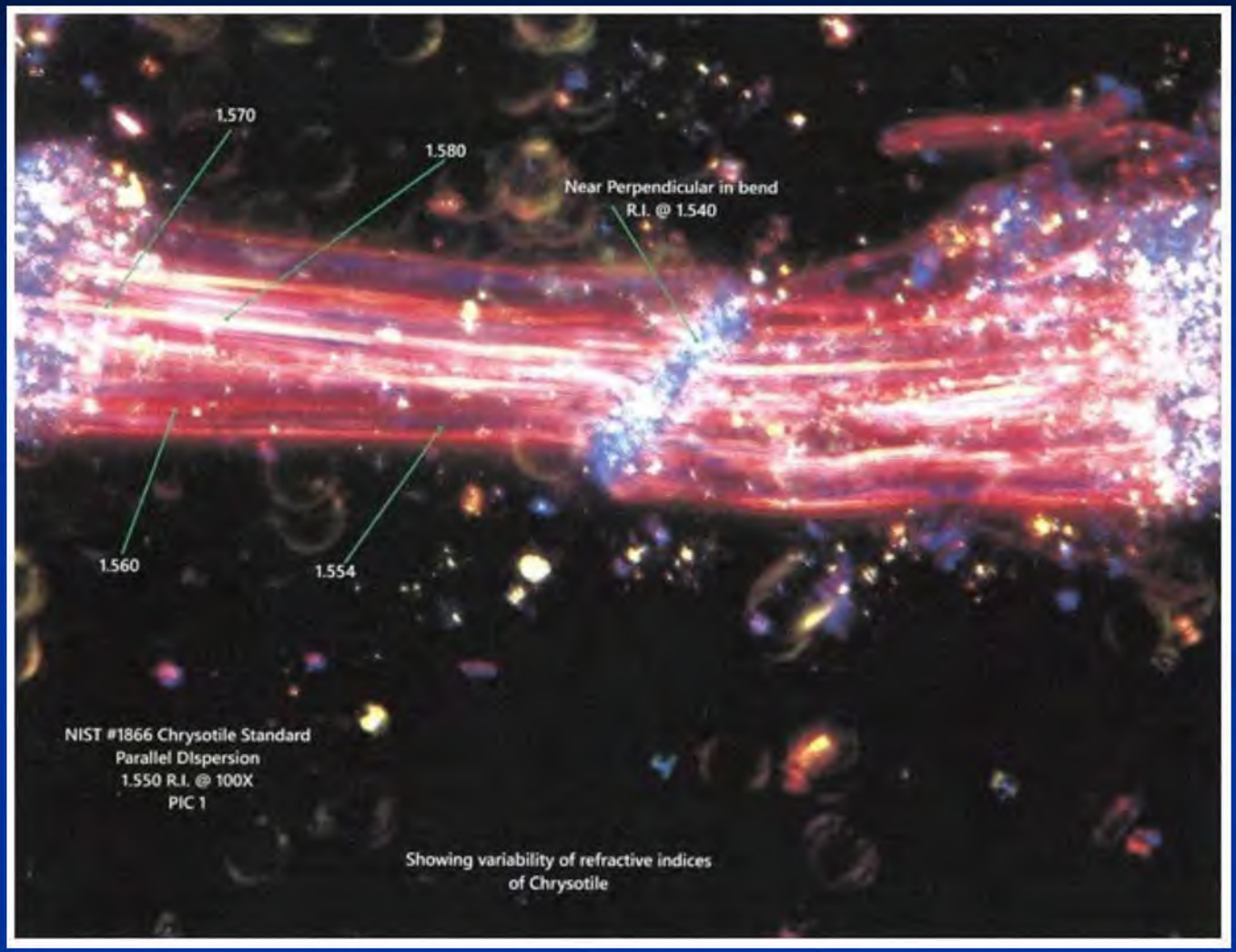

It is wrong for MAS to interpret the variation of dispersion staining color as the variation of refractive index within the bundle.

A mineral's RI is a constant governed by their chemical composition and crystal structure. MAS's theory that chrysotile's RI increases as the particle size decreases is unfounded and defies basic principles of physics. In fact, if such a theory is proved, it would shake the very foundation of physics.

The variation of dispersion staining color is caused by the total reflection occurring at the liquid-solid interface

There is No Variability of Refractive Index within a Bundle

Understanding the formation of distorted dispersion staining color

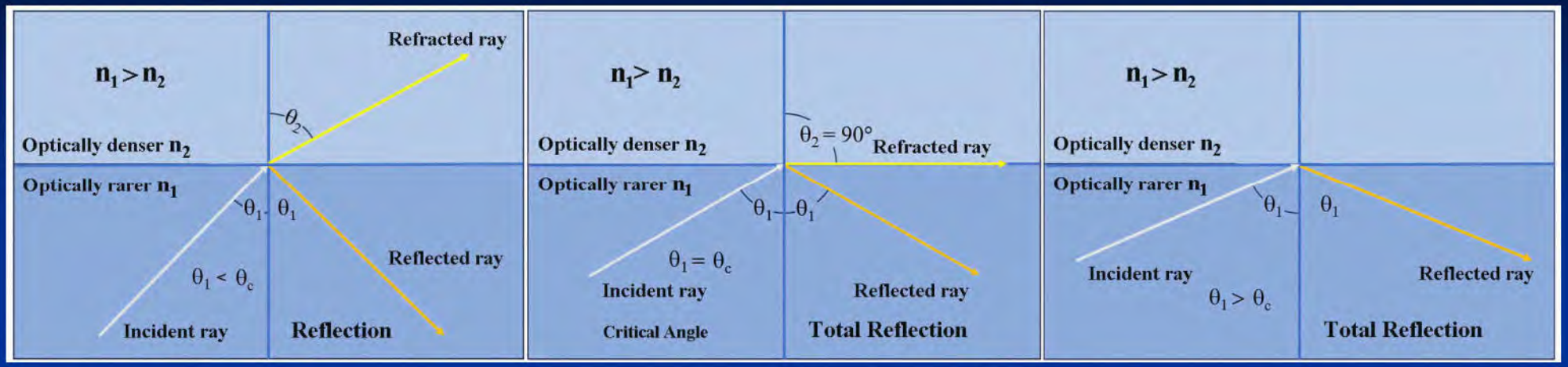

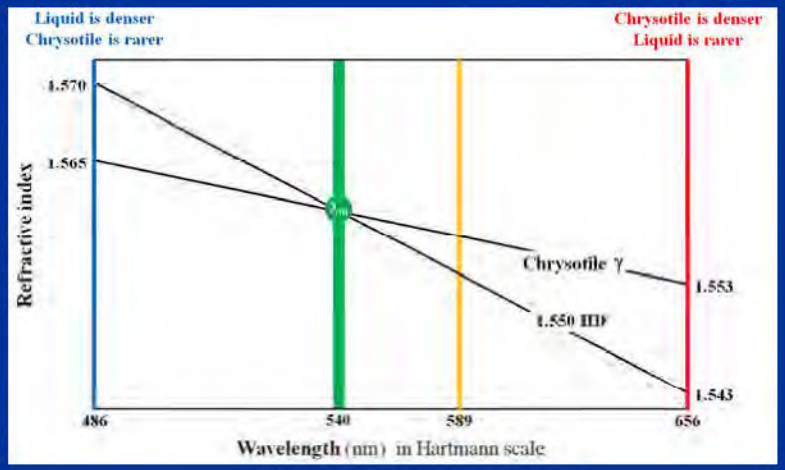

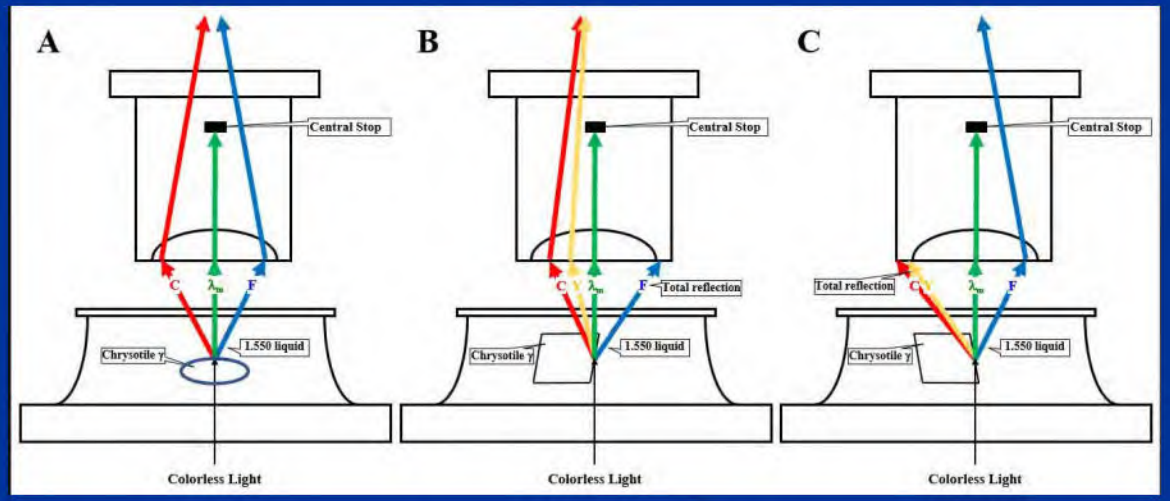

λ	Color	γ	1.551 E	Critical Angle
486 nm	Blue	1.570	1.567	86.5°
656 nm	Red	1.553	1.543	83.5°

When light transmits from an optically denser (greater RI) to an optically rarer (smaller RI) medium, total internal reflection occurs at the critical angle.

The total reflection wavelengths are removed from the non-matching wavelength spectrum, resulting in the distorted dispersion staining color.

There is No Variability of Refractive Index within a Bundle

Table 1. Certified Values of Refractive Index for Chrysotile Asbestos in SRM 1866b

Wavelength (nm)	α Lower Limit[(a)]	α Fitted Value	α Upper Limit	γ Lower Limit	γ Fitted Value	γ Upper Limit
460	1.554	1.558	1.563	1.563	1.568	1.572
480	1.552	1.557	1.561	1.561	1.565	1.569
500	1.551	1.555	1.559	1.559	1.563	1.567
520	1.549	1.553	1.557	1.557	1.561	1.565
540	1.548	1.552	1.556	1.556	1.560	1.564
560	1.547	1.551	1.555	1.554	1.558	1.562
589.3	1.545	**1.549**	1.553	1.552	**1.556**	1.560
600	1.545	1.549	1.553	1.551	1.556	1.560
620	1.544	1.548	1.552	1.550	1.554	1.559
640	1.543	1.547	1.551	1.549	1.553	1.558

The certified refractive index values in the certificate issued by NIST for SRM 1866 apply to every fiber and fiber bundle in the standard reference material.

Refractive Index Does Not Change With the Particle Size

Table 1. Certified Values of Refractive Index for Chrysotile Asbestos in SRM 1866b

Wavelength (nm)	α Lower Limit[a]	α Fitted Value	α Upper Limit	γ Lower Limit	γ Fitted Value	γ Upper Limit
460	1.554	1.558	1.563	1.563	1.568	1.572
480	1.552	1.557	1.561	1.561	1.565	1.569
500	1.551	1.555	1.559	1.559	1.563	1.567
520	1.549	1.553	1.557	1.557	1.561	1.565
540	1.548	1.552	1.556	1.556	1.560	1.564
560	1.547	1.551	1.555	1.554	1.558	1.562
589.3	1.545	**1.549**	1.553	1.552	**1.556**	1.560
600	1.545	1.549	1.553	1.551	1.556	1.560
620	1.544	1.548	1.552	1.550	1.554	1.559
640	1.543	1.547	1.551	1.549	1.553	1.558

A mineral's RI is a constant governed by their chemical composition and crystal structure. MAS's theory that chrysotile's RI increases as the particle size decreases is unfounded and defies basic principles of physics. In fact, if such a theory is proved, it would shake the very foundation of physics.

The NIST SRM 1866 chrysotile RI values, α 1.549 and γ 1.556, were measured by John Phelps, a scientist at NIST, on a single fiber using the spindle stage technique. Dr. Longo's fibers cannot be any thinner than John Phelps's single chrysotile fiber. Dr. Longo's claim is not only unfounded but also without the support of credible measurement data.

Calidria Chrysotile RI Compared to 1866

SAMPLE 1

Sample 1 is a "pure", short range (short fiber) chrysotile from the New Idria serpentinite body of California. The sample is white, very homogeneous, and contains very short fibers/bundles (often < 20μm) of chrysotile. The asbestiform habit of the chrysotile (and the optical properties) are best observed by viewing at high magnification (400 - 500X). The mean refractive indices are 1.560 for γ and 1.555 for α. Chrysotile comprises >95% of the sample.

Of the 257 participating laboratories, eight did not report asbestos for this sample and one reported a different asbestos type. Ten laboratories reported one or both refractive indices outside the acceptance ranges for the chrysotile. Twenty-two laboratories reported an asbestos concentration outside the acceptance range.

The certified 1866 chrysotile RI values are α 1.549 and γ 1.556. The certified Calidria chrysotile RI values are α 1.555 and γ 1.560. Dr. Longo's RI values are another leap beyond the Calidria chrysotile RI values.

MAS Used My Procedure to Measure RI

Table 5

Comparison of Chrysotile Measured Refractive Indexes Between MAS, Dr. McCrone and Dr. Su

	Refractive Index Range Parallel	Refractive Index Range Perpendicular
MAS	ISO 1.568 to 1.561 CSM 1.568 to 1.564	ISO 1.558 to 1.550 CSM 1.556 to 1.550
Dr. McCrone	1.570 to 1.548	1.553 to 1.534
Dr. Su	1.580 to 1.540	1.579 to 1.541

MAS misinterpreted my table (Su, 2003)

American Mineralogist, Volume 88, pages 1979–1982, 2003

A rapid and accurate procedure for the determination of refractive indices of regulated asbestos minerals

SHU-CHUN SU*

Hercules Incorporated, Research Center, 500 Hercules Road, Wilmington, Delaware 19808, U.S.A.

ABSTRACT

By using dispersion staining methods and pre-constructed conversion tables, it is possible to quickly and accurately determine two principal refractive indices (RI) of the six regulated asbestos minerals, chrysotile, grunerite (amosite), riebeckite (crocidolite), tremolite, actinolite, and anthophyllite, in a single immersion oil mount. This procedure is especially suitable for commercial environmental laboratories specializing in the analysis of asbestos components in bulk building materials. The effectiveness of this practical procedure has been proven through rigorous testing and extensive usage over the last decade by the majority of environmental laboratories in the U.S. The principle of this procedure is also readily applicable to RI determination in other applications: mineralogy, forensics, pharmaceutical research, particle identification, etc.

MAS Misinterpreted My Table

TABLE 3. Conversion of the matching wavelength λ_o to the corresponding RI values

Mineral	Chrysotile	Amosite	Crocidolite	Tremolite			Actinolite or Anthophyllite		
Oil $n_D^{25°C}$	1.550	1.680	1.700	1.620	1.610	1.635	1.625	1.610	1.635
Oil Series	E	B	B	E	E	E	E	E	E
RI	$n_\perp$ or $n_\parallel$	$n_\perp$ or $n_\parallel$	$n_\perp$ or $n_\parallel$	$n_\perp$ or $n_\parallel$	$n_\perp$	$n_\parallel$	$n_\perp$ or $n_\parallel$	$n_\perp$	$n_\parallel$
λ_o (nm)									
400	1.[illegible]								1.666
420	1.[illegible]								1.660
440	1.[illegible]								1.655
460	1.[illegible]								1.651
480	1.[illegible]								1.648
500	1.[illegible]								1.645
520	1.[illegible]								1.642
540	1.[illegible]								1.640
560	1.[illegible]								1.638
580	1.[illegible]								1.636
589	1.[illegible]								1.635
600	1.[illegible]								1.634
620	1.548	1.678	1.697	1.618	1.608	1.632	1.623	1.608	1.633
640	1.546	1.677	1.695	1.616	1.606	1.631	1.621	1.607	1.631
660	1.545	1.676	1.694	1.615	1.605	1.630	1.620	1.606	1.630
680	1.544	1.675	1.692	1.614	1.604	1.628	1.619	1.605	1.629
700	1.[illegible]								1.628
720	1.[illegible]								1.627
740	1.[illegible]								1.626
760	1.[illegible]								1.625
780	1.[illegible]								1.624
800	1.[illegible]								1.624
850	1.[illegible]								1.622
900	1.[illegible]								1.621
1000	1.[illegible]								1.618
Δ^L	0.[illegible]								0.0291
Δ^S	0.[illegible]								0.0127
$\Delta^L - \Delta^S$	0.[illegible]								0.0164

Note: Temperature correction: If oil temperature is not 25 °C, for every 1° C decrease (increase) in temperature, add (subtract) 0.001 to (from) the listed values.

The range of each asbestos's RI values in the table must be wider than its possible minimum and maximum RI values.

It doesn't mean the range represents the possible minimum and maximum RI values of chrysotile or other asbestos minerals.

Table 5
Comparison of Chrysotile Measured Refractive Indexes Between MAS, Dr. McCrone and Dr. Su

	Refractive Index Range Parallel	Refractive Index Range Perpendicular
MAS	ISO 1.568 to 1.561 CSM 1.568 to 1.564	ISO 1.558 to 1.550 CSM 1.556 to 1.550
Dr. McCrone	1.570 to 1.548	1.553 to 1.534
Dr. Su	1.580 to 1.540	1.579 to 1.541

MAS misinterpreted the ranges of my table are the possible minimum and maximum values of chrysotile's refractive indices.

The kindergarten stadiometer must be taller than the possible heights of children. It doesn't mean that kindergarten students can be six feet tall.

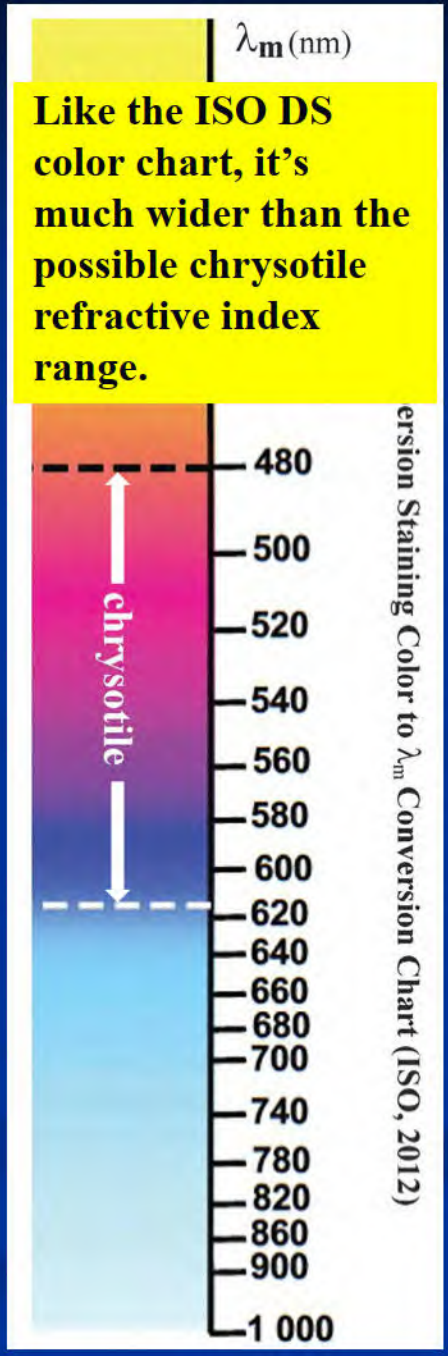

Like the ISO DS color chart, it's much wider than the possible chrysotile refractive index range.

MAS Misinterpreted My Table

Chrysotile

in Cargille 1.560 (E)

λ_m	α							γ						
(nm)	17°C	19°C	21°C	23°C	25°C	27°C	29°C	17°C	19°C	21°C	23°C	25°C	27°C	29°C
300	1.652	1.651	1.650	1.649	1.648	1.647	1.646	1.645	1.644	1.643	1.642	1.641	1.641	1.640
320	1.632	1.631	1.630	1.629	1.628	1.628	1.627	1.627	1.626	1.625	1.624	1.623	1.622	1.621
340	1.618	1.617	1.616	1.615	1.614	1.613	1.613	1.614	1.613	1.612	1.611	1.610	1.609	1.608
360	1.607	1.606	1.606	1.605	1.604	1.603	1.602	1.604	1.603	1.602	1.601	1.600	1.599	1.599
380	1.599	1.598	1.597	1.596	1.595	1.595	1.594	1.596	1.595	1.595	1.594	1.593	1.592	1.591
400	1.593	1.592	1.591	1.590	1.589	1.588	1.587	1.590	1.589	1.588	1.588	1.587	1.586	1.585
420	1.587	1.586	1.585	1.584	1.583	1.583	1.582	1.585	1.584	1.583	1.583	1.582	1.581	1.580
440	1.583	1.582	1.581	1.580	1.579	1.578	1.577	1.581	1.580	1.579	1.578	1.577	1.577	1.576
460	1.579	1.578	1.577	1.576	1.575	1.574	1.573	1.578	1.577	1.576	1.575	1.574	1.573	1.572
480	1.576	1.575	1.574	1.573	1.572	1.571	1.570	1.575	1.574	1.573	1.572	1.571	1.570	1.569
500	1.573	1.572	1.571	1.570	1.569	1.568	1.567	1.572	1.571	1.570	1.569	1.568	1.567	1.567
520	1.570	1.569	1.568	1.567	1.567	1.566	1.565	1.570	1.569	1.568	1.567	1.566	1.565	1.564
540	1.568	1.567	1.566	1.565	1.564	1.563	1.563	1.568	1.567	1.566	1.565	1.564	1.563	1.562
560	1.566	1.565	1.564	1.563	1.562	1.562	1.561	1.566	1.565	1.564	1.563	1.562	1.561	1.560
580	1.564	1.563	1.563	1.562	1.561	1.560	1.559	1.564	1.563	1.562	1.562	1.561	1.560	1.559
600	1.563	1.562	1.561	1.560	1.559	1.558	1.557	1.563	1.562	1.561	1.560	1.559	1.558	1.557
620	1.561	1.560	1.560	1.559	1.558	1.557	1.556	1.562	1.561	1.560	1.559	1.558	1.557	1.556
640	1.560	1.559	1.558	1.557	1.556	1.556	1.555	1.560	1.559	1.559	1.558	1.557	1.556	1.555
660	1.559	1.558	1.557	1.556	1.555	1.554	1.553	1.559	1.558	1.557	1.557	1.556	1.555	1.554
680	1.558	1.557	1.556	1.555	1.554	1.553	1.552	1.558	1.557	1.556	1.556	1.555	1.554	1.553
700	1.557	1.556	1.555	1.554	1.553	1.552	1.551	1.557	1.556	1.556	1.555	1.554	1.553	1.552
720	1.556	1.555	1.554	1.553	1.552	1.551	1.550	1.557	1.556	1.555	1.554	1.553	1.552	1.551
740	1.555	1.554	1.553	1.552	1.551	1.551	1.550	1.556	1.555	1.554	1.553	1.552	1.551	1.550
760	1.554	1.553	1.552	1.552	1.551	1.550	1.549	1.555	1.554	1.553	1.552	1.551	1.550	1.550
780	1.554	1.553	1.552	1.551	1.550	1.549	1.548	1.554	1.553	1.553	1.552	1.551	1.550	1.549
800	1.553	1.552	1.551	1.550	1.549	1.548	1.547	1.554	1.553	1.552	1.551	1.550	1.549	1.548
850	1.551	1.550	1.550	1.549	1.548	1.547	1.546	1.552	1.551	1.550	1.550	1.549	1.548	1.547
900	1.550	1.549	1.548	1.547	1.546	1.546	1.545	1.551	1.550	1.549	1.548	1.547	1.547	1.546
950	1.549	1.548	1.547	1.546	1.545	1.544	1.543	1.550	1.549	1.548	1.547	1.546	1.546	1.545
1000	1.548	1.547	1.546	1.545	1.544	1.543	1.542	1.549	1.548	1.547	1.546	1.546	1.545	1.544

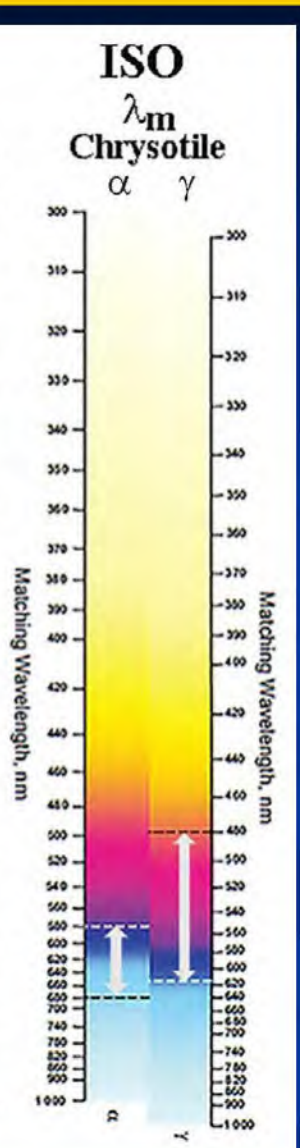

Although the possible RI ranges of chrysotile α & γ are only a small section (between the dotted lines) of the CSDS color chart, the chart must cover the whole λ_m spectrum from 300 to 1000 nm. So does my conversion table. The ranges of the ISO chart and my table must be much wider than the RI range (between the dotted lines) of chrysotile. For people who understand the principle, my table is the numerical version of the ISO graphic chart.

Dr. Longo Misunderstood the RI Liquid's Effect on Mineral's RI

THE MICROSCOPE • Vol. 69:2, pp 51–69, 2022

The Dispersion Staining Technique and Its Application to Measuring Refractive Indices of Non-opaque Materials, with Emphasis on Asbestos Analysis

Shu-Chun Su, Ph.D.
Technical Expert, National Voluntary Laboratory Accreditation Program
National Institute of Standards and Technology[1]

3. *Select a proper RI liquid to mount the sample.*

Mount the suspected asbestos fibers in an appropriate RI liquid according to Table 4 DRIMMC liquid [13] or 5 Cargille liquid [14], which lists two cases: (1) for regulatory, legal, forensic, etc., which requires higher accuracy, and (2) for routine commercial analysis with less stringent accuracy requirements. For high accuracy measurement such as regulatory, legal and forensic analysis, etc., the rule of thumb is to choose RI liquids as close as possible to the RI's to be measured. For example, there are chrysotile minerals whose RIs are significantly higher than those of the standard chrysotile from the NIST SRM 1866 set. In that case, 1.555 or 1.560, instead of 1.550, RI liquids should be used to determine γ (Table 4). When efficiency is a priority and the accuracy requirement is less stringent, choose an RI liquid higher than α and lower than γ so that the two RI's can be determined in a single preparation.

In 2022, I published a paper on the application of the dispersion staining technique to asbestos analysis. I recommended the use of 1.560 RI liquid for measuring the γ of Calidria chrysotile to improve the accuracy of measurement.

The only purpose of switching from 1.550 to 1.560 is to improve the accuracy of RI measurement because chrysotile's RI is a constant and does change with the surrounding liquid medium.

The right diagram shows two beakers, the left one is fatter, representing 1.560 liquid, and the right one is thinner, representing 1.550 liquid. The volume of water represents the γ refractive index.

When the same mineral is measured in two different RI liquids, its RI remains the same, but the matching wavelength λm changes accordingly: the lower liquid produces a shorter λm and the higher liquid produces a longer λm.

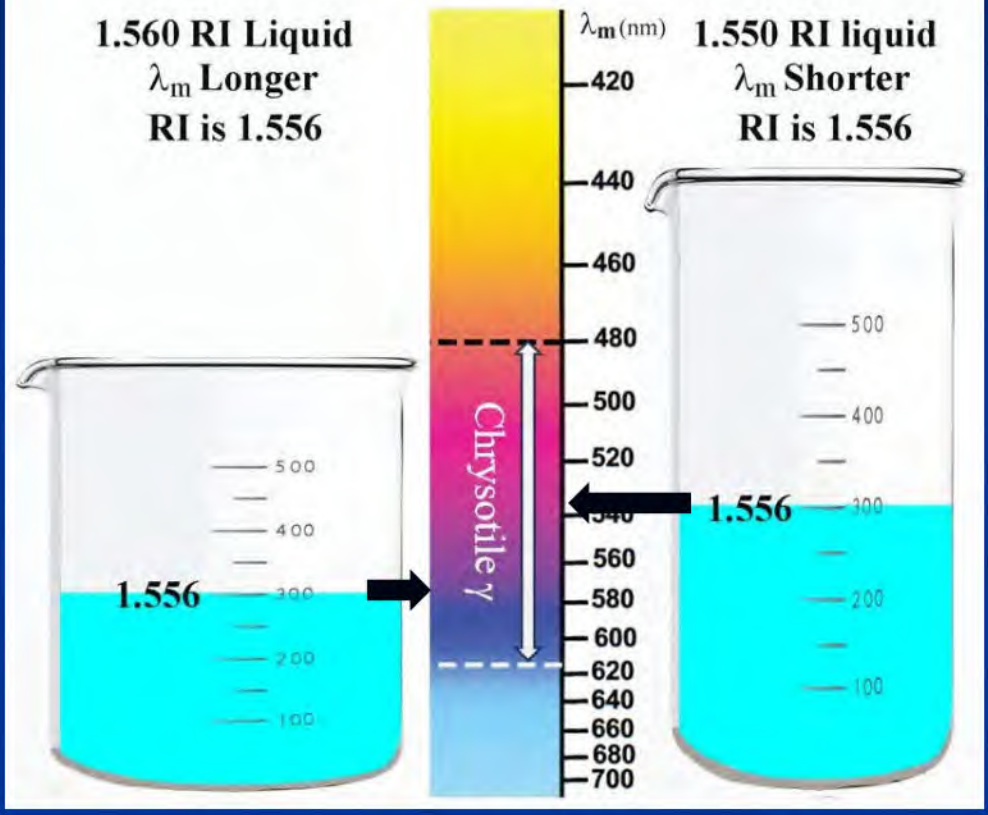

The right diagram shows two beakers, the left one is fatter, representing 1.560 liquid, and the right one is thinner, representing 1.550 liquid. The volume of water represents the γ refractive index. The 300 milliliters of water volume – γ value – didn't change, but the water level – λ_m – did from a shorter (upper) matching wavelength to a longer (lower) matching wavelength.

2024-05-21

Dr. Longo Misunderstood the RI Liquid's Effect on Minerals' RI

M71614-M71643-M71740 J&J Baby Powders

Date	MAS No.			γ		α	
				Low	High	Low	High
2023-02-28	M71614	001	1	1.564	1.564	1.561	1.561
			2	1.565	1.565	1.561	1.561
			3	1.568	1.568	1.557	1.560
			4	1.565	1.568	1.560	1.564
2023-10-19	M71643	001	1	1.566	1.566	1.561	1.561
			2	1.566	1.569	1.557	1.561
			3	1.561	1.561	1.552	1.552
			4	1.568	1.568	1.559	1.559
2024-02-15	M71740	001	1	1.564	1.564	1.560	1.560
			2	1.564	1.564	1.560	1.560
			3	1.565	1.565	1.562	1.562
			4	1.563	1.563	1.561	1.561
			Average	1.565	1.565	1.559	1.560
			Grand Average	1.565		1.560	

Three Types of Chrysotile

Type	α	γ	Birefringence	RI	Source
SRM 1866	1.549	1.556	0.007	Standard	NIST
Calidria	1.555	1.560	0.005	Significantly higher than 1866	NVLAP
New?	1.560*	1.565*	0.005	Significantly higher than Calidria	MAS

* Average of 12 samples in M71614, M71643, and M71740.

In 2022, Dr. Longo switched to 1.560 RI liquid. Without any background in optical crystallography, Dr. Longo mistakenly thought measuring in the 1.560 liquid would increase the fiber's refractive index.

Instead of improving the accuracy of RI measurement, the 1.560 liquid produced a suite of augmented α and γ values.

The left table summarizes 12 pairs of α and γ values from M71614, M71643, and M71740.

Were those data credible (they were not), MAS single-handedly discovered a new type of chrysotile, whose refractive index is significantly higher than the Calidria chrysotile as shown in the left table.

Obviously, there has never been any report of the existence of such a unique type of chrysotile with such peculiar optical properties.

Dr. Shu-Chun Su's Analysis of MAS's Analytical Results

Incorrect Scale Bars

MAS's Inability to Create Scale Bars

Date	MAS No.	Chrysotile Length (µm)		
		Individual	Average	vs. Talc
2020-02-24 M70484	001-001	78.8	61.6	Same partcle size range as talc
	001-002	33.3		
	001-003	38.5		
	001-004	71.3		
	001-005	62.2		
	001-006	57.0		
	001-007	70.4		
	001-008	49.6		
	002-001	58.5		
	002-002	78.5		
	002-003	79.3		
2020-03-18 M71095	001-001	46.7	32.2	Same partcle size range as talc
	001-002	13.3		
	001-003	34.8		
	001-004	34.1		
2020-03-20 M70877	001-001	60.0	37.6	Same partcle size range as talc
	001-002	25.9		
	001-003	23.0		
	001-004	41.5		
2021-05-25 M71228	001-001	105.2	55.2	Same partcle size range as talc
	001-002	59.5		
	001-003	17.2		
	001-004	38.8		
2022-03-11 M71262	001-001	32.8	32.8	Same partcle size range as talc
	001-002	21.6		
	001-003	26.7		
	001-004	50.0		
2023-03-28 M71614	001-001	6.0	4.9	Same partcle size range as talc
	001-002	5.1		
	001-003	3.9		
	001-004	4.8		
2023-10-19 M71643	001-001	3.9	3.8	Same partcle size range as talc
	001-002	6.6		
	001-003	2.2		
	001-004	2.7		
2024-02-15 M71740	001-001	3.6	8.5	Same partcle size range as talc
	001-002	9.4		
	001-003	12.0		
	001-004	8.9		

Drastic variation of "chrysotile" particle size demonstrates continued inaccuracies in measuring particle sizes.

MAS's Inability to Create Scale Bars

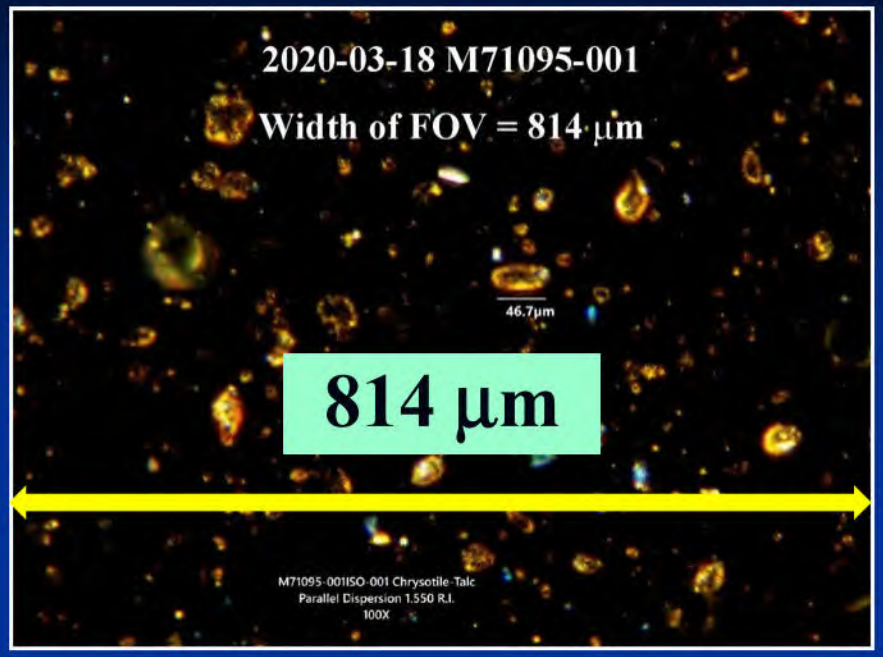

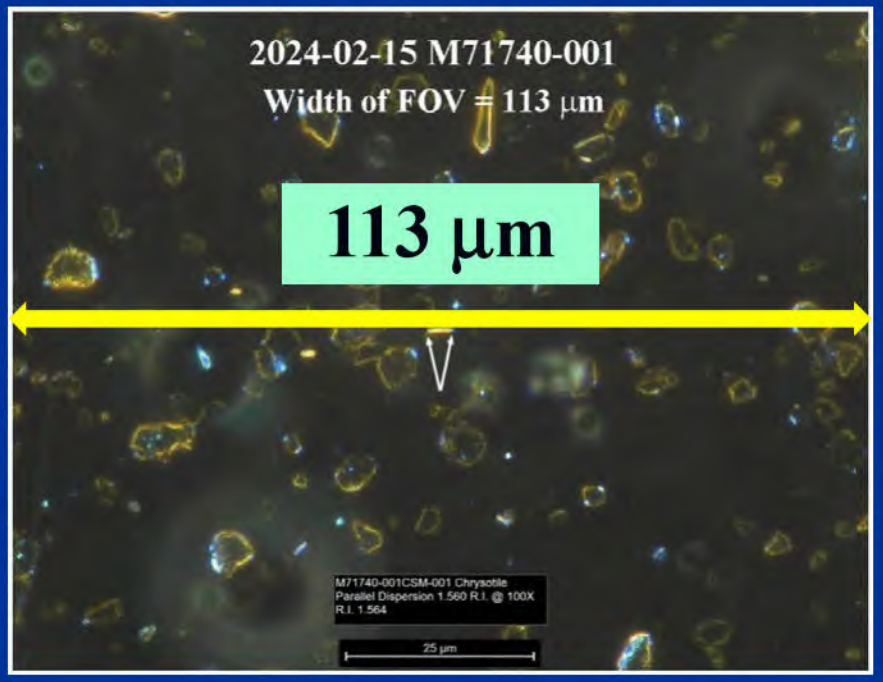

The width of the field of view (FOV) can be calculated from the scale bar length or the width of an object.

Back on 2020-03-18, the 814 µm FOV width was wrong.

Five years later, the mistake remained uncorrected. 2024-02-15 still reported a grossly wrong FOV width of 113 µm.

Regardless of the microscope's make, Olympus Nikon Leitz or Leica, the FOV width for a 10X objective lens is slightly over 1 mm or 1,000 µm.

The only conclusion is that MAS is NOT capable of correctly performing the most fundamental operation procedure of PLM.

What is important is that talc particle sizes in these two micrographs are the same.

Dr. Shu-Chun Su's Analysis of MAS's Analytical Results

Incorrect Particle Size Analysis Results

MAS's Particle Size Analysis Data

Mineral	Minimum (μm)	Average (μm)	Maximum (μm)	Reference
Talc	1.5	9.3	37.0	MAS (2017)
SG-210 Chrysotile	3.0	8.0	10.0	MAS (2023)

- **MAS's particle size measurements in various reports do not conform to the above data.**
- **MAS's data do not conform to the material evidence of USP (2022) and Pier (2017)**
- **The maximum length of SG-210 measured by me is hundreds of micrometers, much longer than 10 micrometers by MAS.**

Incorrect Particle Size Measurement Results

2020-02-24 MAS Rpt JBP-Zimmerman

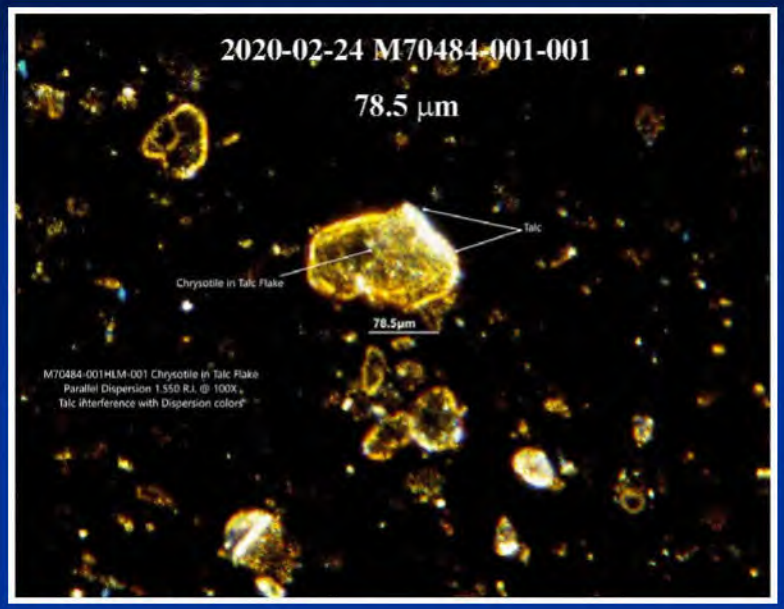

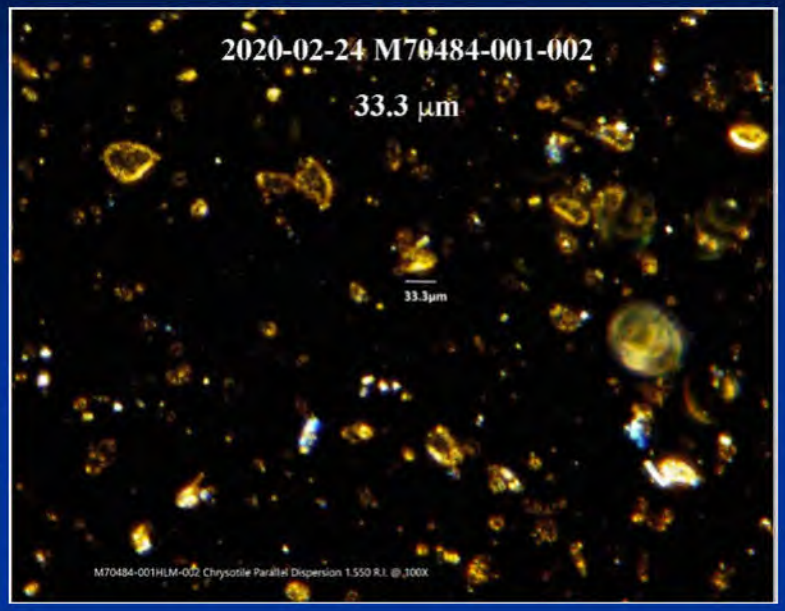

All four chrysotile particles were measured and labeled by MAS.

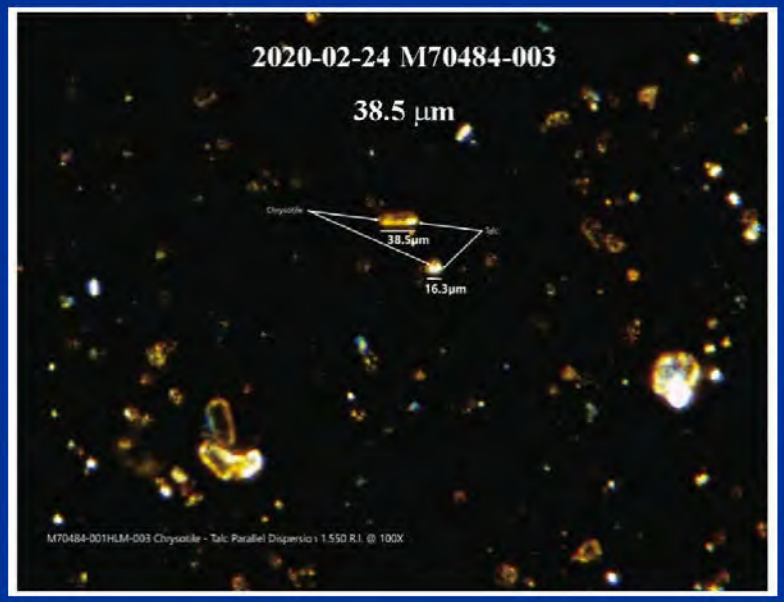

All four chrysotile particles are similar to the particle sizes of the matrix talc particles.

Incorrect Particle Size Measurement Results

2020-02-24 MAS Rpt JBP-Zimmerman

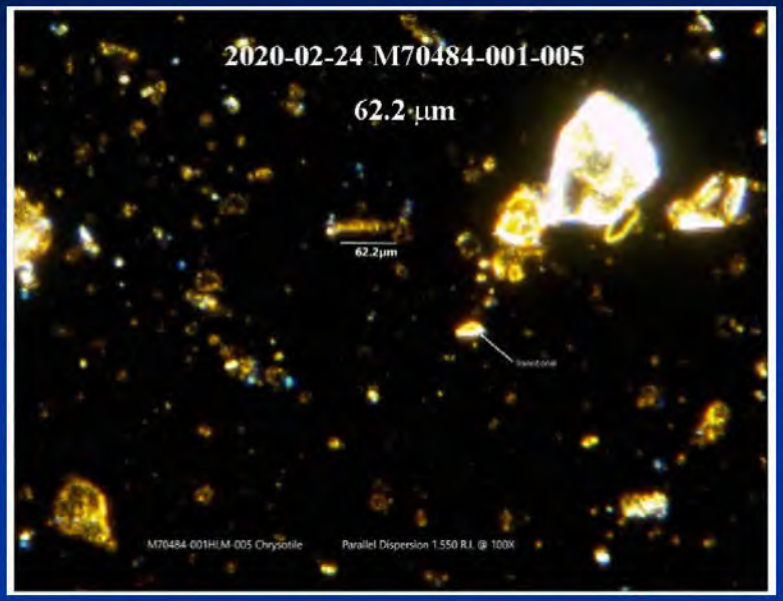

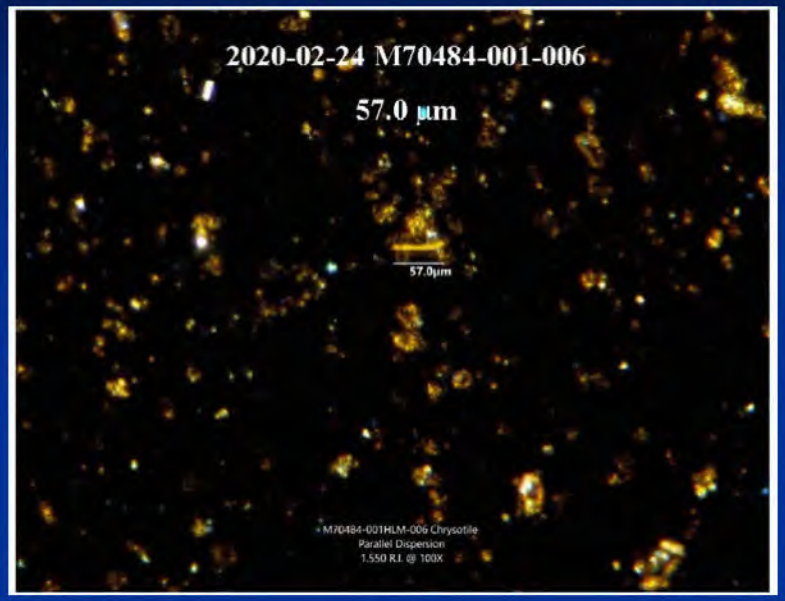

All four chrysotile particles were measured and labeled by MAS.

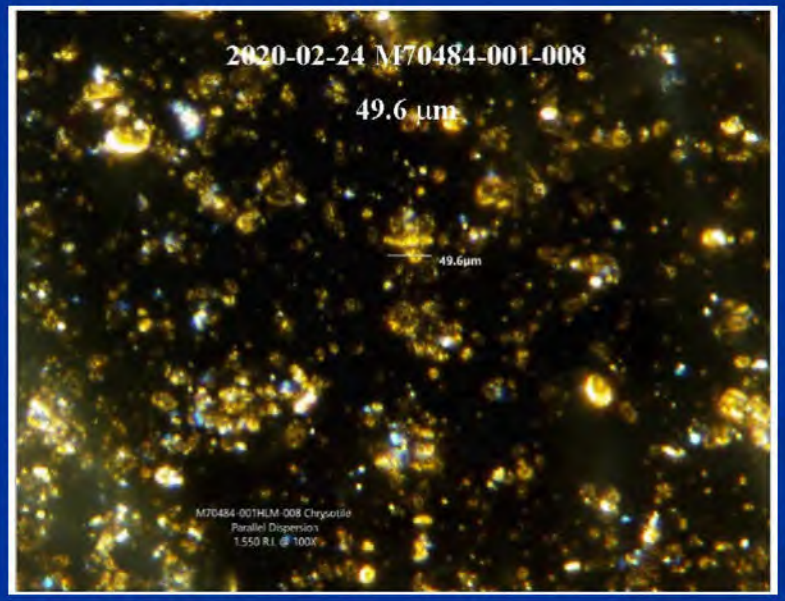

All four chrysotile particles are similar to the particle sizes of the matrix talc particles.

Incorrect Particle Size Measurement Results

2020-02-24 MAS Rpt JBP-Zimmerman

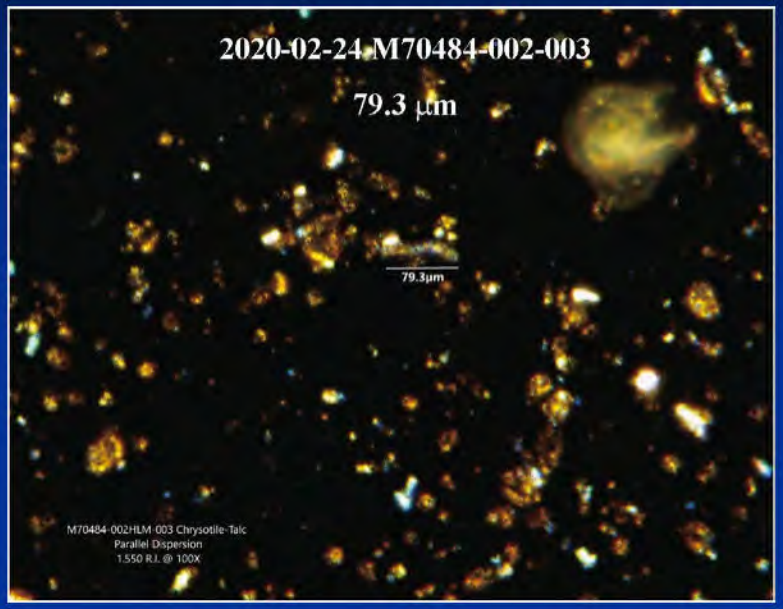

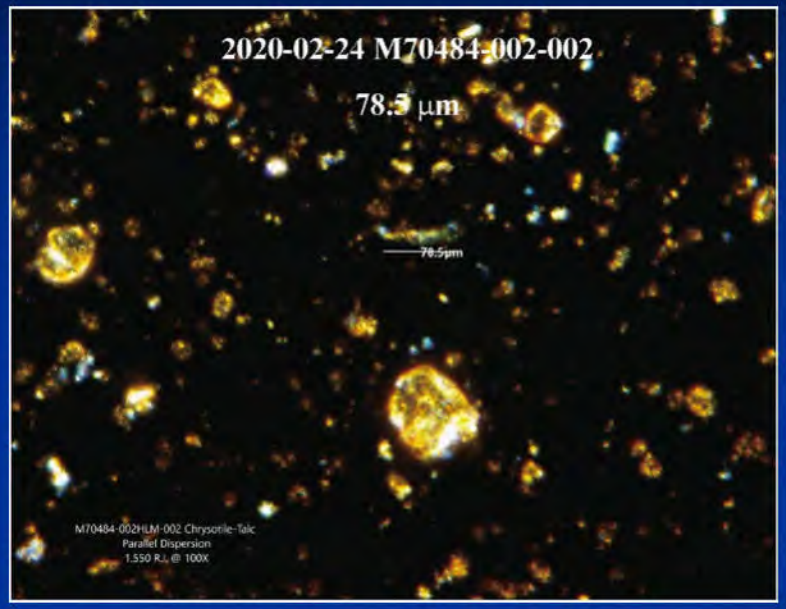

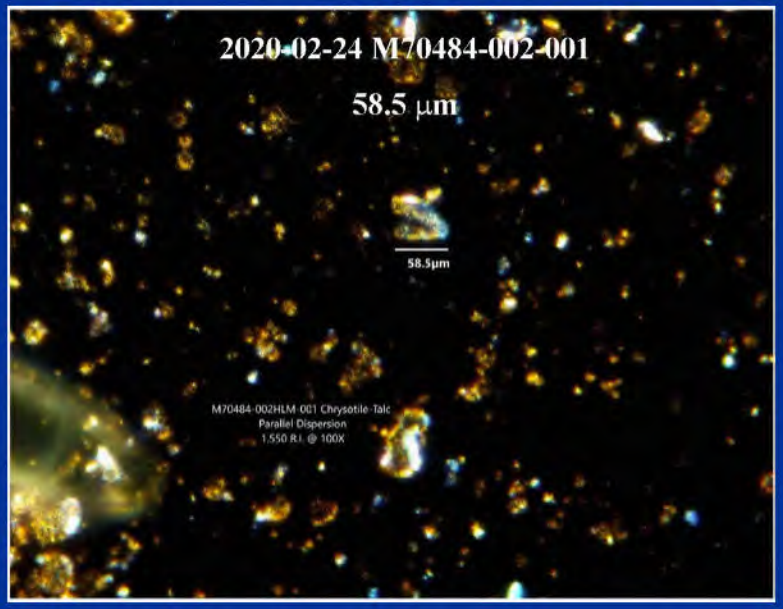

All three chrysotile particles were measured and labeled by MAS.

All four chrysotile particles are similar to the particle sizes of the matrix talc particles.

Incorrect Particle Size Measurement Results

2023-02-28 M71614 Valadez Bottle Report

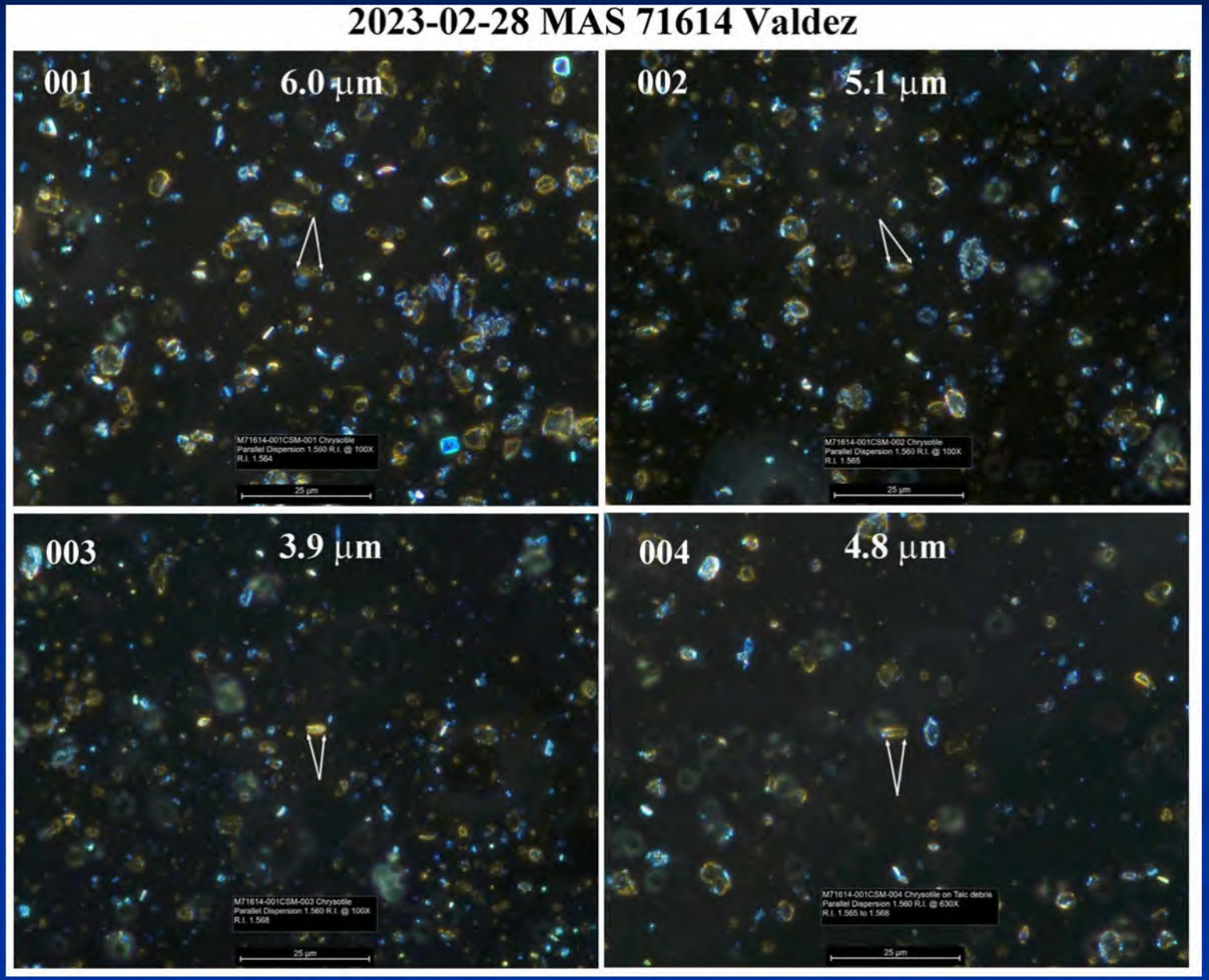

All four chrysotile particles are under 5 micrometers according to the scale bars.

All four chrysotile particles are similar to the particle sizes of the matrix talc particles.

Incorrect Particle Size Measurement Results

2020-03-18 M71095 Rpt JBP-Titley

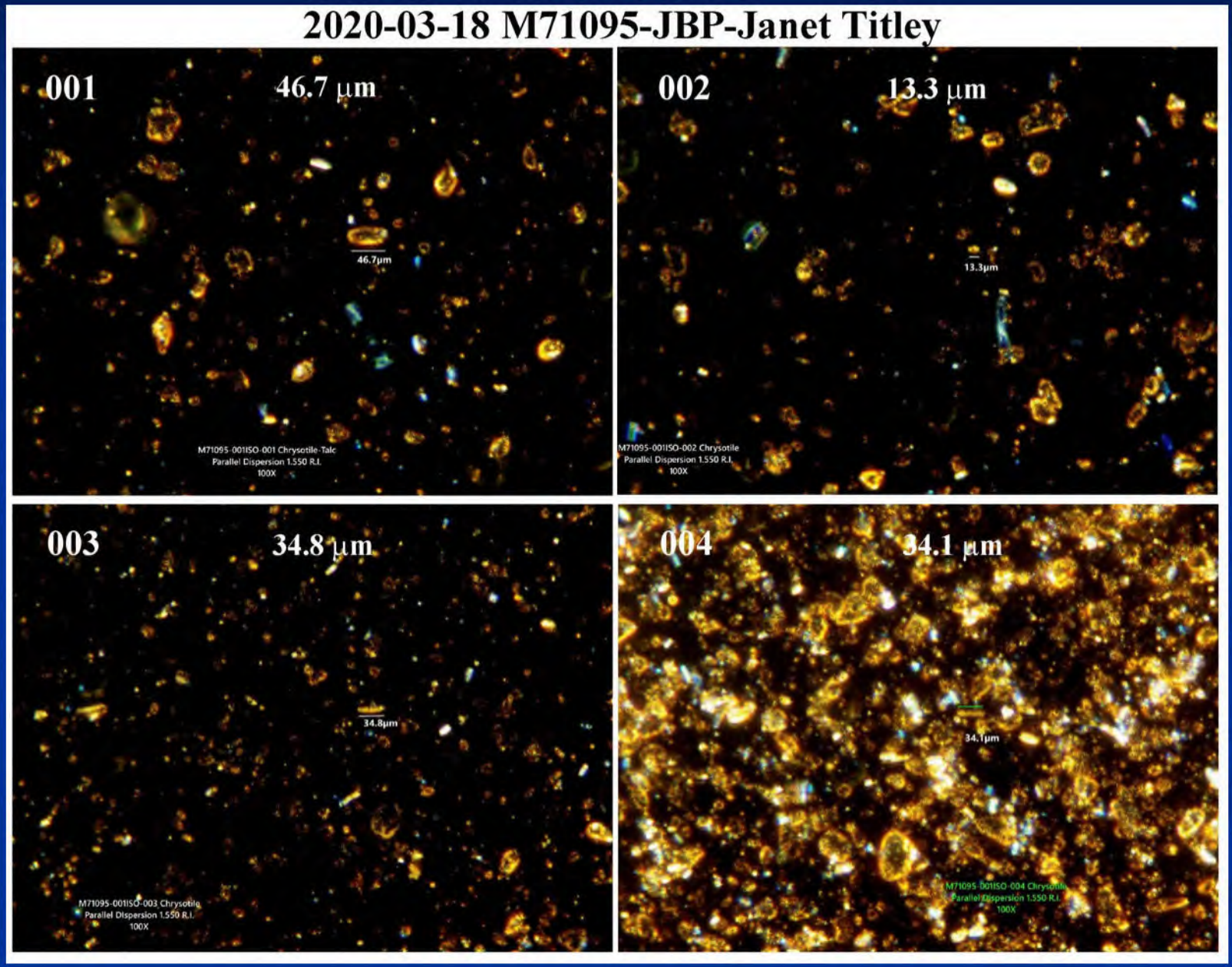

The talc and chrysotile particle sizes of all four samples are much greater than MAS's own data from their SEM analysis.

All four chrysotile particles are similar to the particle sizes of the matrix talc particles.

Incorrect Particle Size Measurement Results

2020-03-20 M70877 Rpt JBP-Doyle

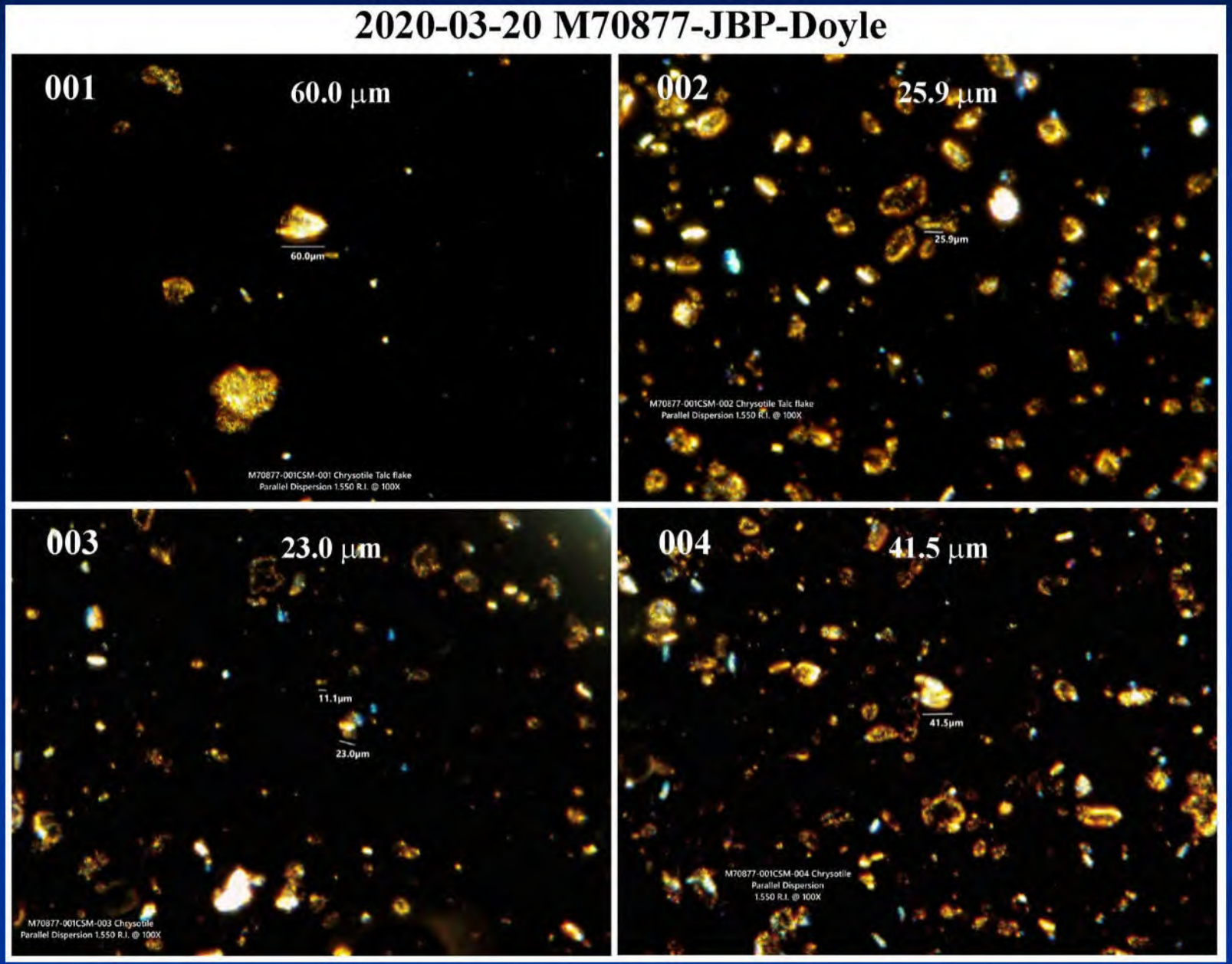

The talc and chrysotile particle sizes of all four samples are much greater than MAS's own data from their SEM analysis.

All four chrysotile particles are similar to the particle sizes of the matrix talc particles.

Incorrect Particle Size Measurement Results

2021-05-25 M71228 OTShelf JBP Purchased Argentina

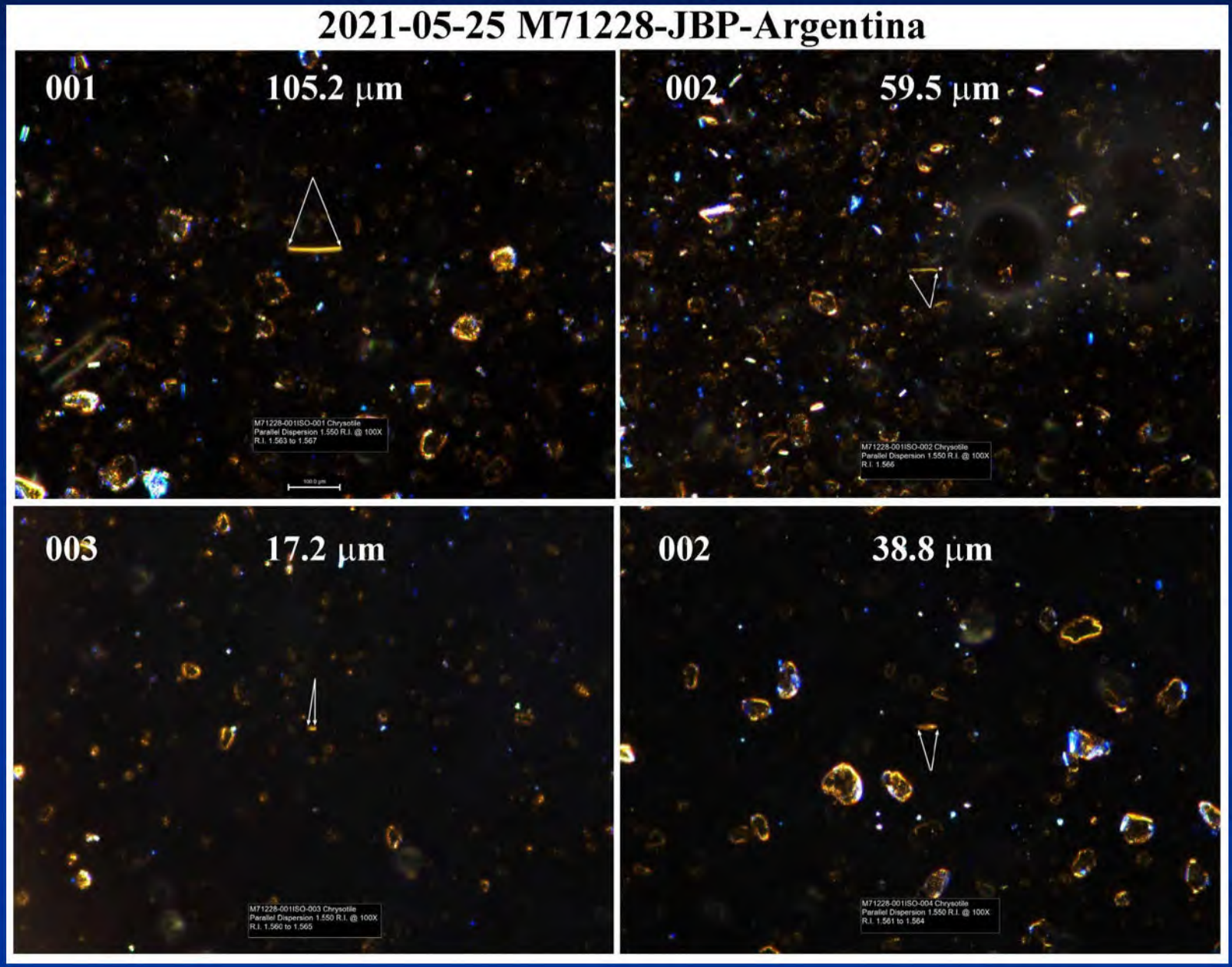

The talc and chrysotile particle sizes of all four samples are much greater than MAS's own data from their SEM analysis.

All four chrysotile particles are similar to the particle sizes of the matrix talc particles.

Incorrect Particle Size Measurement Results

2022-03-11 M71262 Analy of Klayman's JBP & STS Containers

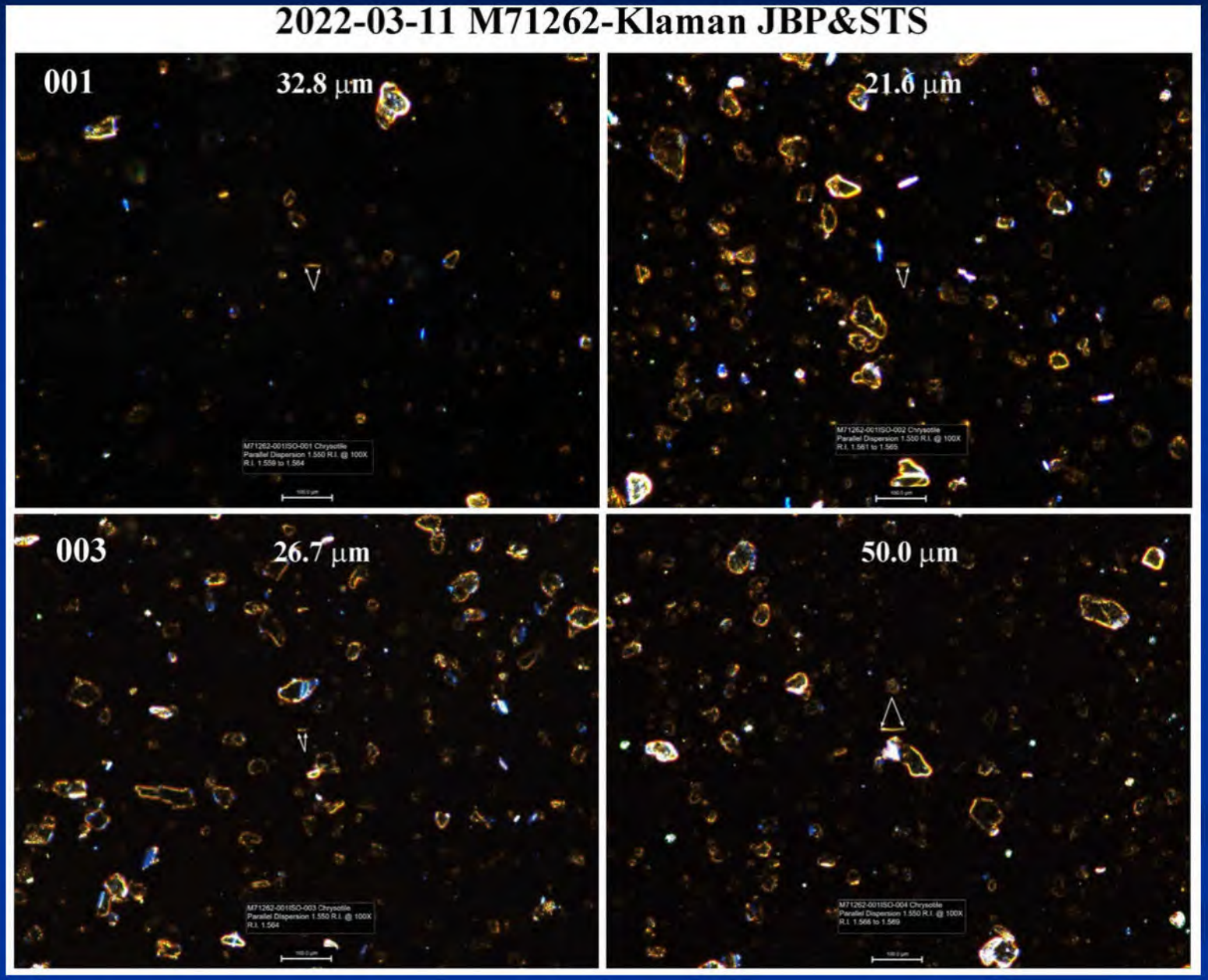

The talc and chrysotile particle sizes of all four samples are much greater than MAS's own data from their SEM analysis.

All four chrysotile particles are similar to the particle sizes of the matrix talc particles.

Incorrect Particle Size Measurement Results

2023-10-19 M71643 Johnson's Baby Powder Compiled Notebook 14-2996

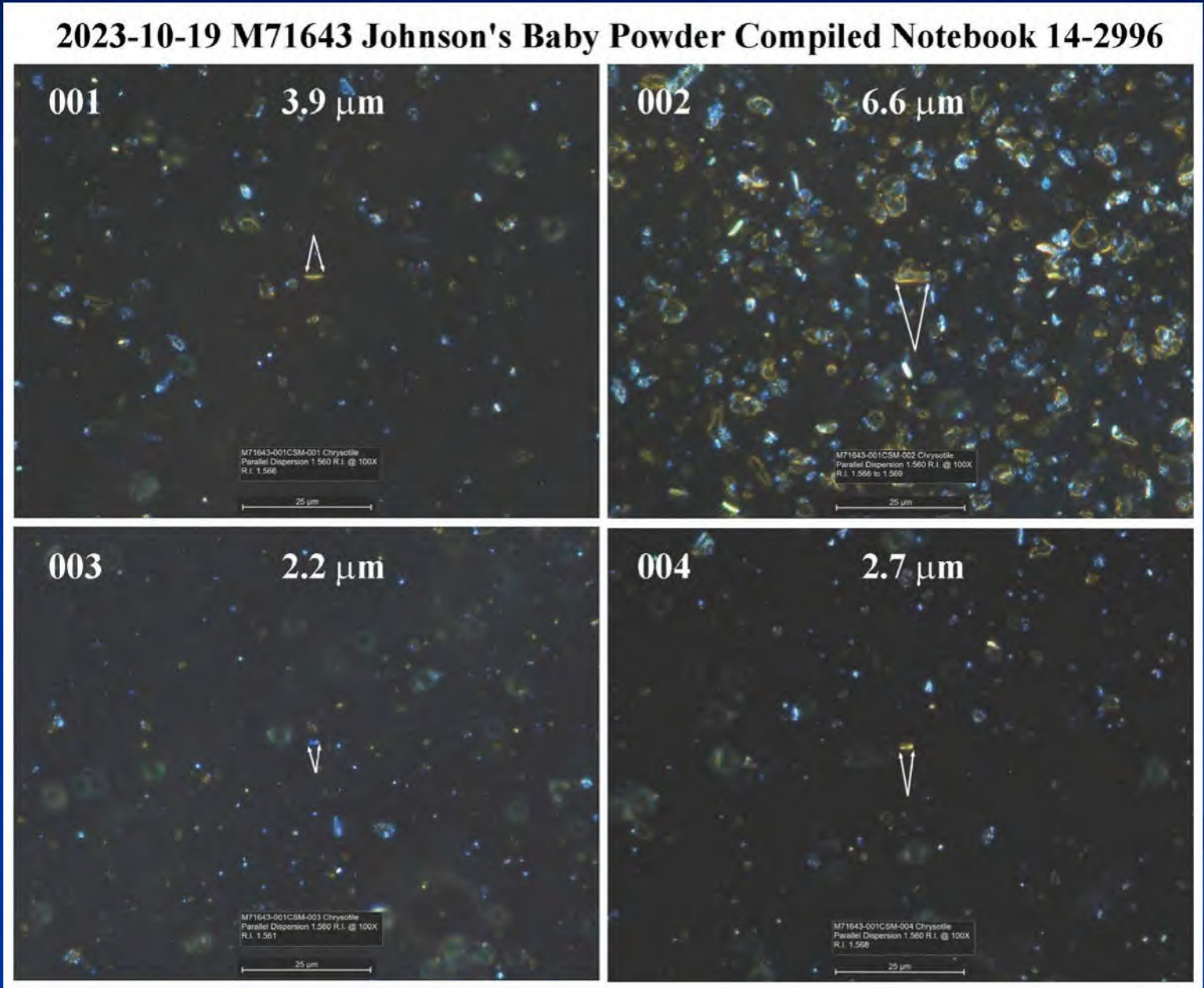

All four chrysotile particles are under 5 micrometers according to the scale bars.

All four chrysotile particles are similar to the particle sizes of the matrix talc particles.

Incorrect Particle Size Measurement Results

2024-02-15 M71740 Analysis of JBP (Rochelle Kirch) Compiled Notebook

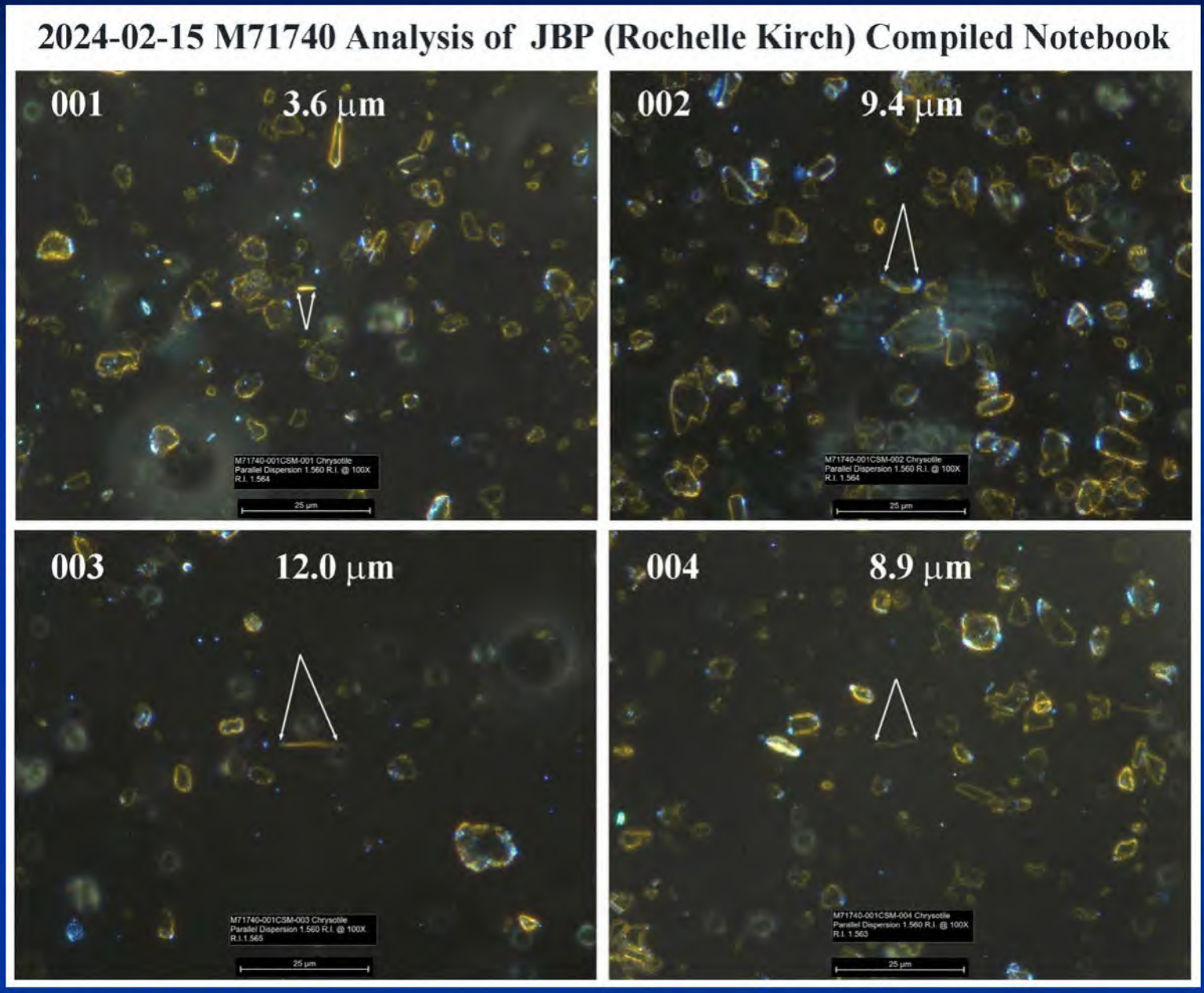

The particle sizes of four chrysotile particles do not conform to MAS's SG-210 Calidria data (2023).

All four chrysotile particles are similar to the particle sizes of the matrix talc particles.

Summary of Eight Particle Size Measurement Results

Date	MAS No.	Chrysotile Length (μm)		
		Individual	Average	vs. Talc
2020-02-24 M70484	001-001	78.8	61.6	Same partcle size range as talc
	001-002	33.3		
	001-003	38.5		
	001-004	71.3		
	001-005	62.2		
	001-006	57.0		
	001-007	70.4		
	001-008	49.6		
	002-001	58.5		
	002-002	78.5		
	002-003	79.3		
2020-03-18 M71095	001-001	46.7	32.2	Same partcle size range as talc
	001-002	13.3		
	001-003	34.8		
	001-004	34.1		
2020-03-20 M70877	001-001	60.0	37.6	Same partcle size range as talc
	001-002	25.9		
	001-003	23.0		
	001-004	41.5		
2021-05-25 M71228	001-001	105.2	55.2	Same partcle size range as talc
	001-002	59.5		
	001-003	17.2		
	001-004	38.8		
2022-03-11 M71262	001-001	32.8	32.8	Same partcle size range as talc
	001-002	21.6		
	001-003	26.7		
	001-004	50.0		
2023-03-28 M71614	001-001	6.0	4.9	Same partcle size range as talc
	001-002	5.1		
	001-003	3.9		
	001-004	4.8		
2023-10-19 M71643	001-001	3.9	3.8	Same partcle size range as talc
	001-002	6.6		
	001-003	2.2		
	001-004	2.7		
2024-02-15 M71740	001-001	3.6	8.5	Same partcle size range as talc
	001-002	9.4		
	001-003	12.0		
	001-004	8.9		

Mineral	Minimum (μm)	Average (μm)	Maximum (μm)	Reference
Talc	1.5	9.3	37.0	MAS (2017)
SG-210 Chrysotile	3.0	8.0	10.0	MAS (2023)

The chrysotile particle sizes of the first three samples were measured and labeled by MAS.

The chrysotile particle sizes of the other five samples were measured in reference to MAS's scale bars.

None of them conforms to MAS's data in the above table.

The particle size range of every chrysotile particle is the same as the matrix talc particles.

There is a great degree of inconsistency in "chrysotile" particle sizes reported by MAS over the last five years.

The only conclusion is that MAS is NOT capable of fixing this systematic error because MAS lacks the ability to perform the most fundamental particle size measuring procedure by PLM.

MAS Misidentified Talc as Chrysotile
Evidence # 2 – Particle Size

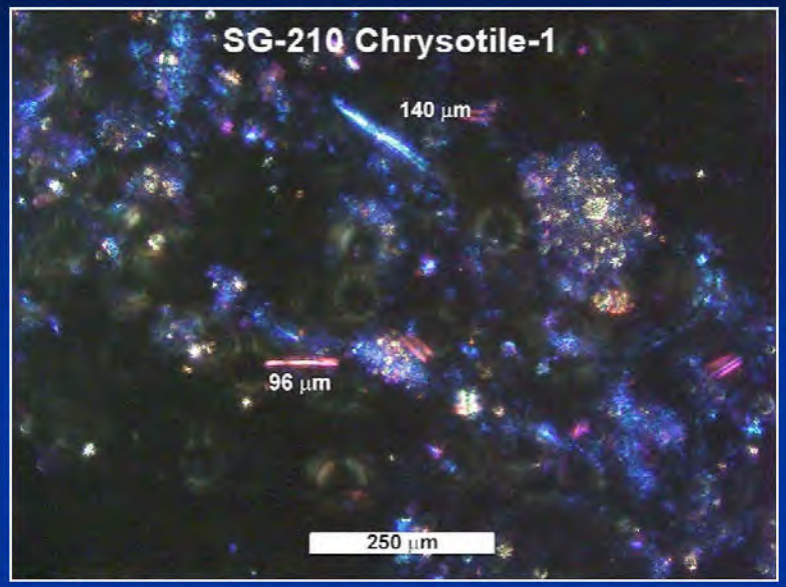

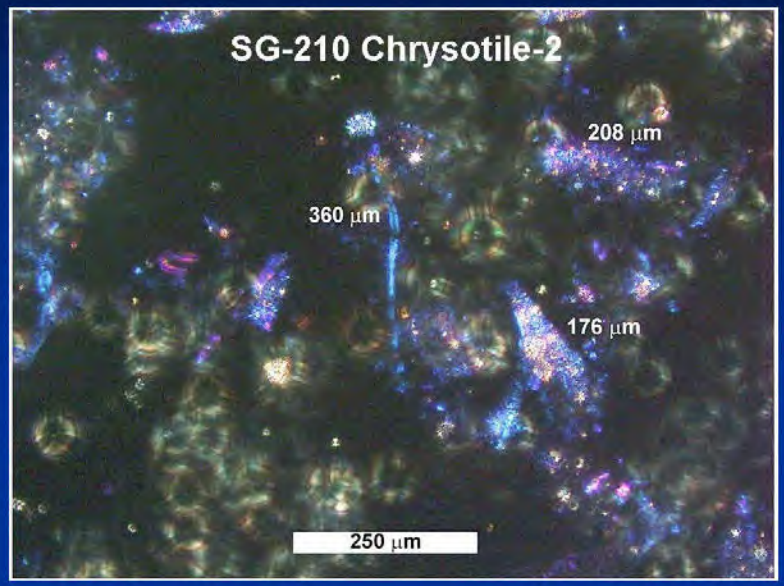

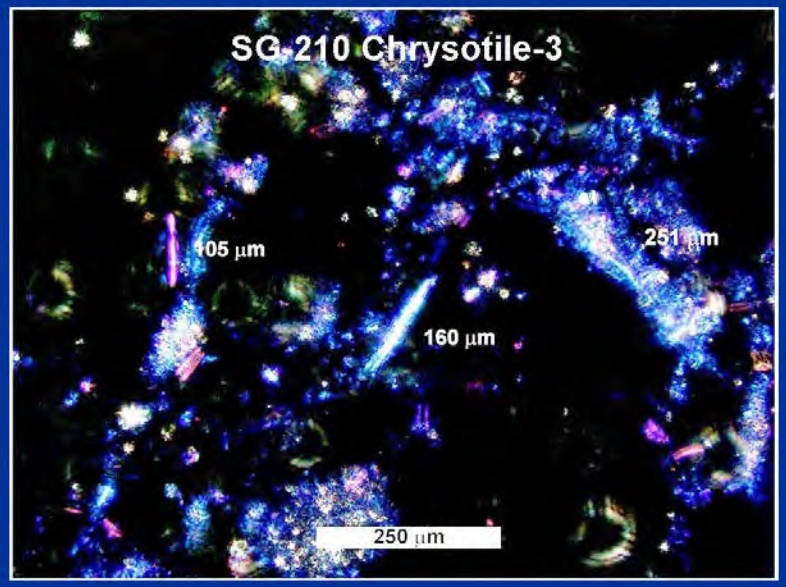

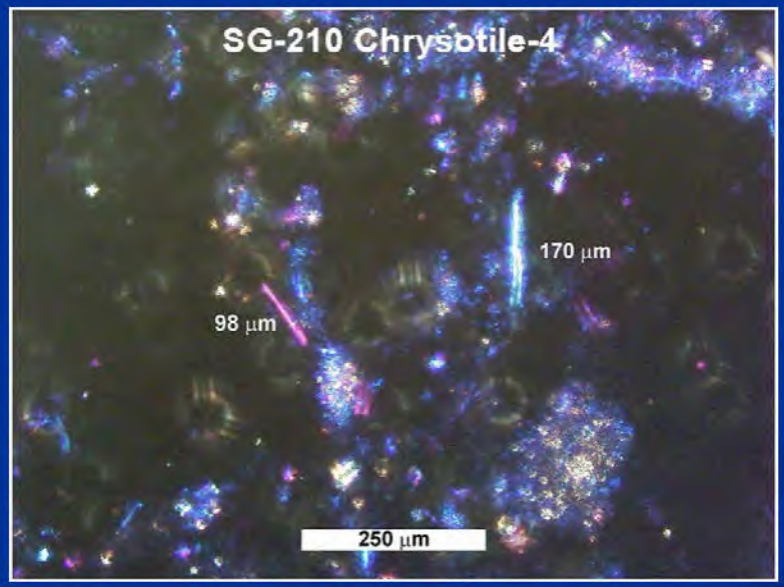

These four images show that Calidria chrysotile structure lengths could be hundreds of micrometers much longer than the 37 micrometers of the SG-210 maximum length reported by MAS.

Tensile Strength of Chrysotile

Structural features of natural and acids modified chrysotile nanotubes

Myroslav Sprynskyy [a], Janusz Niedojadło [b], Bogusław Buszewski [a]

ELSEVIER Chemistry of Solids
Volume 72, Issue 9, September 2011, Pages 1015-1026

Structural features of natural and acids modified chrysotile nanotubes

They are stronger than steel, highly tolerant of corrosion and much cheaper than synthetic fibers. The measured tensile strength of chrysotile fibers has been reported in the range 1.1–4.4 GPa [29].

1.1 to 4.4 GPa or 159,000 – 638,000 Psi

Sprynskyy, M. et. al. (2011) Structural features of natural and acids modified chrysotile nanotubes. Journal of Physics and Chemistry of Solids. Volume 72, Issue 9. Pages 1015-1026. https://doi.org/10.1016/j.jpcs.2011.05.013.

They are stronger than steel, highly tolerant of corrosion and much cheaper than synthetic fibers. The measured tensile strength of chrysotile fibers has been reported in the range 1.1-4.4 Gpa.
Conclusions: The raw chrysotile is presented by bundles of fibers about 50–10 micrometers in size, which are able to splitting with generation of thinner bundles up to one micrometer. The outer diameters of individual nanotubes vary from 15 to 30 nm, while the inner diameters range from 2 to 6 nm. The single chrysolite fibers are presented by cylindrical nanotubes of various forms: rectilinear cylinders (the most widespread), cylinders with cup-like ends, cylinder-in-cylinder and cone-in-cone tubes.

Tensile Strength of Talc

Home > Journal of Packaging Technology and Research > Article

Optimization of Tensile Strength and Shrinkage of Talc-Filled Polypropylene as a Packaging Material in Injection Molding

Research Article
Published: 23 November 2019

Volume 4, pages 69–78, (2020)
Cite this article

Journal of Packaging Technology and Research

Aims and scope →

Submit manuscript →

Abstract

shrinkage of injection-molded TFPP parts under the same molding condition. With the Taguchi optimization approach, it turned out that the tensile strength was increased from 22.07 to 24.40 MPa and the shrinkage was reduced from 3.25 to 2.28%. The optimizing approach and the

2.33 MPa or 338 Psi

Syed, S.F., Chen, J.C. & Guo, G. (2020) Optimization of Tensile Strength and Shrinkage of Talc-Filled Polypropylene as a Packaging Material in Injection Molding. J Package Technol Res 4, 69–78. https://doi.org/10.1007/s41783-019-00077-6

Tensile Strength of Hemp Fibers

Fiber	Tensile strength (MPa)	Young's modulus (GPa)	Density (g cm^{-3})	Refs
Cotton	330–585	4.5–12.6	1.5–1.54	119
Flax	345–1035	27.6–45.0	1.43–1.52	119
Hemp	690–1000	50.0	1.47–1.50	119
Jute	393–800	13–26.5	1.3–1.45	82
Silk	650–750	16	1.3–1.38	82
Kenaf	930	53.0	1.5	119
Ramie	400–1000	61.5	1.5–1.6	119
Sisal	511–635	9.4–15.8	1.16–1.5	119
Banana	500–700	7–20	1.4	120
Softwood	100–170	10–50	1.4	120
Hardwood	90–180	10–70	1.4	120
E-glass	1800	69.0–73.0	2.5	119
HM carbon	2400	380	1.95	121,122
HS carbon	3400	230	1.75	121,122
Kevlar 49	3000	130	1.45	121,122

HM: high modulus, HS: high strength.

690 – 1,000 MPa or 100,050 – 145,000 Psi

Shubhra, T.H. et. al., (2011). Mechanical properties of polypropylene composites: a review. J Thermoplast Compos. 26. 362-391. https://doi.org/10.1177/0892705711428659.

Hemp fiber's tensile strength is slightly lower than chrysotile

Structure of Hemp Fibers

690 – 1,000 MPa or
100,050 – 145,000 Psi

Zhao, S. et. al. (2021) The Physical and Chemical Properties of Hemp Fiber Prepared by Alkaline Pectinase-Xylanase System. https://doi.org/10.21203/rs.3.rs-451112/v1.

Hemp fiber's microtube structure resembles chrysotile

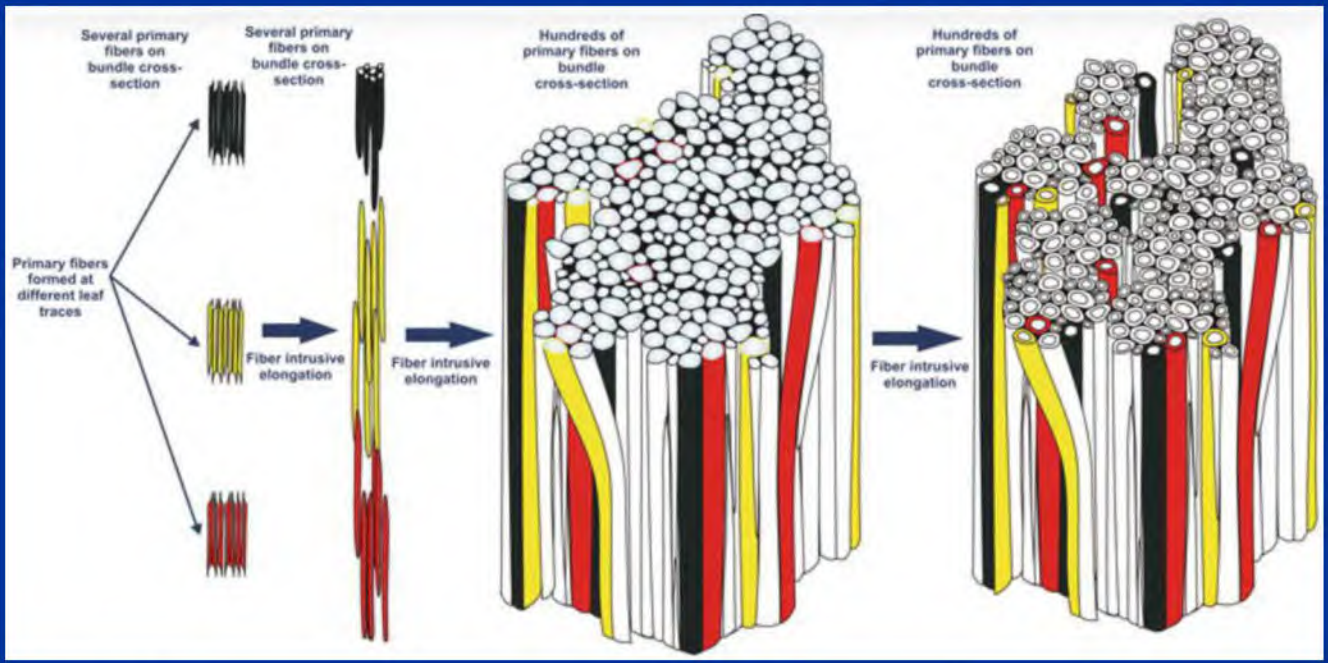

Chrysotile and Talc Are Drastically Different in Tensile Strength

Chrysotile $Mg_3Si_2O_5(OH)_4$

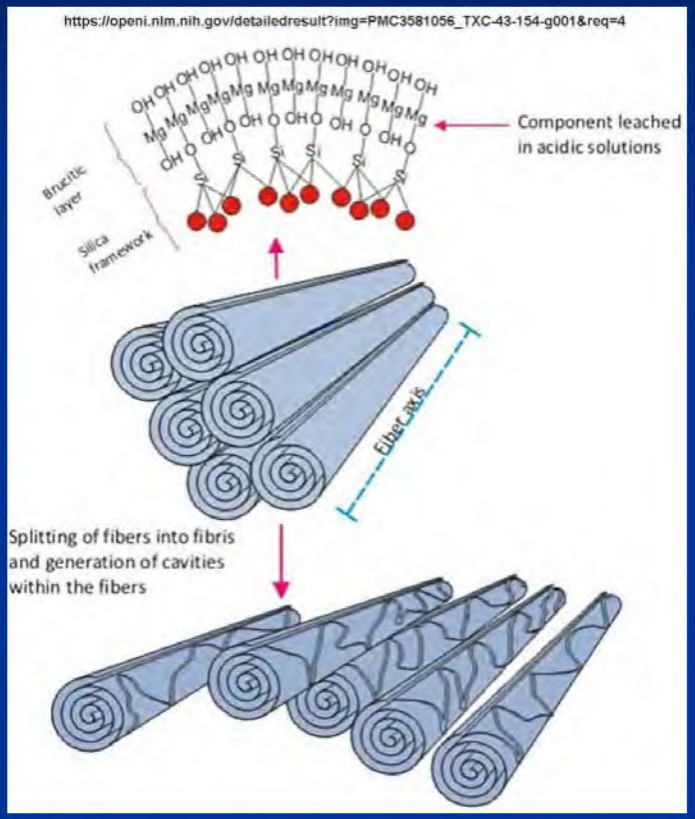

Talc $Mg_3Si_4O_{10}(OH)_2$

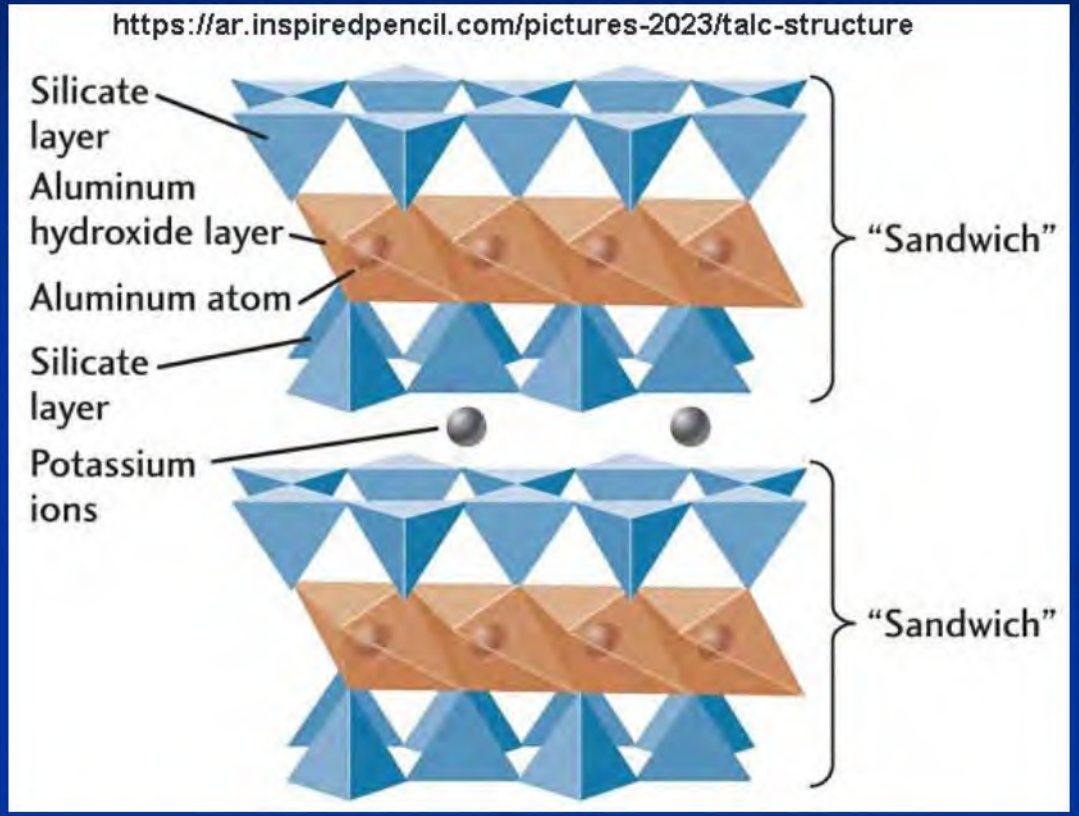

The nanotube structure makes the chrysotile even stronger.

Bonding is weak between and within TOT layers, making talc easily crushable.

Chrysotile's tensile strength is more than 30 times that of talc. With such a high tensile strength, chrysotile does not break down into 325 mesh-size or < 44 μm particles in the milling process of talc.

Chrysotile and Hemp Fiber Are Similar in Tensile Strength

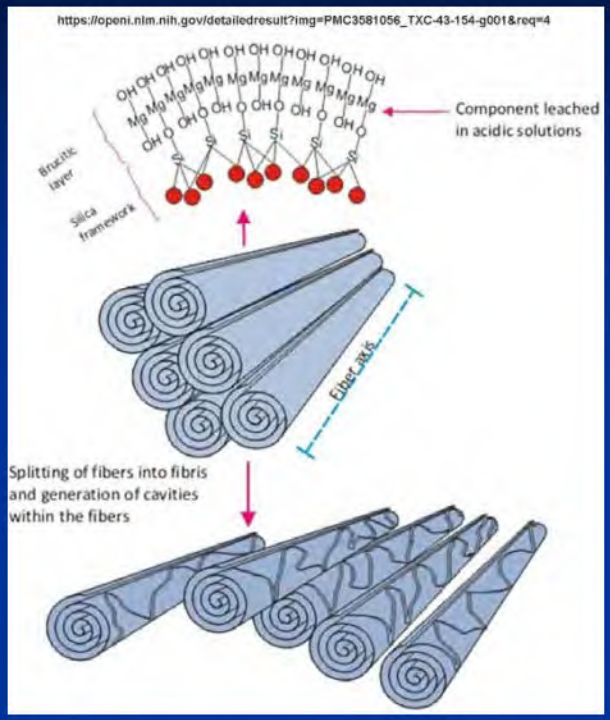

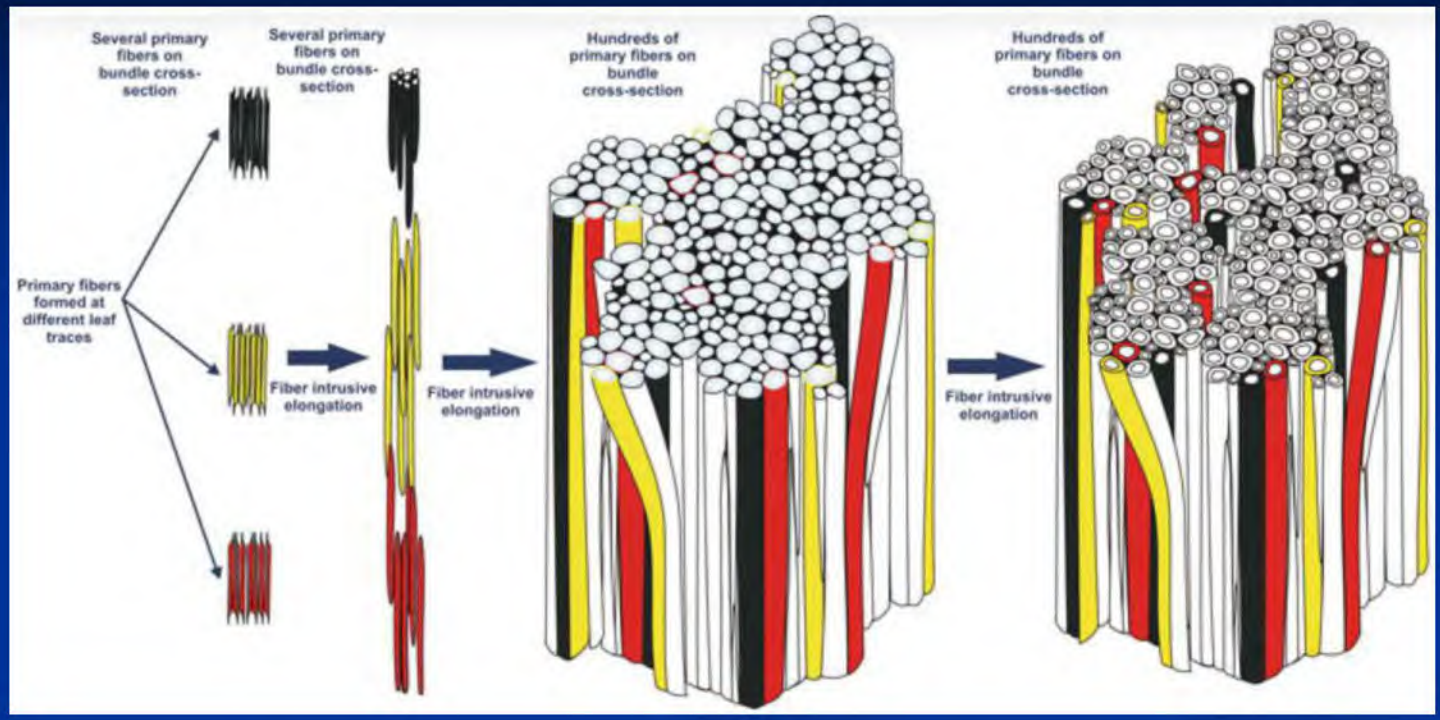

- **The hemp's microtube structure is similar to the nanotube structure of chrysotile, making it also very strong.**
- **Their tensile strengths are similar.**
- **Both are used as the reinforcement components of composite materials**

How Strong Are Chrysotile and Hemp Fiber?

The strong chrysotile fibers are used for various applications.

The strong hemp fibers are used for the construction composite materials.

How These Materials Behave During Mechanical Grinding?

Their high tensile strength and strong bonding make them hard to break into fine powders.

Their softness and weak bonding make them easily break into fine powders.

When Crystal Sugar and Hemp Fibers Are Ground Together

If hemp fibers and sugar crystals are ground together

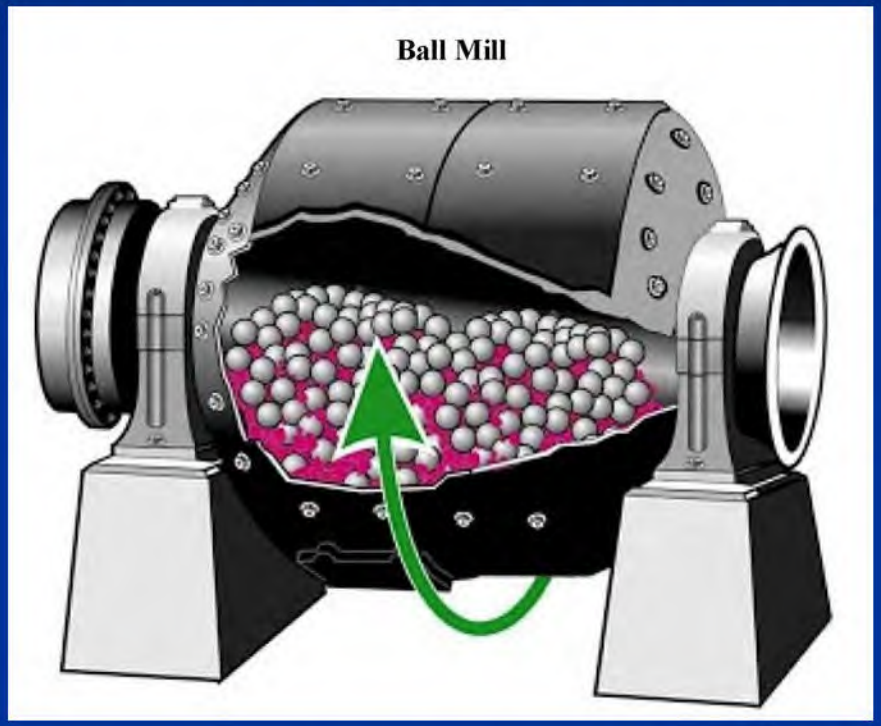

The same is true for talc and chrysotile. USP's research work has proven it.

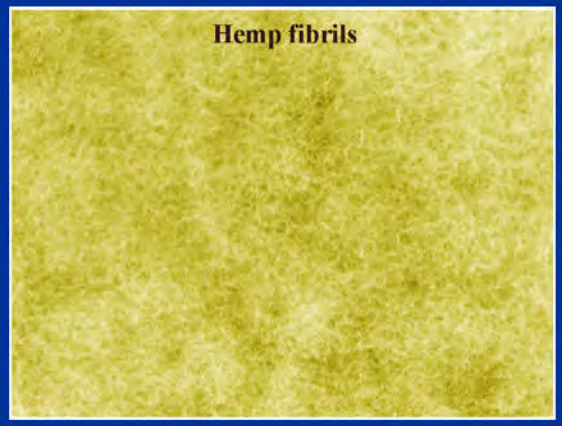

Hemp fibers are crushed and broken into fibrils, but not into fine powders like sugar crystals.

Sugar crystals quickly break into fine powders

USP's experts have conducted extensive research on the topic of asbestos-containing talc.

They wanted to find out how the finished talcum baby powder product should look if the raw talc material contained asbestos.

They spiked an asbestos-free talc sample with asbestos minerals chrysotile and tremolite from NIST SRM 1866 at different concentration levels.

To mimic the baby powder manufacturing process, they ground the asbestos-spiked talc sample inside a balling mill until the talc's particle size reached the commercial specification of the finished baby powder product: under 44 micrometers.

USP's experts studied the finished baby powder samples using various microscopic techniques. The following are pictures taken under optical microscope.

NIST Standard Chrysotile in Talcum Powder (USP, 2022)

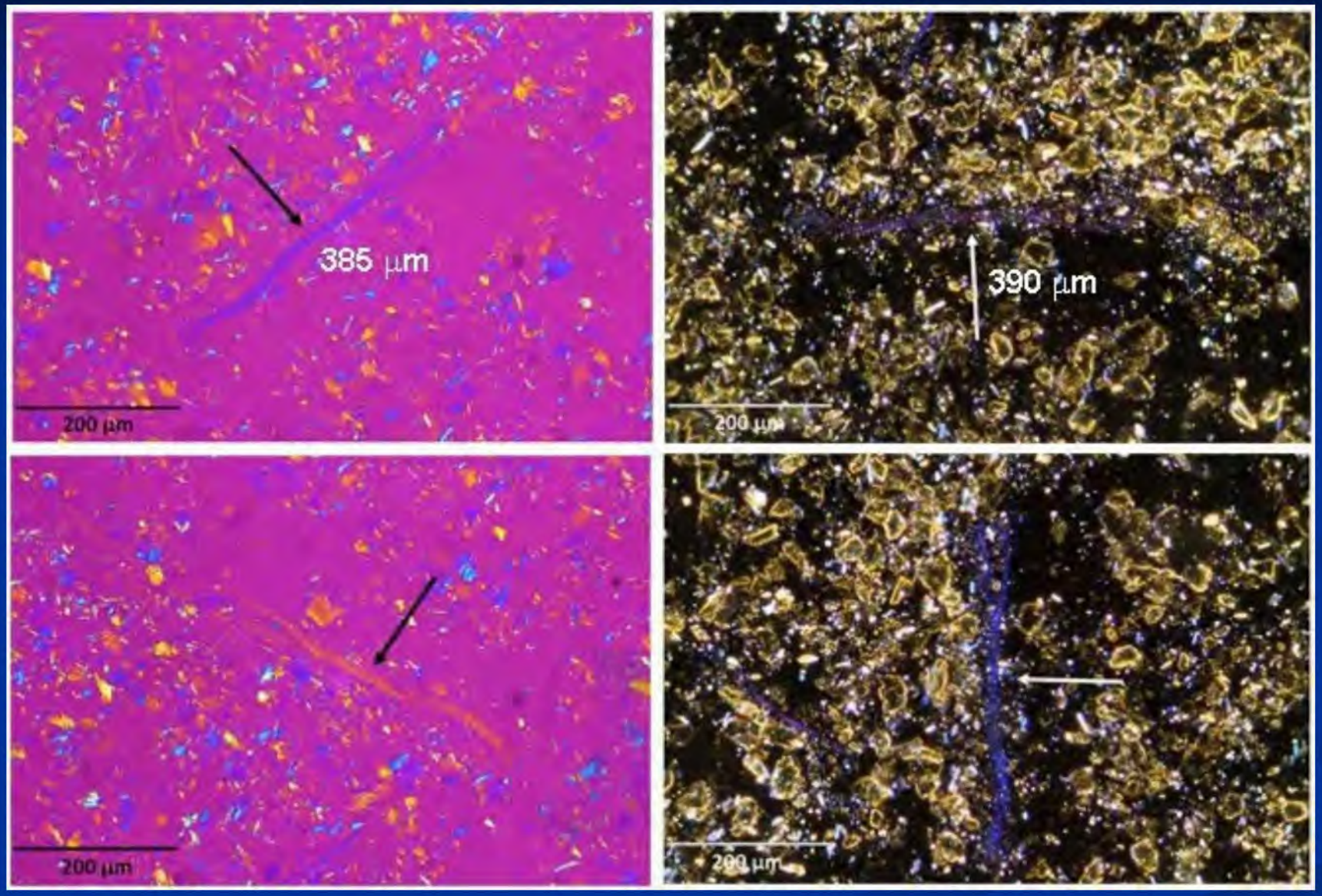

0.1% standard Chrysotile-spiked talc. Chrysotile fibers' lengths are much longer than talc particles.

NIST Standard Chrysotile in Talcum Powder (USP, 2022)

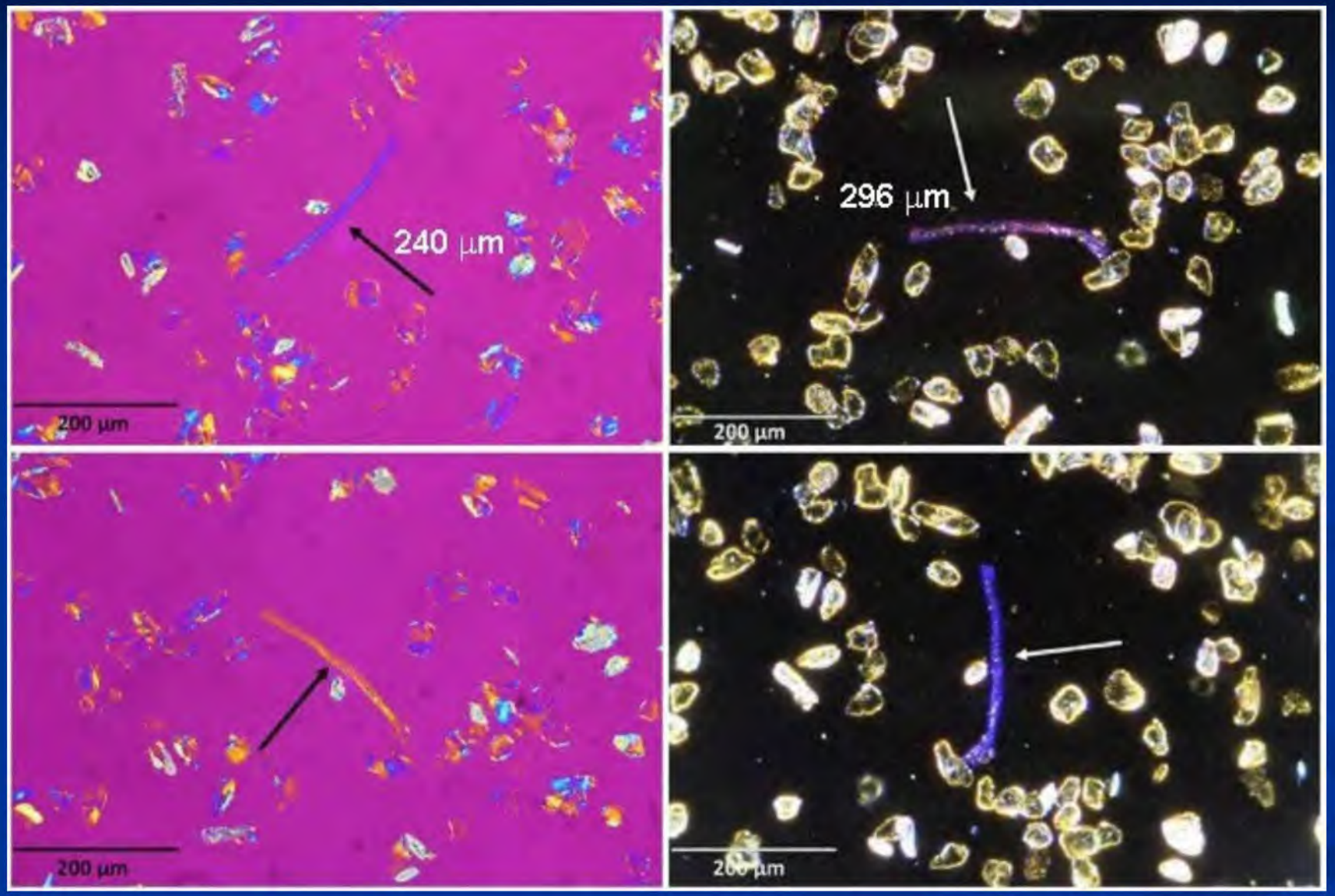

0.01% standard Chrysotile-spiked talc. Chrysotile fibers' lengths are much longer than talc particles.

NIST Standard Chrysotile in Talcum Powder (USP, 2022)

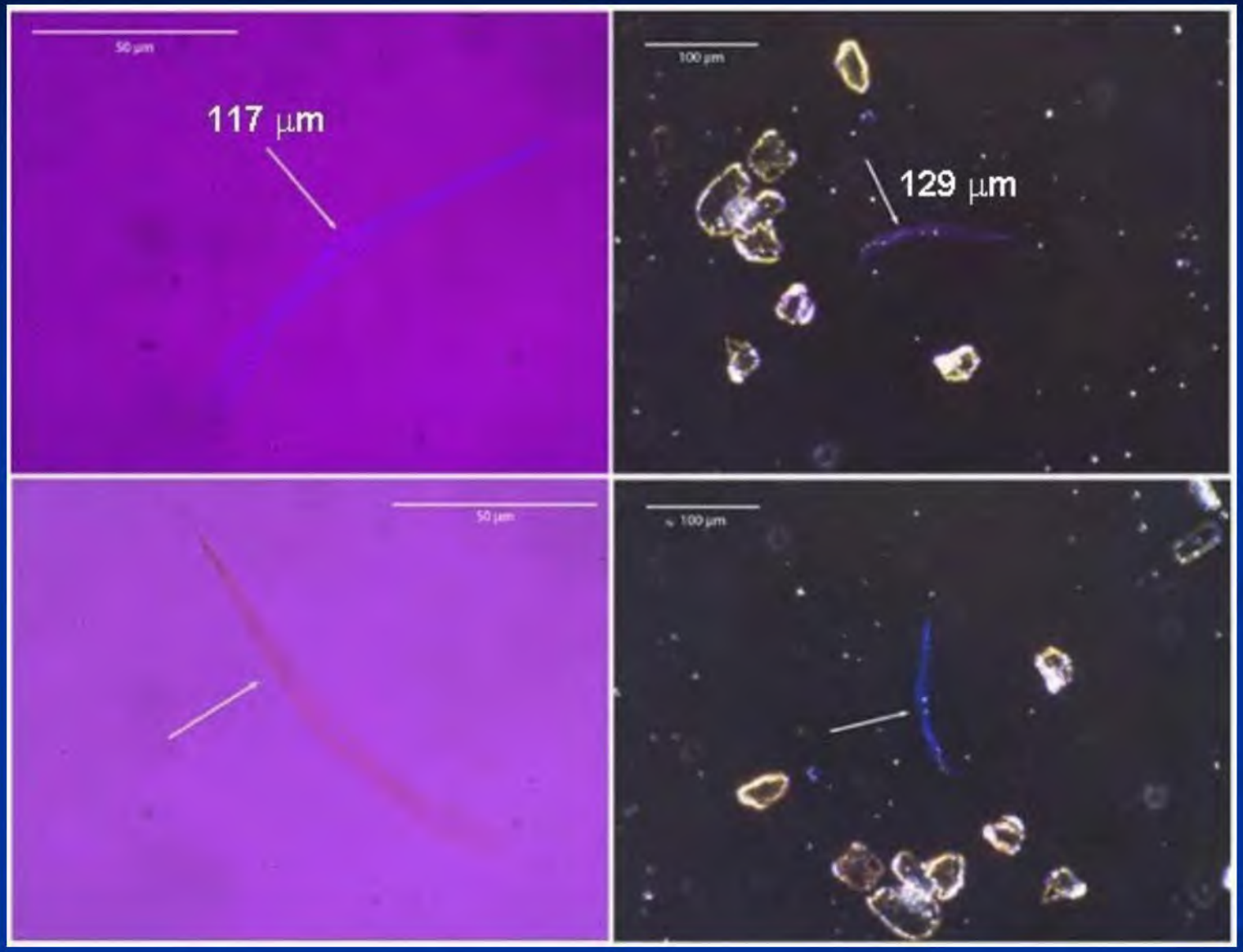

0.001% standard Chrysotile-spiked talc. Chrysotile fibers' lengths are much longer than talc particles.

Calidria Chrysotile in Talc Powder Samples

The above are all NIST standard chrysotile.
How about Calidria chrysotile?

Calidria Chrysotile in Talcum Powder (Pier, 2017)

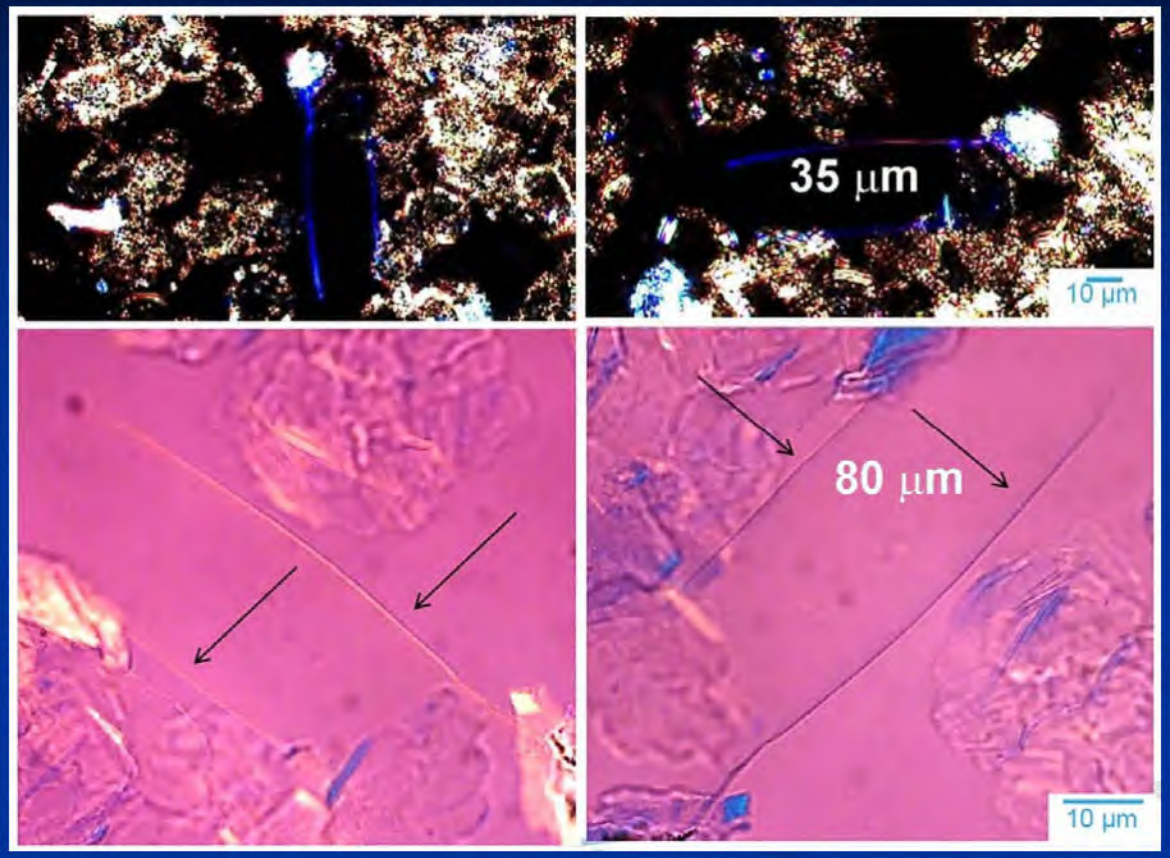

0.05% Calidria chrysotile-spiked talc powder under PLM.
After talc is ground into the baby powder particle sizes (325 mesh or < 44 μm),
There are still longer (80 mm) Calidria chrysotile in the sample.

Conclusions Derived from the Above Evidence

- **The minute amount (e.g. 0.0003 – 0.0006%) of chrysotile found in J&J baby powder products by MAS must have been formed together with talc during the geological formation process. When the raw talc rock ore is used to produce baby powder products, the chrysotile is ground together with talc in balling mills.**
- **Because of its extremely high tensile strength chrysotile crystals do not break down to the same particle size range as talc crystals. Therefore, the particles of the same size as talc particles cannot be chrysotile.**

Dr. Shu-Chun Su's Analysis of MAS's Analytical Results

Incorrect Quantification Procedure

MAS's Quantitation Procedure Defies Common Sense

REMOTE DEPOSITION OF WILLIAM E. LONGO, PhD
March 22, 2024

Page 150

So, okay, well, let's -- and that's why the SG-210 is so valuable because it's about the same size.

So then you take what the recovery is, you know, and then you can calculate what -- all our reports will have a weight corrected, that's the measurement of the difference between the heavy fraction and the light fraction.

Q. And the percentage reporting, is that like a qualitative visual estimate from what the analyst is seeing on the slides as opposed to a quantitative calculation when I look at that, your PLM reports on chrysotile on Johnson & Johnson samples?

A. Yes. There's only two ways that you can do the estimated weight percent. You can do point counting, which we don't do because we found it not very accurate, but you have a visual estimate of the percentage you're seeing and that's what you write down, and it's usually a range.

Q. Okay. That's what your laboratory does, this sort of visual estimate of what you're seeing in terms of area by a percent basis, right?

A. Right.

Q. Okay. And then when I see -- you know, when you report that in terms of chrysotile bundles per gram, the way that you calculate that number for

Priority-One Court Reporting Services Inc. – A Veritext Company
718-983-1234

In Dr. Longo's deposition on March 22, 2024 he claims that EPA's Point Counting is not very accurate and used Visual Estimate for quantitation

MAS Did Not Follow EPA's Quantitation Procedure

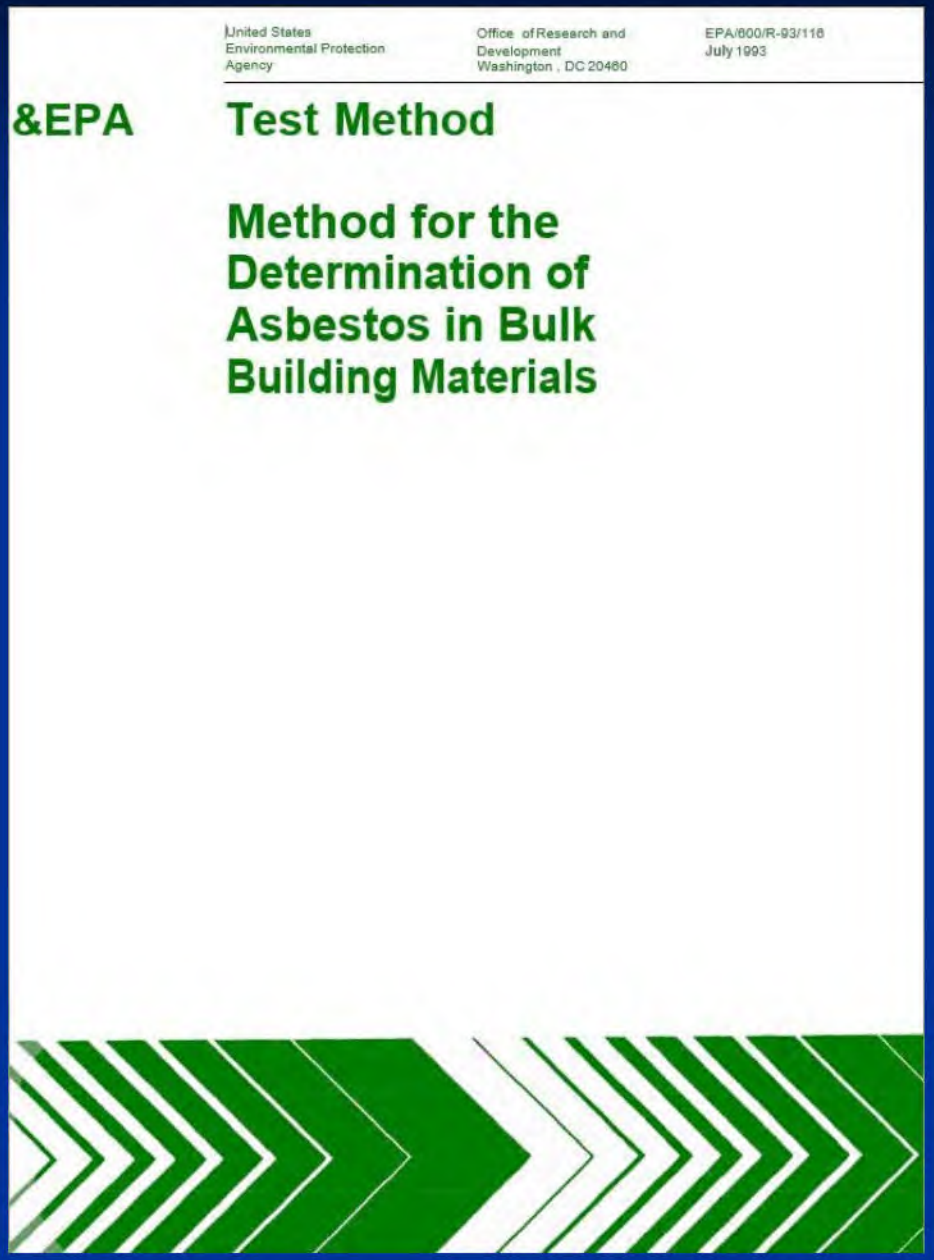
United States Environmental Protection Agency | Office of Research and Development Washington, DC 20460 | EPA/600/R-93/116 July 1993

&EPA

Test Method

Method for the Determination of Asbestos in Bulk Building Materials

Baby powder is a friable material.

This Latin adjective comes from the verb "friare," which means "**to crumble**." "Friare" in turn is related to the verb "fricare" ("to rub"), the source of the English noun "friction." "Friable" is used to describe something that can be easily reduced to a powdered form. In contemporary usage, it is often found in the discussion of asbestos.

Friable Definition & Meaning - Merriam-Webster

Point counting quantitation is required by U.S. EPA (1982) EPA-600-82-020 Interim method for the determination of asbestos in friable materials.

1.7.2.4 Quantitation of Asbestos Content

Asbestos quantitation is performed by a point-counting procedure.

MAS did not follow the official EPA 600 M4 82-200 point counting procedure for quantitation of asbestos content in friable materials.

Reference Chart for Visual Estimate (Su, 2022)

THE MICROSCOPE
Vol. 69:4, pp 160–162, 2022
https://doi.org/10.59082/RFCG4507

Area Percentage Charts to Aid Visual Estimation of Asbestos Concentration in Bulk Asbestos Samples

Shu-Chun Su, Ph.D.
Technical Expert, National Voluntary Laboratory Accreditation Program
National Institute of Standards and Technology

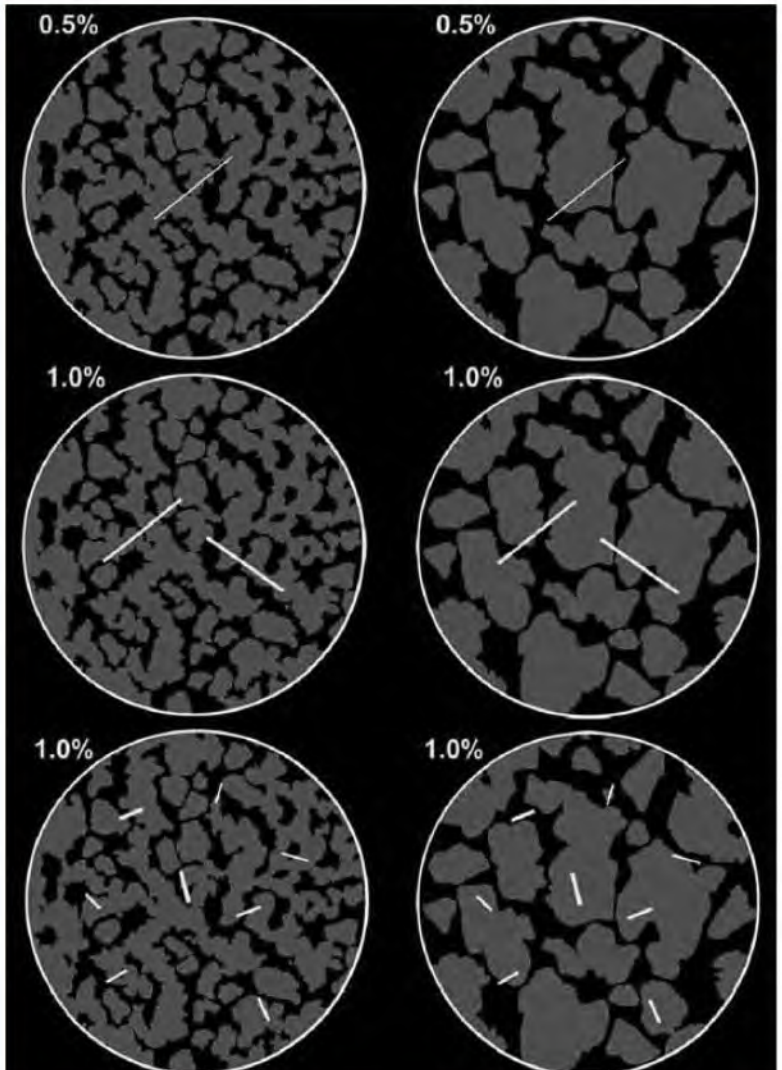

Figure 3. 0.5–1.0% with 65% of the field of view filled with matrix.

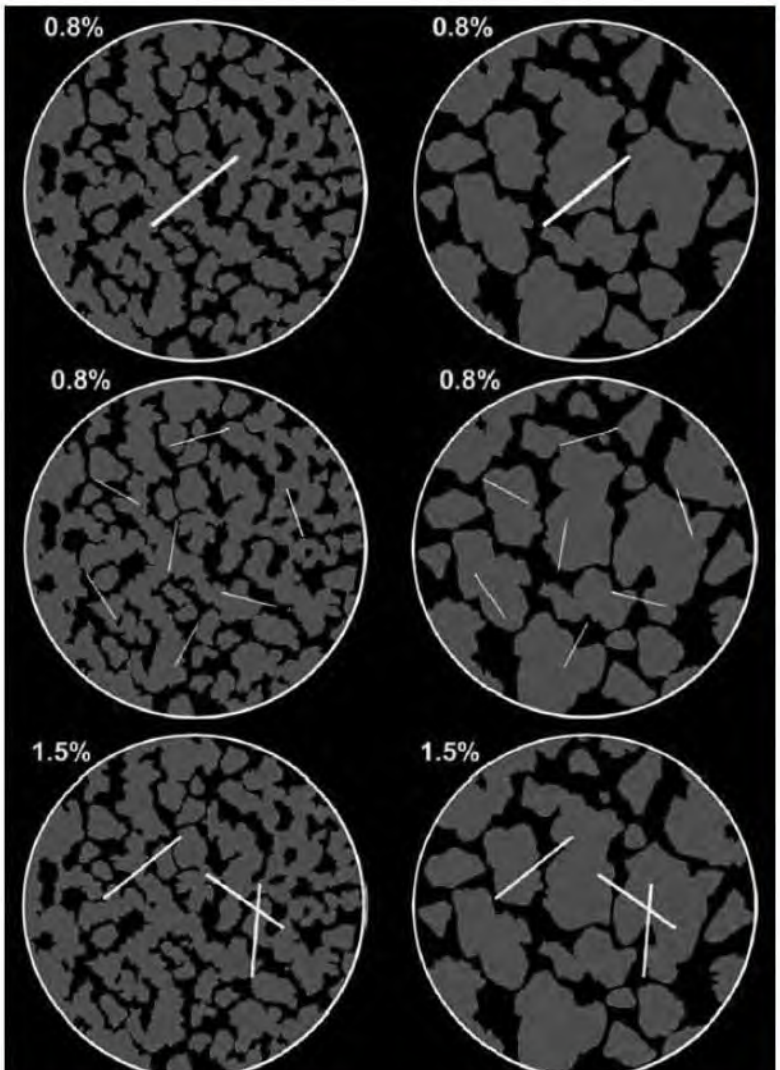

Figure 4. 0.8–1.5% with 65% of the field of view filled with matrix.

These are the asbestiform reference charts at 0.X% to meet AHERA requirement for differentiating ACM (asbestos containing material) from Non-ACM. The differentiating factor is 1% by weight:

ACM > 1%
Non-ACM ≤ 1%
These charts have been widely used by US asbestos laboratories and were formally published in 2022 by Shu-Chun Su.

Can the Asbestos% in the Image be Visually Estimated?

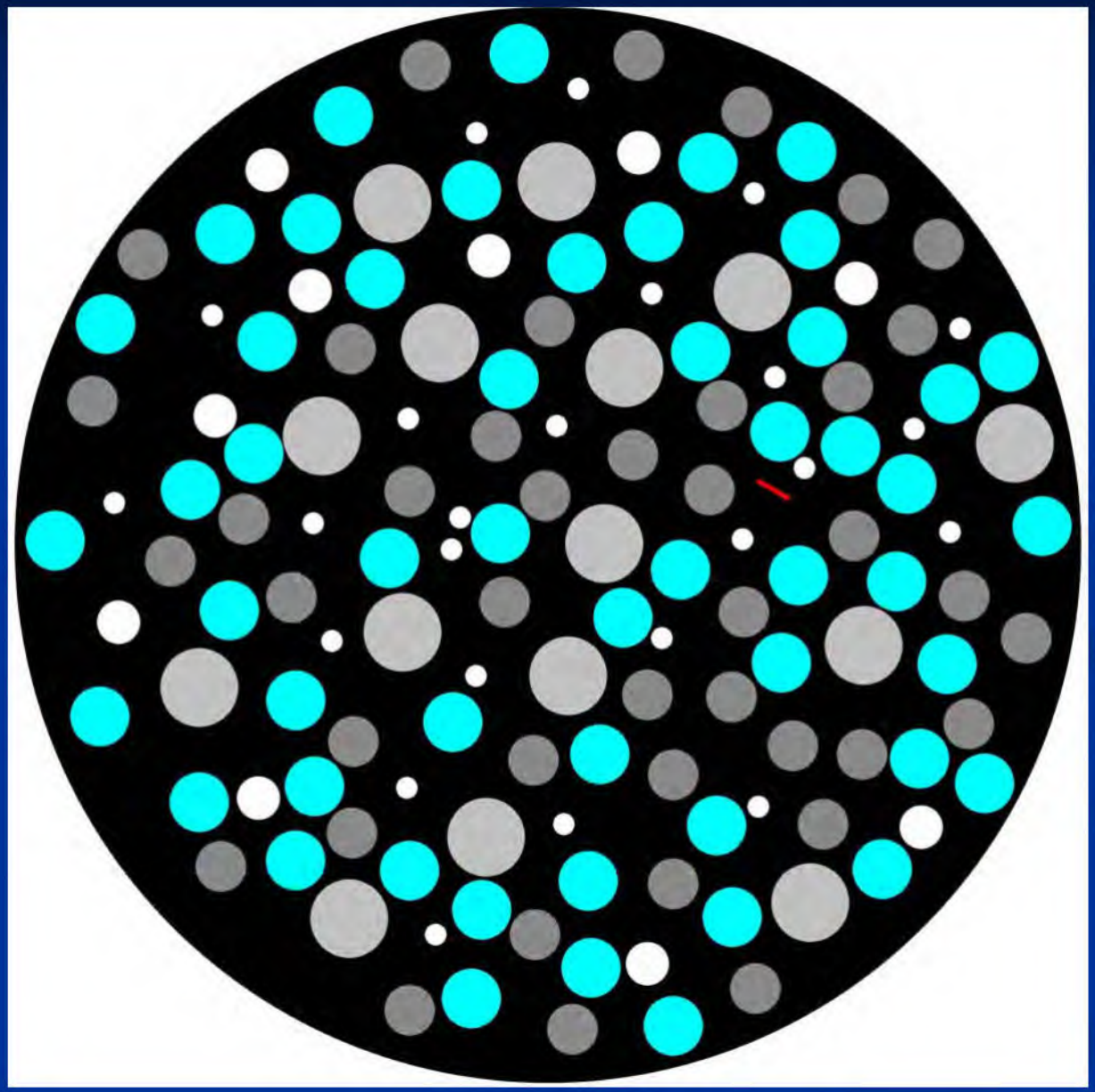

The red fiber is asbestos. The round objects are talc particles.

There is no established analytical protocol to do Visual Estimate at such low concentration levels.

Can 0.002 – 004% Be Visually Estimated?

2023-02-28 - Valadez Bottle Report

Table 2
Overall Summary of the JBP Asbestos Sample Analysis Results

MAS Sample #	ATEM Amphibole Asbestos	ISO-NY PLM Wt. % Amphibole Asbestos	CSM-PLM w/o HLS Chrys %	CSM Weight Recovery Light fraction	CSM Chrys % Weight Corrected**
M71614-001	<52,000	NSD	0.002-0.004	15.8%	0.0003-0.0006

*NSD: No Structure Detected **Weight Corrected

- According to Dr. Longo's March 22, 2024 deposition, the 0.002 – 004% CSM-PLM w/o HLS Chrys% was visually estimated.
- Can anyone visually estimate the red fiber's percentages among the matrix round objects?

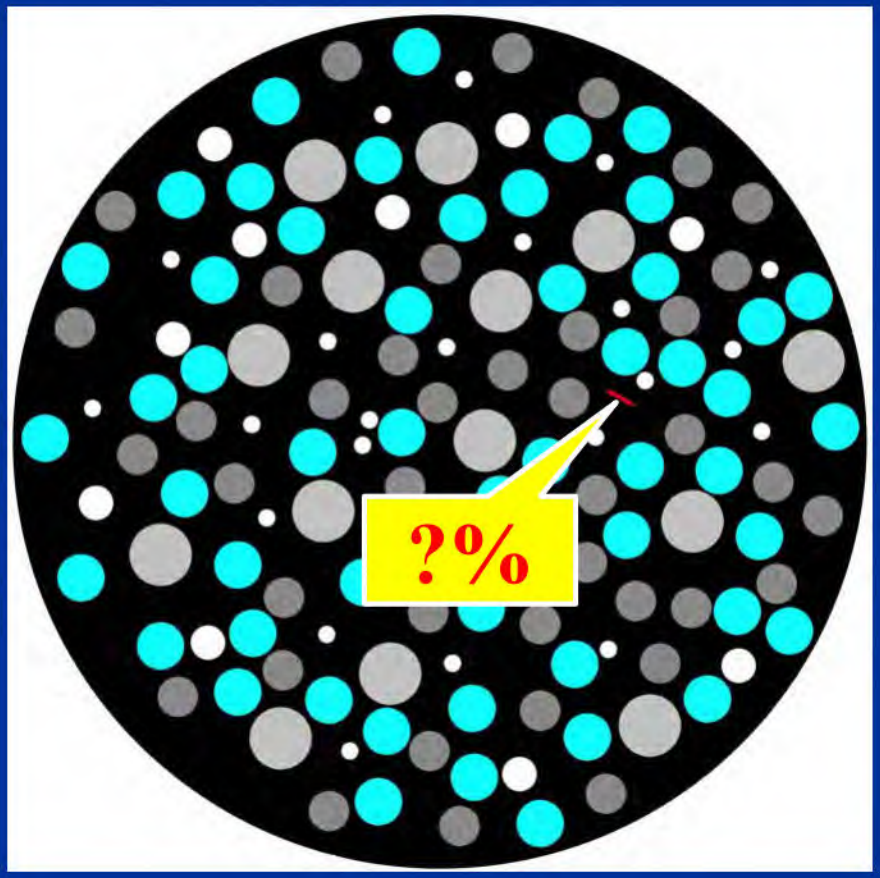

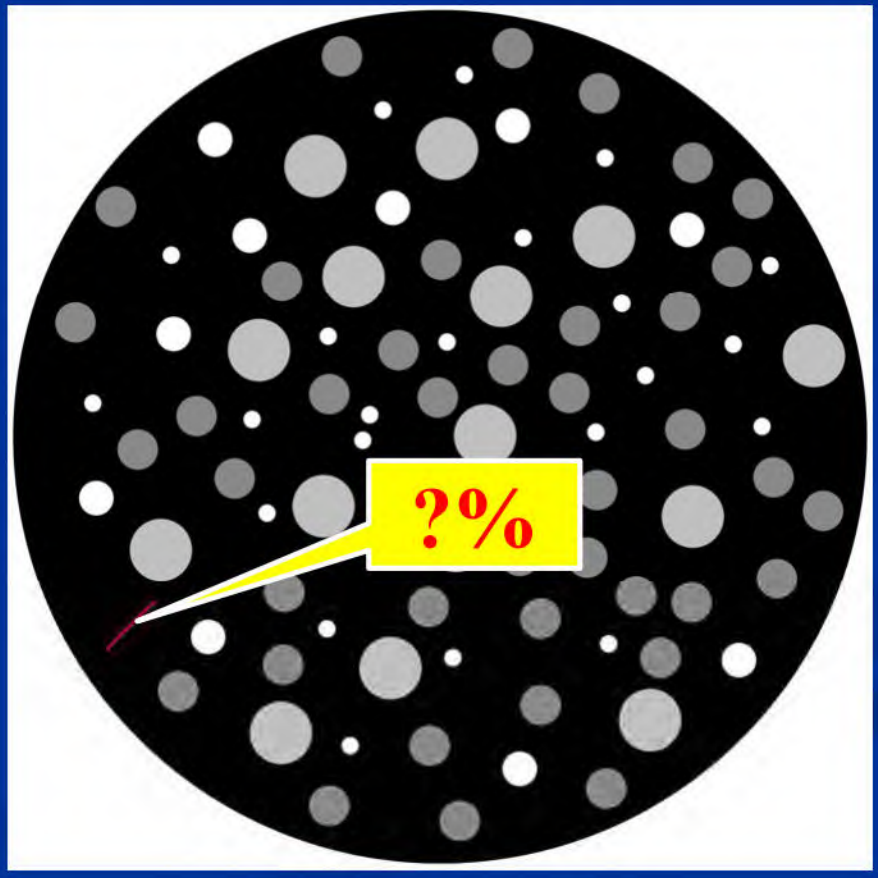

Dr. Shu-Chun Su's Analysis of MAS's Analytical Results

Impossible Error Rate of Visual Estimate

MAS's 0.005% Error Rate Defies Common Sense

REMOTE DEPOSITION OF WILLIAM E. LONGO, PhD
April 2, 2024

Kayme Clark (NJ) - WilliamLongoVol2-20240402.PDF

these that I do. So, it's just a visual estimate.
It's their opinion.

Q. And it's a qualitative number, qualitative assessment, right?

A. A visual estimate -- it typically may have an error rate of .005 percent or something. They're all qualitative. Every time somebody does PLM and puts a weight percent down, it's called qualitative.

Q. Okay. That error rate that you just referenced, where did you pull that from? That's not from your --

A. It --

(Court Reporter clarification.)

BY MR. HYNES:

Priority-One Court Reporting Services Inc. - A Veritext Company
718-983-1234

LONGO, Ph.D. - DIRECT

Page 186

Q. I was going to say, that error rate isn't specific to this chrysotile by PLM?

A. No. It's more specific. And, typically, NVLAP, they would send you a known sample, and you had a range of where it could be. You know, if it was 10 percent. And I forget what they allowed before they started knocking points off.

Q. So, that is based on NVLAP

In Dr. Longo's April 2, 2024 deposition, he claimed that MAS's typical error rate of Visual Estimate was 0.005%

It is not qualitative but quantitative.

NVLAP's acceptable error rate of Calibrated Visual estimate or CVE is a single-digit percentage, for example, ± 5%, not an error rate at the third decimal place.

The 0.005% Error Rate of Visual Estimate Defies Common Sense

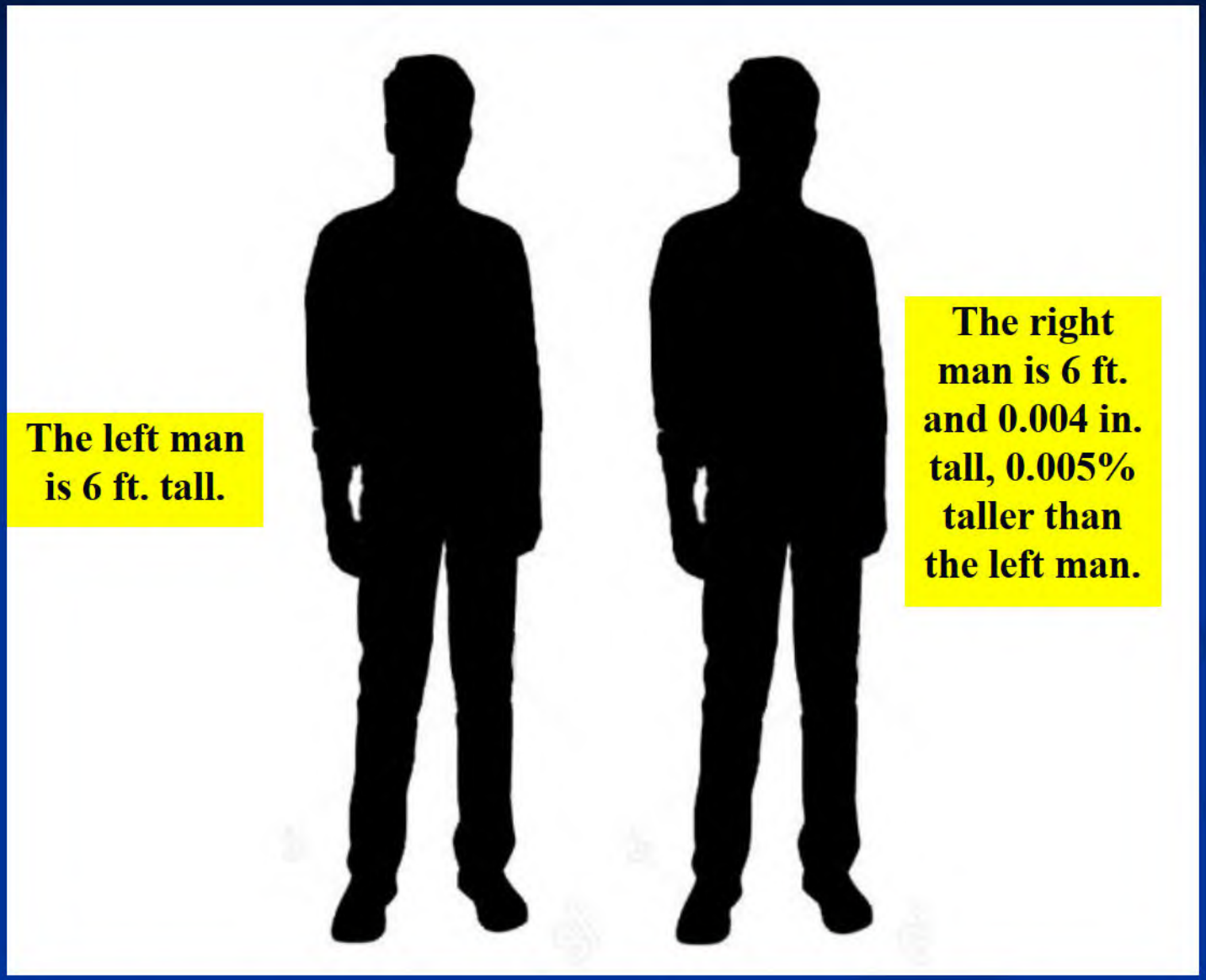

Can a human being visually tell the difference that the right man is taller by 0.004 inches? No.

Dr. Shu-Chun Su's Analysis of MAS's Analytical Results

Incorrect Extrapolation Procedure.

MAS's Analytical Results of J&J Talcum Powder

Valadez J & J Baby Powder Container

MAS's Analytical Results of J&J Talcum Powder

2023-02-28 Valadez Bottle Report

Table 2
Overall Summary of the JBP Asbestos Sample Analysis Results

MAS Sample #	ATEM Amphibole Asbestos	ISO-NY PLM Wt. % Amphibole Asbestos	CSM-PLM w/o HLS Chrys %	CSM Weight Recovery Light fraction	CSM Chrys % Weight Corrected**
M71614-001	<52,000	NSD	0.002-0.004	15.8%	0.0003-0.0006

*NSD: No Structure Detected **Weight Corrected

Table 3
Overall Summary of the Calculated Chrysotile
BIR CSM-PLM Data
(RI Fluid 1.650)

MAS Sample #	Chrysotile RI Values CSM-PLM	Birefringence Calculations
M71614-001	1.568-1.564 1.564-1.557	0.004-0.007 avg. = 0.006
	α range γ 1.564-1.557 1.568-1.564	Avg. = 0.006

Table 6
Chrysotile
Range of Parallel and Perpendicular RIs

Chrysotile Bundle No.	RI Fluid	CSM PLM (with HLS) Parallel RI	CSM PLM (with HLS) Perpendicular RI	BIR Calculations γ - α
M71614-001	1.560			
1		1.564	1.561	0.003
2		1.565	1.561	0.003
3		1.568	Avg. 1.559	0.009
4		Avg. 1.567	Avg. 1.562	0.005
		Avg. 1.566	Avg. 1.561	0.005

Estimation of the Number of Chrysotile Bundles Detected for CSM PLM Methods

Using the number of chrysotile bundles counted during the PLM analysis, and the amount of talcum powder analyzed in a specified area on the cover slip mount per the two glass slides, the amount of chrysotile bundles per gram of talcum powder sample can be calculated.

Total chrysotile bundles in the sample is calculated as shown in the following equation:

$$(A1 \div A2) \times (CB) \div W = TCB/W$$

Where:
A1: The total area (972 mm²) that the talcum powder occupies on the two glass slides.
A2: The area (23.5 mm²) in the fields of view that the talcum powder occupies on the two glass slides.
CB: Number of chrysotile bundles detected in a positive sample by PLM analysis.
W: Weight of total talcum powder placed on the two glass slides.
TCB/W: Total number of chrysotile bundles per weight (grams) of talcum powder.

The results of CSM sample preparation analysis calculations are shown in Table 4.

Table 4
Summary of Estimated Chrysotile Bundles per gram Calculations
For the CSM PLM Results

MAS Sample #	wt. of sample grams	No. of Chrys Bundles counted	CSM/ISO Chrysotile Bundles/g	CSM/ISO* Chrysotile Bundles/g
M71614-001	0.0007	6	354,000	56,000*
			Avg. = 354,000	Avg. = 56,000*

Weight corrected*

MAS's Conclusions

- This baby powder contains 0.0003 – 0.0006% of chrysotile.
- Each gram of talc contains 56,000 chrysotile bundles.

MAS PLM Extrapolation Procedure Is Unpublished, Unvalidated, Unreliable, and Not Scientifically Justified

Estimation of the Number of Chrysotile Bundles Detected for CSM PLM Methods

Using the number of chrysotile bundles counted during the PLM analysis, and the amount of talcum powder analyzed in a specified area on the cover slip mount per the two glass slides, the amount of chrysotile bundles per gram of talcum powder sample can be calculated.

Total chrysotile bundles in the sample is calculated as shown in the following equation:

$$(A1 \div A2) \times (CB) \div W = TCB/W$$

Where:

A1: The total area (972 mm^2) that the talcum powder occupies on the two glass slides.

A2: The area (23.55 mm^2) in thirty fields of view that the talcum powder occupies on the two glass slides.

CB: Number of chrysotile bundles detected in a positive sample by PLM analysis.

W: Weight of total talcum powder placed on the two glass slides.

TCB/W: Total number of chrysotile bundles per weight (grams) of talcum powder.

The results of CSM sample preparation analysis calculations are shown in Table 4.

Table 4
Summary of Estimated Chrysotile Bundles per gram Calculations For the CSM PLM Results

MAS Sample #	wt. of sample grams	No. of Chrys Bundles counted	CSM/ISO Chrysotile Bundles/g	CSM/ISO* Chrysotile Bundles/g
M71614-001	0.0007	6	354,000	56,000*
			Avg. = 354,000	Avg. = 56,000*

Weight corrected*

Out of a 1.5 oz. container, MAS separated out 0.0007 grams of talc powder for analysis.

Out of the 0.0007 grams sample, Only 2.4% or 0.000017 grams was actually counted.

Based on the counting results of the 0.000017-gram sample, MAS concluded that one gram of talc powder contains 56,000 chrysotile bundles.

The results of 0.000017 grams were extrapolated to 1 gram of talc powder. The extrapolation factor is 58,824 times!

0.000017-Gram PLM Results Extrapolated to 1 Gram of Talc

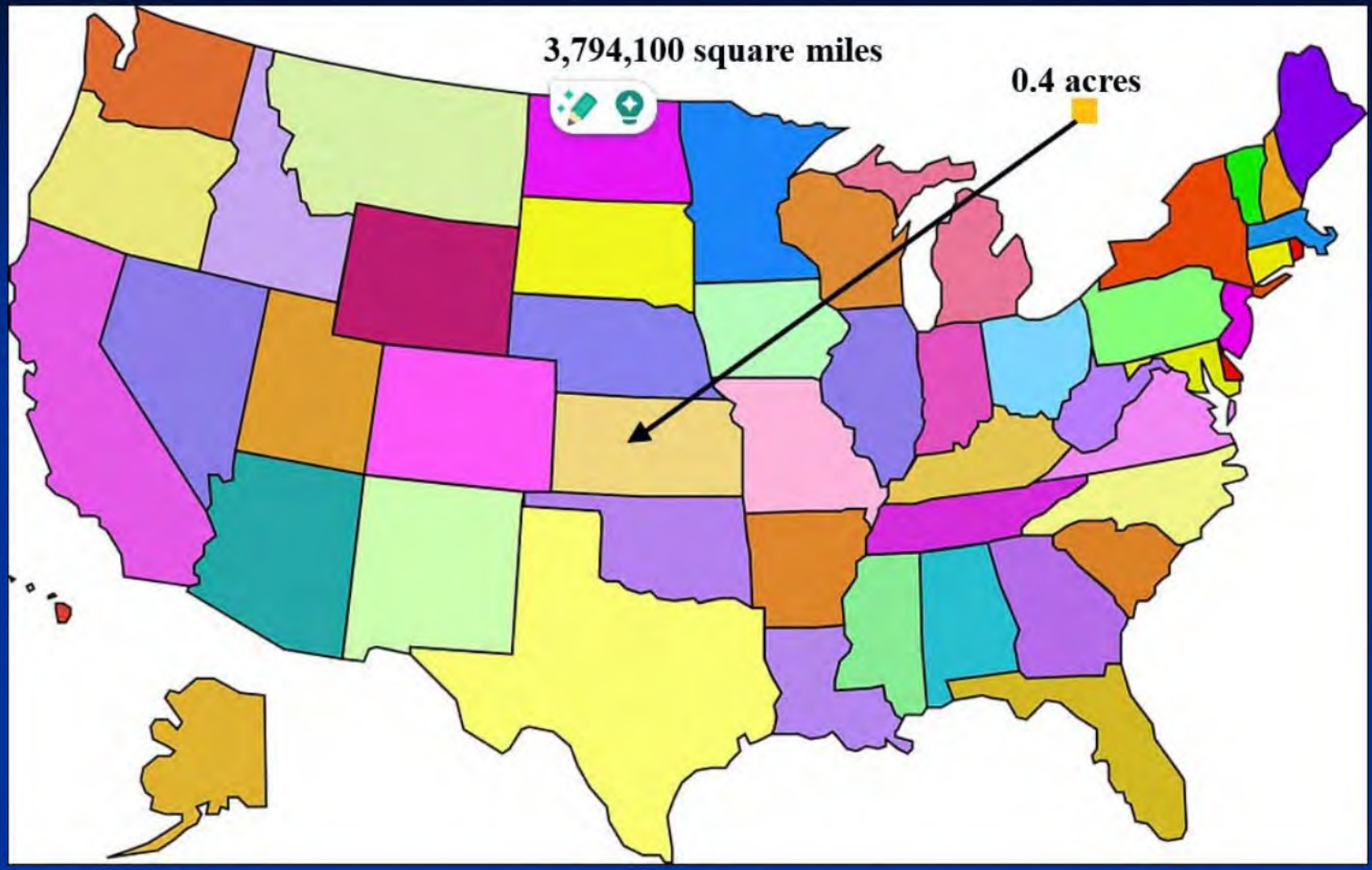

The total area of the United States is three million seven hundred ninety-four thousand one hundred square miles. Using 0.000017-gram results to extrapolate to 1 gram of talc is like using a survey of the soil of a 0.4-acre backyard in a Kansas home to represent the soil of the whole United States.

0.000017-Gram PLM Results Extrapolated to 1 Gram of Talc

A motor vehicle plant produces 58.000 cars in a year.

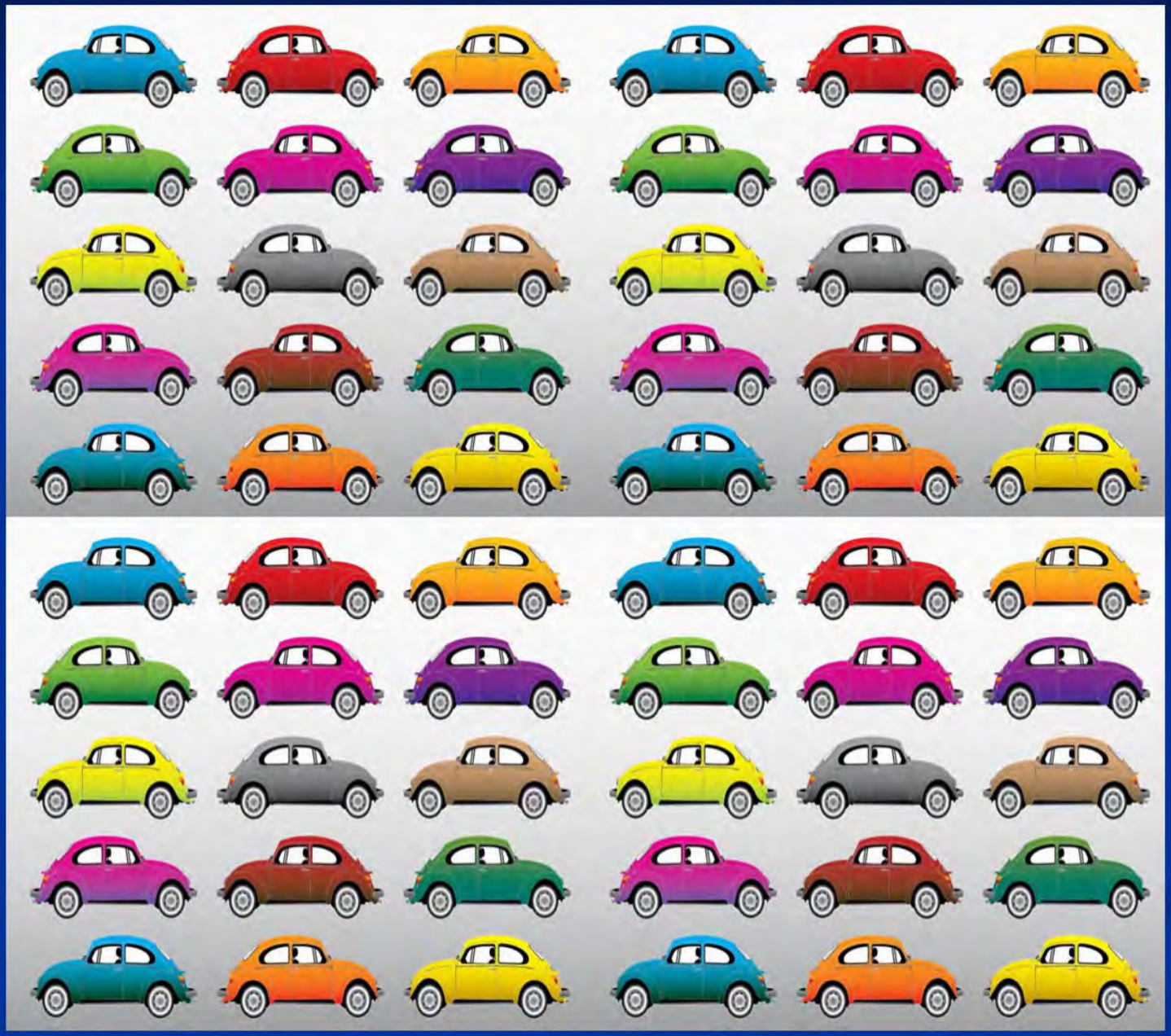

Using the measurement results of 0.000017 grams sample to evaluate 1 gram of talc is like using the Quality Control check results of one vehicle to represent all 58,000 vehicles produced in a year. It is not an acceptable practice.

0.000017-Gram PLM Analysis is Far From Sufficient to Ensure a < 5% False Positive

- Any analytical procedure has errors. Asbestos analysis is no exception.
- There are two types of analytical errors: Type 1 – False Positive and Type 2: False Negative.
- For litigation-related analysis, the False Positive error rate must be kept under 5% or 1%
- In other words, the analytical procedure's Confidence Level (CL) must be at least 95% to ensure a < 5% False Positive error rate.
- In product liability analysis, a 95% CL test has a 5% probability of wrongly implicating an innocent product.
- MAS should pay more attention to the established sampling protocol and arbitrarily choose the amount of sample to be analyzed, which results in unacceptable False Positive rates.

A Sample Size of 0.000017-Grams is Far From Sufficient to Ensure a < 5% False Positive

Equation for Calculating Sample Size

$$n = p(1-p)\left(\frac{z}{E}\right)^2$$

where

- n – sample size that is large enough to attain the specified maximum allowed error and confidence level
- p – a rough estimate of population proportion (B%)
- E – MAE (maximum allowed error)
- z – critical value from normal distribution corresponding to the specified confidence level

  $z = 1.96$ for 95% confidence level

  $z = 2.575$ for 99% confidence level

Nate: 1. Given z and p, this equation can be used to calculate the margin of error associated with a specific n

2. The derivation of this equation is omitted in this presentation, which can be found in general probability/statistics texts

June 10, 2008 Shu-Chun Su: CARB M-435 22 of 40

All reliable methodologies require a sample size calculation to ensure a 95% Confidence Level and keep the False Positive error rate under 5%. Above is an example that I provided to the California Air Resources Board in 2008.
MAS did not perform any such calculation as part of its PLM methodology, which is scientifically inappropriate.

A Sample Size of 0.000017-Grams is Far From Sufficient to Ensure a < 5% False Positive

Equation for Calculating Sample Size

$$n = p(1-p)\left(\frac{z}{E}\right)^2$$

where

- n – sample size that is large enough to attain the specified maximum allowed error and confidence level
- p – a rough estimate of population proportion (B%)
- E – MAE (maximum allowed error)
- z – critical value from normal distribution corresponding to the specified confidence level

  $z = 1.96$ for 95% confidence level

  $z = 2.575$ for 99% confidence level

Nate: 1. Given z and p, this equation can be used to calculate the margin of error associated with a specific n

2. The derivation of this equation is omitted in this presentation, which can be found in general probability/statistics texts

June 10, 2008 Shu-Chun Su: CARB M-435 22 of 40

The above equation can be used to calculate the Confidence Level for known sample size, population proportion, and maximum allowed error. The Confidence Level of 2023-02-28 Valadez Bottle Report is far below 50%, making the False Positive error rate much greater than 50%. Such a False Positive error rate is totally unacceptable. A responsible laboratory will never adopt such a sampling scheme to make the False Positive error rate greater than 50%.

Dr. Shu-Chun Su's Analysis of MAS's Analytical Results

Internally Conflicting Quantification Results.

Internally Conflicting Quantification Results

2021-05-25 OTShelf JBP Purchased Argentina (M71228-001)

MAS reported 137,000 chrysotile bundles constituting a 0.005 – 0.006%wt. asbestos concentration.

Date of Report	2021-05-25
MAS No.	71228-001
Product	Argentina
Chrysotile %	0.005 - 0.006
Chrysotile Bundles per gram of baby powder	137000
Image of 71228-001 Chrysotile	p.39
Scale bar length (µm)	100
Length of Scale Bar on screen (pixel)	95.0
Chrysotile length on screen (pixel)	97.0
Chrysotile length (µm)	102.1
Chrysotile width on screen (pixel)	9.0
Chrysotile width (µm)	9.5
Chrysotile thickness (µm)	9.5
Single chrysotile volume (μm^3)	9164.02
Single chrysotile volume (mm^3)	0.0000091640
Total volume of chrysotile bundles (mm^3)	1.255470
Talc density (g/cm^3)	2.72
Volume of 1 gram chrysotile (cm^3)	0.368
Volume of 1 gram chrysotile (mm^3)	367.6
Percentage of chrysotile	0.34%

Table 2
Overall Summary of Off-The-Shelf JBP Container Sample Analysis Results

MAS Sample #	ISO-PLM w/o HLS Chrysotile %	Chrysotile Bundles Counted ISO	CSM/ISO-PLM with HLS chrysotile %	Chrysotile Bundles Counted CSM-ISO	Weight Recovery CSM-ISO	CSM/ISO-PLM with HLS chrysotile %
M71216-001	0.016-0.017	53	*0.022-0.023	70	24.2%	**0.005-0.006
M71216-002	0.009-0.012	33	0.014-0.015	48	21.4%	0.003
M71216-003	0.016-0.017	39	0.019-0.020	63	21.3%	0.004
	Range 0.009-0.017	Avg. 41 Bundles	Range 0.014-0.023	Avg. 60 Bundles	Avg. 22.3%	Range 0.003-0.006

*CSM chrysotile weight concentrations not weight corrected. **CSM chrysotile weight concentrations recovery corrected

Table 5
Summary of Estimated Chrysotile Bundles per gram Calculations for the JBP ISO & CSM PLM Results

MAS Sample #	ISO-PLM Wt of Sample Grams	No. of Chry Bundle counted	Chrysotile Bundles/g	Wt. of Sample in Grams	No. of Chry Bundles counted	Chrysotile Bundles/g
M71228-001	0.0010	53	567,000	0.0010	70	749,000
M71228-002	0.0010	33	353,100	0.0010	48	514,000
M71228-003	0.0009	39	464,000	0.0011	63	613,000
	Avg. 0.0097	Avg. 42 Chry Bundles	Avg. 461,000	Avg. 0.00103	Avg. 60 chry Bundles	Avg. 625,000

Reported: 0.005 – 0.006; Calculated: 0.34%. Differing by 62 times.

The conclusion is that MAS's quantification results are NOT credible.

Dr. Shu-Chun Su's Analysis of MAS's Analytical Results

Inaccurate and Unreliable Sample Preparation Procedure.

Incorrect Sample Preparation Procedure

2020 - 2024 HLS Resaults

Date	MAS No.			Light Fraction %
2020-09-17	M71666	001	1	17.0
			2	14.6
			3	13.4
2021-05-25	M71216	001	1	24.2
			2	21.4
			3	21.3
2023-02-28	M71614	001	1	15.9
2023-10-19	M71643	001	1	19.7
2024-02-15	M71740	001	1	25.7

Since MAS's chrysotile concentration is at the 0.00x% level, talc is then at 99+% level.
If the Heavy Liquid Separation (HLS) sample preparation procedure was correctly performed, the Light Fraction would be < 1%.
MAS's two-digit Light Fraction results clearly indicate that MAS was NOT capable of correctly performing the HLS sample preparation procedure.

Summary of Deficiencies of MAS's Analytical Procedures

- Inability to ensure a 95% Confidence Level of quantification.
- Inability to correctly interpret dispersion staining colors.
- Inability to calibrate dispersion staining colors.
- Inability to understand the basic relationship between the material's refractive index and the refractive index of liquids used for measurement.
- Inability to conduct calibrated visual estimate (CVE).
- Inability to check the internal consistency of analytical data.
- Inability to correctly measure particle size under a polarized light microscope.
- Inability to correctly create scale bars.
- Inability to understand the fundamental physics principles governing the relationship between a material's refractive index and its physical dimension.
- Inability to understand the fundamental geological principles governing the formation of minerals and mineral ore deposits.

References in Presentation

Aveston, J. (1969) The mechanical properties of asbestos. Journal of Materials Science, 4, 625-633.MAS (2020). https://doi.org/10.1007/BF00550118.

ISO 22262-1 ISO 22262-1

MAS (2020) 2020-03-18 MAS Rpt JBP-Titley.pdf

MAS (2020) 2020-03-20 MAS Rpt JBP-Doyle.pdf

MAS (2021) 2021-05-25 MAS OTShelf JBP Purchased Argentina (M71228).pdf

MAS (2021) 2021.09.05 - Dr. Longo Report Avon, Clinique, EL.pdf

MAS (2022) 2022-03-11 MAS Analy of Klayman's JBP & STS Containers (M71262).pdf

MAS (2023) 2023-02-28 - Valadez Bottle Report.pdf

MAS (2023) 2023.10.19 (M71643-001) Talcum Powder Analysis of Johnson's Baby Powder Compiled Notebook 14-2996.pdf

MAS (2024) 2024-02-15 M71740 Analysis of JBP (Rochelle Kirch) Compiled Notebook.pdf

MAS (2024) Kayme Clark (NJ) – William Longo Ph.D. Deposition-Vol. 1-20240327.

MAS (2024) Kayme Clark (NJ) – William Longo Ph.D. Deposition-Vol. 2-20240402.

Mumpion, F.A. and Thompson, C.S. (1973) Mineralogy And Origin of the Coalinga Asbestos Deposit. Clays and Clay Minerals. 23, 131 – 143.

Pier, J (2017) Wet Sieve Concentration Applied to Chrysotile in the Analysis of Talc for Asbestos. Johnson Conference, Burlington, VT.

Sprynskyy, M. et. al. (2011) Structural features of natural and acids modified chrysotile nanotubes. Journal of Physics and Chemistry of Solids. Volume 72, Issue 9. Pages 1015-1026. https://doi.org/10.1016/j.jpcs.2011.05.013.

Su, S.C. (2003) A rapid and accurate procedure for the determination of refractive indices of asbestos minerals. American Mineralogist, 88, 1979-1982.

Su, S.C (2022) The Dispersion Staining Technique and Its Application to Measuring Refractive Indices of Non-opaque Materials, with Emphasis on Asbestos Analysis, The Microscope, 69:2, pp 51–69; https://doi.org/10.59082/ZGWM6676.

Su, S.C. (2022) Area Percentage Charts to Aid Visual Estimation of Asbestos Concentration in Bulk Asbestos Samples, The Microscope 69:4, pp 160-162

Syed, S.F. et. al. (2020) Optimization of Tensile Strength and Shrinkage of Talc-Filled Polypropylene as a Packaging Material in Injection Molding. J Package Technol Res 4, 69–78. https://doi.org/10.1007/s41783-019-00077-6.

Shubhra, T.H. et. al. (2011) Mechanical properties of polypropylene composites: a review. J Thermoplast Compos. 26. 362-391. https://doi.org/10.1177/0892705711428659.

USP (2022) 41. USP-NF 〈1901〉 Theory and Practice of Asbestos Detection in Pharmaceutical Talc.pdf

Zhao, S. et. al. (2021) The Physical and Chemical Properties of Hemp Fiber Prepared by Alkaline Pectinase-Xylanase System. https://doi.org/10.21203/rs.3.rs-451112/v1.